DEVELOPMENT OF MAIN SHAFT SEALS FOR ADVANCED AIR BREATHING PROPULSION SYSTEMS

SEMIANNUAL REPORT NO. 2
1 JANUARY 1966 THROUGH 30 JUNE 1966
9 SEPTEMBER 1966

NASA

PREPARED FOR
NASA-LEWIS RESEARCH CENTER CLEVELAND, OHIO 44135
UNDER CONTRACT NAS 3-7609

Pratt & Whitney Aircraft DIVISION OF UNITED AIRCRAFT CORPORATION

PREFACE

This program started 29 June 1965 under contract NAS3-7609 and will extend with Tasks I & II for a period of twenty four (24) months. Semiannual progress reports will be submitted on the 20th of the month at the end of each six month period. This is the second of these reports and covers activities for the period ending June 30, 1966.

Richard M. Slayton is Project Manager for Pratt & Whitney Aircraft for this program.

The following National Aeronautics and Space Administration personnel have been assigned to this project.

Contracting Officer	J. H. DeFord
Project Manager	D. P. Townsend
Research Advisor	L. P. Ludwig
Contract Administrator	T. J. Charney

PWA-2879

SEMIANNUAL REPORT

DEVELOPMENT OF MAINSHAFT SEALS

FOR

ADVANCED AIRBREATHING PROPULSION SYSTEMS

Prepared for

National Aeronautics and Space Administration

September 9, 1966

Contract NAS3-7609

Technical Management
NASA Lewis Research Center
Cleveland, Ohio

Airbreathing Engine Division
D. P. Townsend
Project Manager
L. P. Ludwig
Research Advisor

Prepared by: R. L. Thomas
R. L. Thomas
Asst. Project Engineer

A. J. Parks
A. J. Parks
Asst. Project Engineer

R. M. Slayton CHK.
R. Slayton
Project Manager

Approved by: R. P. Shevchenko
R. P. Shevchenko
Sr. Project Engineer

Pratt & Whitney Aircraft
400 Main Street
E. Hartford, Connecticut

#13

SUMMARY

This report covers the work accomplished during the second 6-month period (January 1966 through June 1966) of the NAS3-7609 contract which was initiated 29 June 1965 and extends for a total of 24 months.

Briefly, the objective of the work to be accomplished is to analyze, design, procure, and test four types of mainshaft seals for advanced gas turbine applications.

A program summary is presented in Figure 1. The work accomplished during this 6-month period is outlined below.

1. Contacts with vendors were continued in relation to the seals to be evaluated.

2. Detailed analytical studies of all seal configurations to be tested were continued.

3. The remaining three design concepts and detailed drawings were submitted to NASA for approval. These design concepts consisted of the following seal configurations:

   a. Orifice compensating hydrostatic face seal with piston ring secondary.
   b. Face contact seal with bellows secondary.
   c. Externally pressurized hydrostatic seal.

4. Approval was received from NASA for the following seal concepts:

   a. Orifice compensating hydrostatic face seal.
   b. Face contact seal with bellows secondary.

5. Procurement of mainshaft seal rig (A) parts was completed. Also, procurement of parts for a second mainshaft seal rig (B) was completed.

6. Procurement of the inert gas rig and the instrumentation validation rig was started and completed.

7. Procurement of all approved seals has commenced. The first two orifice compensating seal assemblies were received from Stein Seal Company.

8. Mainshaft seal rig (A) was assembled and the face contact seal with piston ring secondary (Build 1) was run 16 hours while undergoing preliminary dynamic checkout.

9. Build 2 of the face contact seal with piston ring secondary completed 35 hours running time including some test points at 250°F oil in and 800°F air temperature at sliding speeds of up to 400 feet per second. The engine simulation tests of this seal are currently continuing.

10. The instrumentation validation rig assembly was completed during June 1966 and is ready for mounting on the test stand.

11. Mainshaft seal rig (B) with the orifice compensating hydrostatic face seal, was assembled in June 1966.

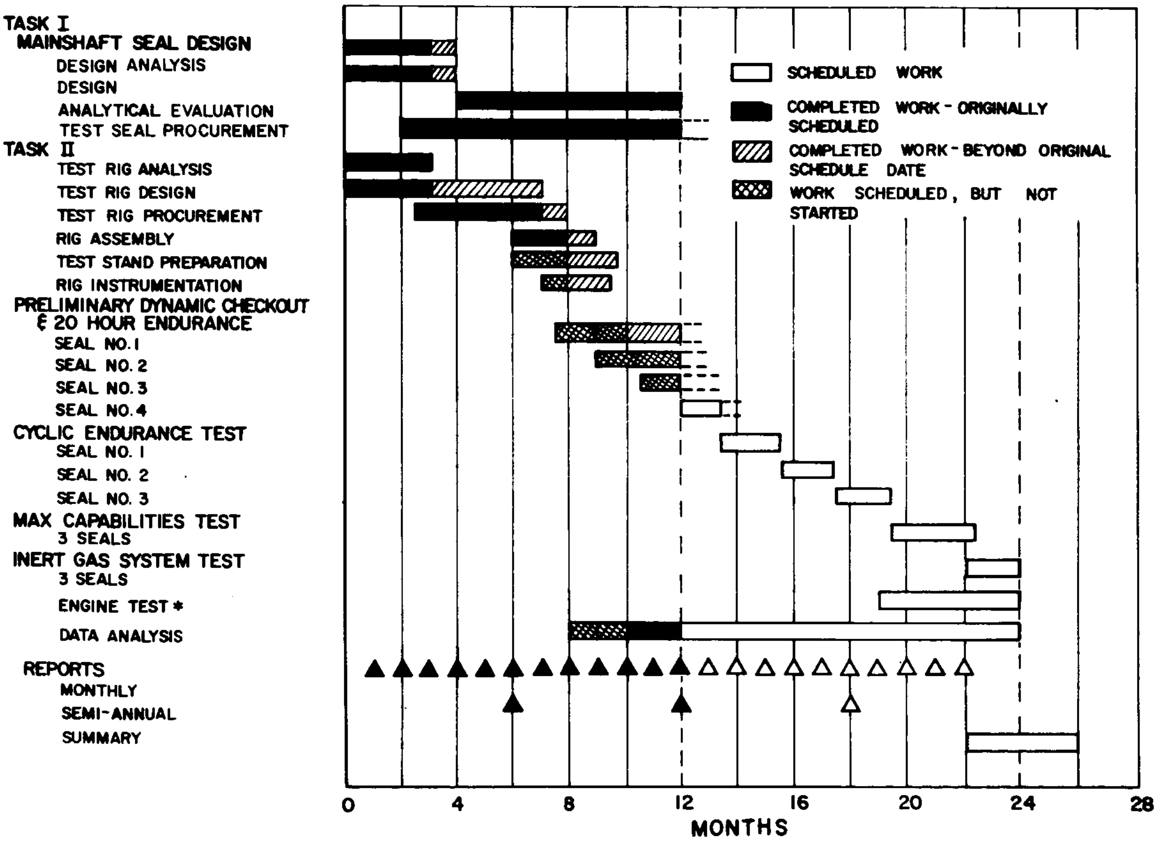

* CONTINGENT UPON PERFORMANCE OF SEAL AND AVAILABILITY OF ENGINE FOR TESTING. SEE LETTER OF TRANSMITTAL DATED FEB. 26, 1965

Figure 1 Mainshaft Seal Program Summary

TABLE OF CONTENTS

	Page No.
PREFACE	ii
SUMMARY	iii
LIST OF ILLUSTRATIONS	vii
1.0 INTRODUCTION	1
2.0 DISCUSSION	2
2.1 Task I - Mainshaft Seal Design	2
2.1.1 Summary	2
2.1.2 Mainshaft Seal Analyses	2
2.1.2.1 Orifice Compensated Hydrostatic Face Seal With Piston Ring Secondary (Stein)	3
2.1.2.2 Externally Pressurized Orifice Compensated Hydrostatic Face Seal (Stein)	4
2.1.2.3 Carbon Face Contact Seal with Bellows Secondary Seal (Stein)	5
2.1.3 Mainshaft Seal Calculations	6
2.1.3.1 Orifice Compensated Hydrostatic Face Seal with Piston Ring Secondary (A) and Externally Pressurized Orifice Compensated Face Seal (B)	7
2.1.3.1.1 Inertial Loadings	7
2.1.3.1.2 Frictional Force on Piston Rings	10
2.1.3.1.3 Geometry Assurance Check (Deflection Analysis)	13
2.1.3.1.4 Collars (Seal Plate Deflection Analysis)	17
2.1.3.1.5 Shroud, Windback (Stress Calculations)	22
2.1.3.1.6 Compression Springs	24
2.1.3.1.7 Leakage and Restoring Force	24
2.1.3.2 Carbon Face Contact Seal With Bellows Secondary Seal (C)	41
2.1.3.2.1 Inertial Loadings	41
2.1.3.2.2 Required Total Loadings (Summary)	42
2.1.3.2.3 Face Pressure Forces	42
2.1.3.2.4 Collars (Deflection Analysis)	43
2.1.4 Seal-Housing Deflection Analysis (P&WA Design)	45
2.1.4.1 Deflection and Rotation Equations	46
2.1.4.1.1 For Body (1)	46
2.1.4.1.2 For Body (2)	47
2.1.4.1.3 For Body (3)	48
2.1.4.1.4 For Body (4)	48
2.1.4.1.5 For Body (5)	49
2.1.4.1.6 Relations Between P_2, P_4, and P_5	50
2.1.4.1.7 Slopes and Deflections	50

TABLE OF CONTENTS (Cont'd)

	Page No.
2.1.5 Thermal Analysis	53
2.2 Task II - Mainshaft Seal Evaluation	59
2.2.1 Statement of Objective	59
2.2.2 Progress	59
2.2.2.1 NASA Approval of Seal Designs	59
2.2.2.2 Seal Procurement	60
2.2.2.3 Test Stand and Facilities	60
2.2.2.4 Test Rig A	60
2.2.2.4.1 Rig Procurement and Assembly	61
2.2.2.4.2 Rubbing Contact Face Seal with Piston Ring Secondary - Build 1	61
2.2.2.4.3 Rubbing Contact Face Seal with Piston Ring Secondary - Build 2	61
2.2.2.5 Test Rig B	62
2.2.2.6 Inert Gas Test Rig	62
2.2.2.7 Instrumentation Validation Rig	62
APPENDIX A	83
Distribution List	109

LIST OF ILLUSTRATIONS

Figure	Title	Page
1	Mainshaft Seal Program Summary	iv
2	Orifice Compensated Hydrostatic Seal With Piston Ring Secondary	4
3	Externally Pressurized Orifice Compensated Hydrostatic Face Seal	5
4	Carbon Face Contact Seal With Bellows Secondary	6
5	SEAL B: Face Leakage to Sump - Pi = 335 psia.	28
6	SEAL B: Face Leakage to Sump - Pi = 135 psia.	29
7	SEAL B: Face Leakage to Sump - Pi = 95 psia.	30
8	SEAL B: Face Leakage to Sump - Pi = 235 psia.	31
9	SEAL A: Design Characteristics of Self-Energized Face Seal-Curves in Error Due to Incorrect P_A Value (P_A = 300;100 psia)	32
10	SEAL A: Design Characteristics of Self-Energized Face Seal - Seal Design Based on Fig. 9 (P_A = 315 psia)	33
11	SEAL A: Design Characteristics of Self-Energized Face Seal - Seal Design Based on Fig. 9 (P_A = 115 psia)	34
12	SEAL A: Design Characteristics of Self-Energized Face Seal - Seal Design Based on Fig. 9 (P_A = 75 psia)	35
13	SEAL A: Design Characteristics of Self-Energized Face Seal - Seal Design Based on Fig. 9 (P_A = 215 psia)	36
14	SEAL A: Design Characteristics of Self-Energized Face Seal Using Correct Value of P_A (P_A = 315 psia)	37
15	SEAL A: Design Characteristics of Self-Energized Face Seal Using Correct Value of P_A (P_A = 115 psia)	38
16	SEAL A: Design Characteristics of Self-Energized Face Seal Using Correct Value of P_A (P_A = 75 psia)	39

LIST OF ILLUSTRATIONS (Cont'd)

Figure	Title	Page
17	SEAL A: Design Characteristics of Self-Energized Face Seal Using Correct Valve of P_A (P_A = 215 psia)	40
18	Temperature Map of Carbon Seal For Design Conditions	55
19	Pressure Drop Per Unit Length (psi/in) as a Function of Oil Flow-Rate Per Passage (lb/hr) With Passage Diameter as Parameter	56
20	Heat Transfer As a Function of Oil Flow Rate Per Passage With Passage Diameter as Parameter	57
21	Schematic Diagram of Test Facilities X-81 Stand	63
22	Mainshaft Seal Rig 29360 - Overall View of Interior of X-81 Stand Showing Test Rig, Gear Box and Drive Engine	63
23	Mainshaft Seal Rig 29360 - Close-Up of Test Rig and Gear Box As Mounted in X-81 Test Stand	64
24	Mainshaft Seal Rig 29360 - View of X-81 Stand Control Panel and Specialized Instrumentation Required for NASA Contract.	64
25	Rig Layout Showing Materials Used	65
26	Preliminary Dynamic Checkout Program P&WA Rubbing Contact Seal With Piston Ring Secondary Leakage Calibration - Build 1	66
27	Mainshaft Seal Rig 29360 - Shaft Assembly in Gisholt Dynetric Balance Machine Supports During Balance Operation.	67
28	Mainshaft Seal Rig 29360 - Shaft Assembly in Gisholt Dynetric Balance Machine Supports During Balance Operation.	67
29	Mainshaft Seal Rig 29360 - View of Shaft and Rear Bearing Support Assembly.	68

LIST OF ILLUSTRATIONS (Cont'd)

Figure	Title	Page
30	Mainshaft Seal Rig 29360 - Front Hub Assembly Prior to Final Assembly of Rig	68
31	Mainshaft Seal Rig 29360 - Rear View of Instrumentation Support Assembly in Rig Housing	69
32	Mainshaft Seal Rig 29360 - Front View of Outer Case Showing Roller Bearing Support	69
33	Mainshaft Seal Rig 29360 - Rig Hub Assembly Prior to Installation of the Test Seal Assembly	70
34	Mainshaft Seal Rig 29360 - P&WA Rubbing Contact Seal With Piston Ring Secondary Assembly Shown With Instrumentation Installed	70
35	Mainshaft Seal Rig 29360 - Front View of Rig With the Seal Assembly Installed	71
36	Mainshaft Seal Rig 29360 - Front View of Rig With The Insulation Shield Installed Over the Seal Assembly Support	71
37	Mainshaft Seal Rig 29360 - Rig Hub Assembly After 16.0 Hours Running of the Preliminary Dynamic Checkout Program on the P&WA Rubbing Contact Seal With Piston Ring Secondary	72
38	Mainshaft Seal Rig 29360 - P&WA Rubbing Contact Seal With Piston Ring Secondary After 16.0 Hours Running of the Preliminary Dynamic Checkout Program	72
39	Mainshaft Seal Rig 29360 - PWA 771 Seal Plate With LCIC Hardface After 16.0 Hours Running of the Preliminary Dynamic Checkout Program Against the P&WA Rubbing Contact Seal With Piston Ring Secondary	73
40	Mainshaft Seal Rig 29360 - Close-Up View of Carbon Lip Wear Path on the PWA 771 Seal Plate with LCIC Hardface	73

LIST OF ILLUSTRATIONS (Cont'd)

Figure	Title	Page
41	Mainshaft Seal Rig 29360 - Rear View of the Oil Cooled Seal Plate Showing Oil Scoop With Oil Inlet Holes.	74
42	Mainshaft Seal Rig 29360 - Rear View of the Oil Cooled Seal Plate Showing Oil Scoop With the Enlarged Oil Inlet Holes	74
43	Preliminary Dynamic Checkout Program P&WA Rubbing Contact Seal With Piston Ring Secondary Leakage Calibration - Build 2	75
44	Mainshaft Seal Rig 29360 B Build 1. Front Hub Assembly Prior to Final Assembly	76
45	Mainshaft Seal Rig 29360 B. Build 1. Front Hub Assembly Prior to Final Assembly	76
46	Mainshaft Seal Rig 29360 B. Build 1. Stein Seal Company Orifice Compensating Hydrostatic Face Seal With Piston Rig Secondary	77
47	Mainshaft Seal Rig 29360 B - Build 1. Component Parts of the Stein Seal Company Orifice Compensating Hydrostatic Face Seal With Piston Rig Secondary	77
48	Mainshaft Seal Rig 29360 B - Build 1. Stein Seal Company Orifice Compensating Hydrostatic Carbon Seal Ring Assembly.	78
49	Mainshaft Seal Rig 29360 B - Build 1. Rear Side of Stein Seal Company Orifice Compensating Hydrostatic Carbon Seal Ring Assembly.	78
50	The Shaded Areas of These Two Layouts Illustrates the Changes Made to the Rig to Permit Testing of Seals Using an Inert Gas Blanket on the Oil Sump.	79
51	Instrumentation Validation Rig (TL-67996) (Torque Measuring Not Shown)	80

LIST OF ILLUSTRATIONS (Cont'd)

Figure	Title	Page
52	Instrumentation Validation Rig 29401 - Build 1. Test Seal Assembly Installed in Rig Cover.	81
53	Instrumentation Validation Rig 29401 - Build 1. Close-Up of Test Seal Assembly Installed in Rig Cover	81
54	Instrumentation Validation Rig 29501 - Build 1. Rig Hub Assembly Prior to Installation of the Test Seal Assembly	82
55	Film Riding Face Seal Assembly - Orifice Compensated Type With Metallic Piston Ring Secondary	83
56	Seal Carrier For Orifice Compensated Seal	84
57	Assembly Guard For Orifice Compensated Seal	85
58	Seal Assembly For Orifice Compensated Seal	86
59	Steel Band For Orifice Compensated Seal	87
60	Seal Ring Carbon For Orifice Compensated Seal	88
61	Shroud Windback For Orifice Compensated Seal	89
62	Piston Ring For Orifice Compensated Seal	90
63	Seal Plate For Orifice Compensated Seal	91
64	Orifice For Orifice Compensated Seal	91
65	Teflon Holder For Instrumented Version of Orifice Compensated Seal	92
66	Teflon and Gap Shield for Instrumented Version of Orifice Compensated Seal	93
67	Special Windback for Instrumented Version of Orifice Compensated Seal	94
68	Carbon Face Contact Bellows Secondary Seal Assembly	95

LIST OF ILLUSTRATIONS (Cont'd)

Figure	Title	Page
69	Bore Guide for Face Contact Bellows Secondary Seal	96
70	Bellows Front Fitting For Face Contact Bellows Secondary Seal	97
71	Bellows Rear Fitting For Face Contact Bellows Secondary Seal	98
72	Windback for Face Contact Bellows Secondary Seal	99
73	Carbon Seal Assembly For Face Contact Bellows Secondary Seal	100
74	Seal Assembly Band For Face Contact Bellows Secondary Seal	101
75	Carbon Wafer for Face Contact Bellows Secondary Seal	102
76	Seal Carrier For Face Contact Bellows Secondary Seal	103
77	Alignment Ring For Face Contact Bellows Secondary Seal	104
78	Seal Plate For Face Contact Bellows Secondary Seal	105
79	Teflon Holder For Instrumented Version of Face Contact Bellows Secondary Seal	106
80	Teflon and Gap Shield For Instrumented Version of Face Contact Bellows Secondary Seal	107
81	Special Windback For Instrumented Version of Face Contact Bellows Secondary Seal	108

1.0 INTRODUCTION

The objective of this program is the analysis, design and testing of four types of mainshaft seals for advanced airbreathing propulsion systems. Testing will be conducted under simulated engine operating conditions to:

1. determine design components and features of an improved mainshaft seal,
2. establish seal operational limits in terms of temperature, speed, and pressure differential, and
3. establish a measure of seal reliability (wear and stability).

2.0 DISCUSSION

2.1 TASK I MAINSHAFT SEAL DESIGN

2.1.1 Summary

The work to be accomplished under this task is to analyze and design four seal assemblies that have the potential capabilities of operating at the following conditions:

Seal Sliding Speed	0 to 500 ft/sec
Seal Pressure Differential	0 to 300 psi
Gas Temperature	Ambient to 1300°F
Oil Sump Temperature	Ambient to 500°F

These four seal assemblies are further defined in the work statement of the contract to be of four types:

1. Orifice compensating hydrostatic face seal. (Seal Designation A - Stein)
2. Externally pressurized hydrostatic face seal. (Seal Designation B - Stein)
3. Face contact seal with bellows secondary seal. (Seal Designation C - Stein)
4. Face contact seal with piston ring secondary seal (PWA)

During the 6-month period from January 1, 1966 to June 30, 1966 covered by this report, analysis were performed on each of these four seal types. The following paragraphs present a detailed discussion of the results of these analytical studies.

2.1.2 Mainshaft Seal Analysis

Four seal assemblies were designed to meet the contractual specifications. A table outlining some significant features of these four designs is given in Table 1. In each of the succeeding subsections, a diagram of each seal assembly along with a general description is presented. The Pratt & Whitney Aircraft seal assembly was discussed in the first semiannual report, PWA-2683, so it will not be presented here.

TABLE 1

MAINSHAFT SEAL CHARACTERISTICS

Seal Designation	Film Riding	Orifice Compensated	Single Piston Ring Secondary	Double Piston Ring Secondary	Bellows Secondary	Capable of Being Externally Pressurized
A (Stein)	X	X	X			
B (Stein)	X	X		X		X
C (Stein)					X	X
P&WA Design				X		

A	Orifice compensated hydrostatic face seal
B	Externally pressurized orifice compensated hydrostatic face seal
C	Face contact with bellows secondary
PWA	Face contact with piston ring secondary

2.1.2.1 Orifice Compensated Hydrostatic Face Seal with Piston Ring Secondary - (Seal A Stein)

This is a film riding seal (Figure 2) which allows the high pressure air at the inside diameter to be introduced to an annular groove in the carbon face (1). The air is introduced through three supply lines, each of which contains an assembly of four orifices in series (2). The orifices are installed for the purpose of metering the flow and lowering the pressure before allowing the air to enter the annular face groove. The air introduced to the groove creates a "back pressure" which tends to impede the leakage air from the I.D. (3) (which is at a higher pressure) from flowing across the face of the seal. The leakage air, plus the air introduced to the groove, then flows across the outer lip to the O.D. of the seal (4), thus creating the "film" for the seal to ride on.

When the seal face and seal plate are in firm contact, the pressure in the face pocket will equal the load pressure because of the negligible pressure drop across the orifice when there is no flow. As the seal opens, the flow through the orifice creates a large pressure drop so that the pressure force in the face pocket diminishes with increase in clearance between face and face plate. As the face pocket pressure diminishes, the restoring force increases.

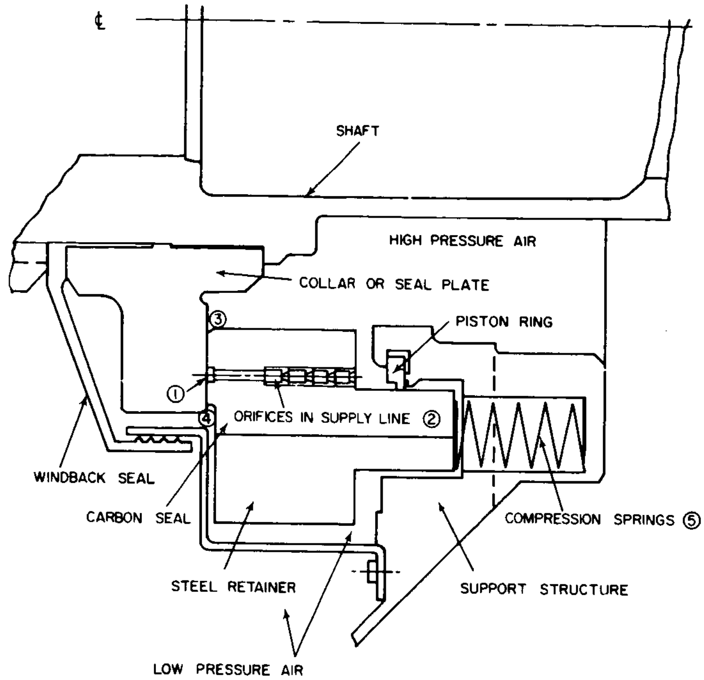

Figure 2 Orifice Compensated Hydrostatic Seal With Piston Ring Secondary

2.1.2.2 <u>Externally Pressurized Orifice Compensated Hydrostatic Face Seal - (Seal B Stein)</u>

This is a film riding seal (Figure 3) which allows either the high pressure air at the inside diameter or (through the use of fittings) some external high pressure gas supply (such as nitrogen) to be introduced to an annular groove in the carbon face. This high pressure gas is used to create a "back pressure" to impede air-flow from the high pressure I. D. (1). The gas introduced to the groove plus the leakage flow then flows across the outer lip to the O. D. of the seal (2), thus creating the "film" for the seal to ride on. The four orifices per assembly (3) in each of the three supply lines are arranged in series and are installed for the purpose of metering the flow and lowering the pressure before allowing the gas to enter the annular groove at the interface. When the seal is tight against the seal plate, the pressure in the interfacial groove is approximately equal to the pressure in the rear chamber since leakage is low and the loss in the orifice is negligible. As the face opening increases, the leakage will increase and the orifice drop will become appreciable, thus causing a net restoring force.

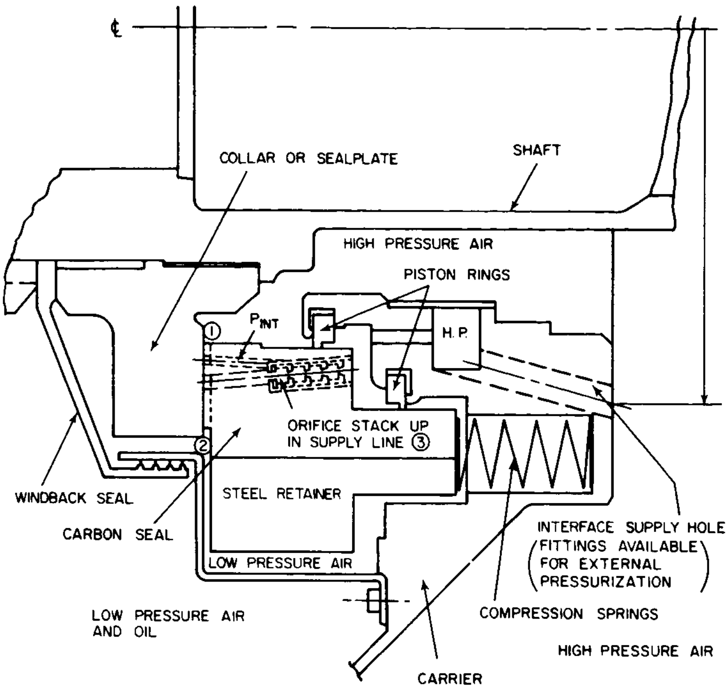

Figure 3 Externally Pressurized Orifice Compensated Hydrostatic Face Seal

2.1.2.3 Carbon Face Contact Seal With Bellows Secondary Seal - (Seal C Stein)

This face seal (Figure 4) is comprised of a carbon primary seal and a bellows secondary seal. The high pressure air is at the I.D. of the seal (1). Air at a high pressure leaks through labyrinth seal(5) and exists at pressure (P) at location(4). Gas (such as nitrogen) is introduced inside the bellows at location (6) at some pressure (P + 5 psi). This gas then exits from the bellows at location (3) where it still exists at pressure (approximately P + 5 psi). The nitrogen then has two flow paths. Some of the nitrogen leaks across the carbon face seal toward the O.D. (2) and the remainder since it is at pressure (P + 5 psi), leaks through a second labyrinth seal toward location (4) where air exists at pressure P. The air-nitrogen mixture is then vented to the atmosphere. The pressure of the nitrogen is not necessarily required to be P + 5, but this value was chosen to emphasize the point that it is desirable to have the nitrogen leak from point (3) to point (4) to ensure that air does not leak from point (4) to point (3). In order to accomplish this, the nitrogen must be at some higher pressure level than the air at point (4).

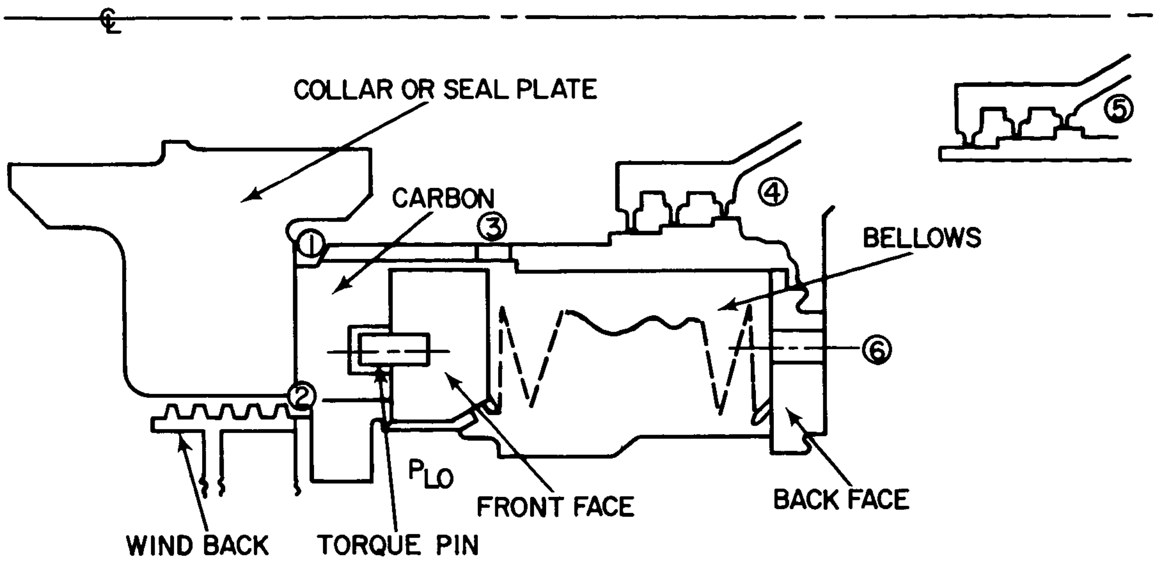

Figure 4 Carbon Face Contact Seal With Bellows Secondary

2.1.3 Mainshaft Seal Calculations

For each of the four seal designs, comparable design systems were formulated consisting of the calculation of: (1) seal-carrier and plate deflections, (2) inertial and frictional forces, (3) restoring and closing forces, (4) face leakages, and (5) thermal maps of the seal assembly. Table 2 references these calculations to the respective sections in this report and/or Semiannual Report No. 1 (PWA-2683).

A discussion in the first semiannual report stated that the forces acting to close a seal, the net closing force to make the stationary seal contact the rotating face plate, should be a constant value independent of changes in the pressure drop across the seal. The basic equation defining this closing force is:

$$\left\{\begin{array}{l}\text{net}\\ \text{closing}\\ \text{force}\end{array}\right\} = \left\{\begin{array}{l}\text{spring}\\ \text{closing}\\ \text{force}\end{array}\right\} \pm \left\{\begin{array}{l}\text{friction}\\ \text{force}\end{array} \pm \begin{array}{l}\text{inertial}\\ \text{force}\end{array}\right\} + \left\{\begin{array}{l}\text{pressure}\\ \text{closing}\\ \text{force}\end{array}\right\} - \left\{\begin{array}{l}\text{interfacial}\\ \text{pressure}\\ \text{lifting force}\end{array}\right\}$$

The spring force is designed to overcome the frictional force and the inertial force. Consequently, the net closing force is equal to the difference between the pressure closing and lifting forces. Using this as a design basis, the following calculations are presented.

TABLE 2

Seal Designation	Deflection Analysis	Inertial & Frict. Forces	Restoring & Closing Forces	Face Leakage	Thermal Analysis
A (Stein)	Prel.: Pg. 13-23 Detail: To be Initiated	Pg. 7-10 Pg. 10-12	Pg. 24 Pg. 28	Pg. 28	Analysis has been Initiated
B (Stein)	Prel. : Pg. 13-23 Detail: To be Initiated	Pg. 7-10 Pg. 10-13	Pg. 24 Pg. 24-27	Pg. 27	Analysis has been Initiated
C (Stein)	Prel.: Pg. 43-44 Detail: To be Initiated	Pg. 41-42	Pg. 42	-	To be Initiated
P&WA Design	Pg. 45-53	1st Semi-Annual* Pg. 8-9	1st Semi-Annual* Pg. 10	-	Pg. 53-59

*PWA-2683

A. Orifice compensated hydrostatic face seal.
B. Externally pressurized orifice compensated hydrostatic face seal.
C. Face contact with bellows secondary.
PWA Face contact with piston ring secondary

2.1.3.1 Orifice Compensated Hydrostatic Face Seal with Piston Ring Secondary (A) and Externally Pressurized Orifice Compensated Face Seal Inertial Loadings (B)

The orifice compensated hydrostatic face seal (A) and the comparable externally pressurized hydrostatic seal (B) which is capable of being externally pressurized are very similar in design so the calculations relating to both will be treated as one unit. The development presented in this subsection is primarily for seal (A). Where results differ, the comparable result for seal (B) will be found to the right of the result for (A). The difference is due to a slight increase in size of seal (B).

2.1.3.1.1 Inertial Loadings - In calculating inertial loadings, the weight of the steel band and carbon seal are first calculated. In turn, the equivalent face force F_I is determined at various conditions of ΔP.

Loadings

A. Inertia -

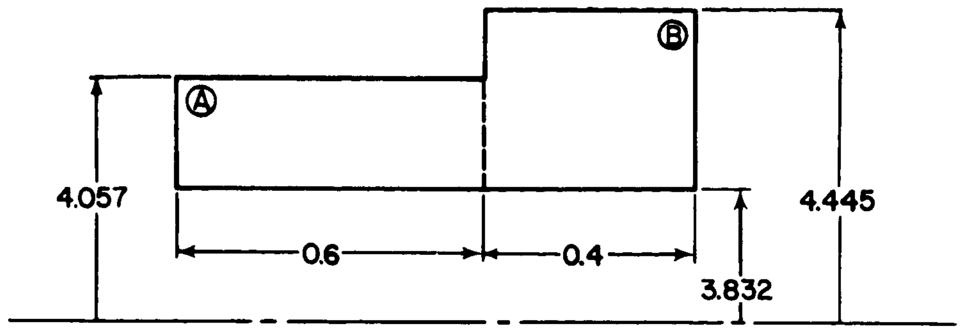

1. Steel band (P.R. Seal Ring)

wt. of A = $\rho\pi(R_o^2 - R_i^2)\,\ell$

$= .28\ \pi(4.057^2 - 3.832^2)(.6) = .95$

wt. of B = $.28\ \pi(4.445^2 - 3.832^2)(.4) = \underline{1.76}$

total steel band weight = 2.71 lb.

2. Carbon seal

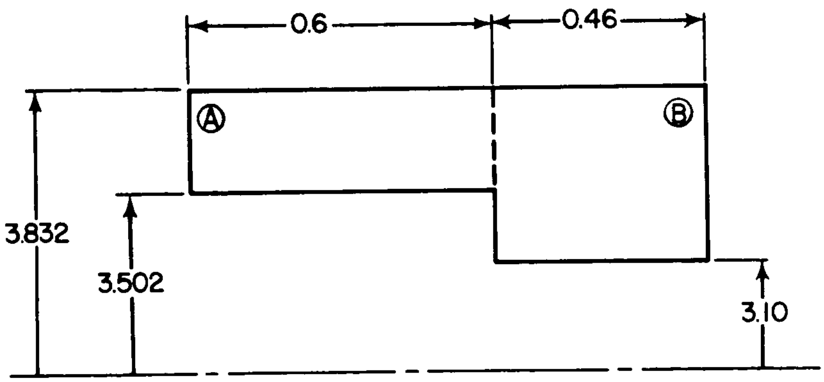

wt. of A = $.065\ \pi(3.832^2 - 3.502^2)(.6) = .296$

wt. of B = $.065\ \pi(3.832^2 - 3.1^2)(.46) = \underline{.476}$

total carbon seal weight = .772 lb.

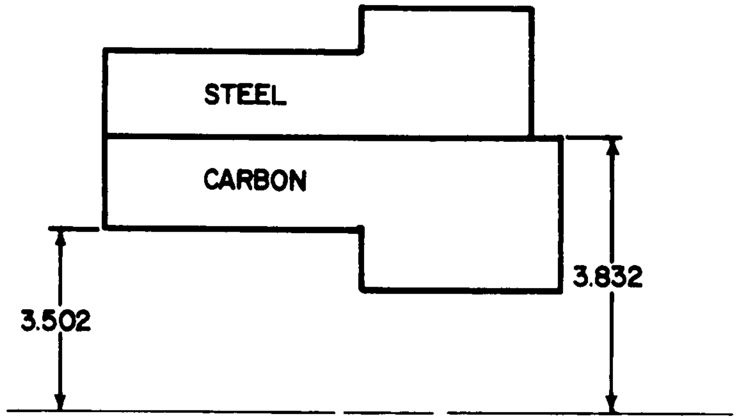

Total weight of steel and carbon:

$$\begin{aligned} \text{steel weight} &== 2.71 \text{ lb.} \\ \text{carbon weight} &= \underline{\ .77 \text{ lb.}} \\ & \quad\ 3.48 \text{ lb.} \end{aligned}$$

$$\text{wt./in. of circum.} = \frac{3.48 \text{ lb.}}{2\pi\,(3.502)} = .158 \text{ lb./in.}$$

At the condition of $\Delta P = 300$ psi, the velocity is 500 ft/sec. Consequently,

$$\text{Speed} = \left(500 \frac{\cancel{ft}}{\cancel{sec}}\right)\left(60 \frac{\cancel{sec}}{\cancel{min}}\right)\left(\frac{1 \text{ rev.}}{2\pi\ 3.502\ \cancel{in}}\right)\left(12 \frac{\cancel{in}}{\cancel{ft}}\right) = 16,371.1 \text{ rpm.}$$

$$\omega = 16,371 \times 2\pi/60 = 1712 \text{ rad sec}^{-1}$$

$$\omega^2 = 2.93 \times 10^6 \text{ rad sec}^{-2}$$

Assume:

1. runout $= 6. \times 10^{-4}$ in. T.I.R.
2. simple harmonic motion: $x = \sin \omega t \rightarrow \ddot{x} = -\omega^2 \cancel{\sin}^{\,x}\ \omega t$
   where x = axial displacement
   x_{max} = 1/2 runout

Then,

$$G = \frac{\omega^2 x_{max}}{g_c} = \frac{2.93 \times 10^6\ (3 \times 10^{-4})}{3.86 \times 10^2} = 2.28 \quad \text{(dimensionless)}$$

Table of Resulting Inertial Loads:

Cond. - ΔP, psi	Vel., ft/sec.	Vel. ratio	$(\text{Vel. ratio})^2$	G	F_I, equiv. face force, lb/in.
100	200	2/5	4/25	.3646	.0576
calc.	332			1.	.158
200	400	4/5	16/25	1.458	.230
300	500	1	1	2.28	.36

where $F_I = .158 \times G$

where vel. ratio = vel./500

2.1.3.1.2 Frictional Force on Piston Rings

Dimensions Used :

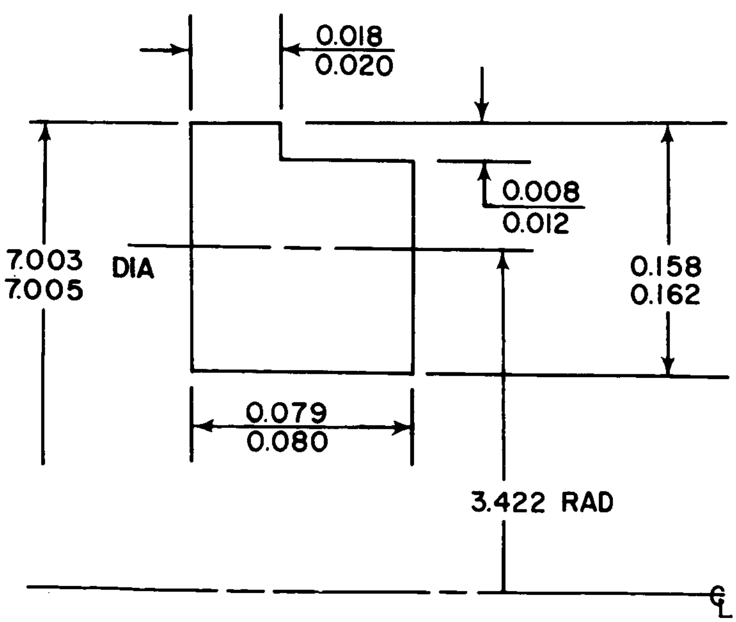

Free Body Diagram :

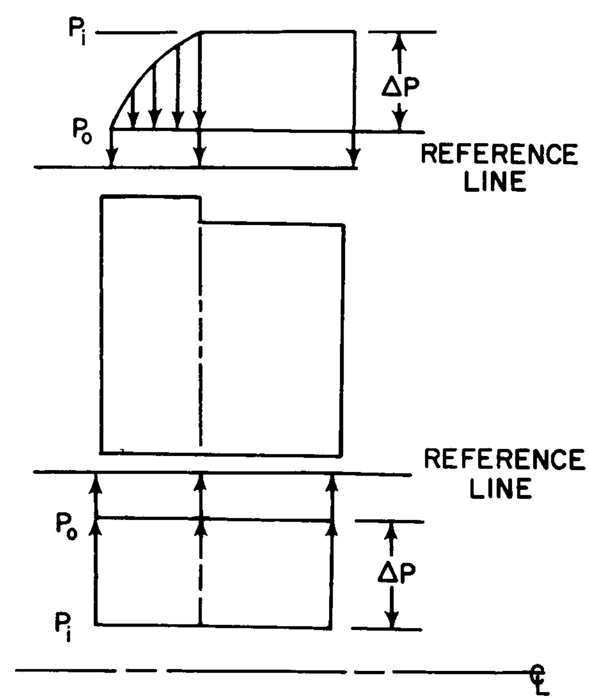

Major Definitions:

F_{rp} = Force per circumferential inch on piston ring in radial direction due to ΔP. $= \Delta P[1 - k](.019)$

F_{rs} = Force per circumferential inch on piston ring in radial direction due to its tendency to restore itself to its original shape

F_{rt} = Total force per circumferential inch on piston ring in radial direction. $(F_{rt} = F_{rp} + F_{rs})$

F_{pr} = Force on piston ring in axial direction due to friction.

Note: F_{rs} = .15 lbf/in. of circum. uniform mechanical loading dam width = 0.019"

C_f = .2 = coefficient of friction

P_o = 14.7 psia = outlet pressure

k = pressure profile modification constant = fraction of ΔP that is considered to act over dam area = f (r, geometry)

Table of Piston Ring Loads:

P_i, psia	ΔP, psi	$r = P_o/P_i$	K	1 - K	F_{rp}, lb/in	$F_{rt} = F_{rp} + F_{rs}$	$F_{pr} = F_{rt} \times C_f$
114.7	100	0.1282	.629	.371	0.705	0.85	0.1710
214.7	200	0.0684	.646	.354	1.344	1.494	0.2988
314.7	300	0.0467	.652	.348	1.98	2.13	0.426

Piston Ring Design

1. Large Piston Ring

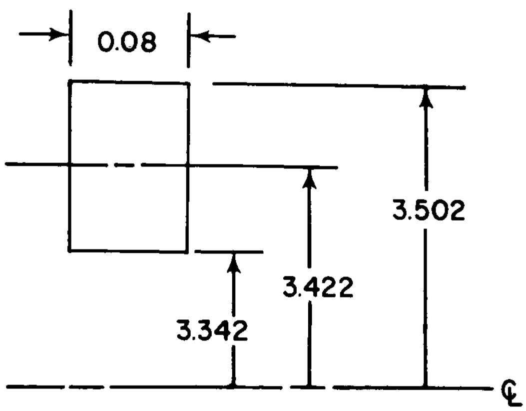

$$I = \frac{1}{12}(.08)(.16)^3 = 2.73 \times 10^{-5} \text{ in}^4$$

$$\text{Gap Closure} = \frac{9.43\, F_{rs} R_m^4}{EI}$$

$$\text{Gap Closure} = \frac{9.43\,(.15)(3.422)^4}{30 \times 10^6 \times 2.73 \times 10^{-5}}$$

where:

$F_{rs} = .15 \dfrac{\text{lbf}}{\text{in. of circum.}}$

R_m = mean radius

E = mod. of elast.

I = moment of inertia

Gap Closure = distance ring must be closed to produce radial restoring force, F_{rs}.

Gap Closure = .2368 in (A) .2401 in (B)

$$\sigma_{pr} = \frac{d\,(E)(\text{gap closure})}{9.43\ Rm^2}$$

$$\sigma_{pr} = \frac{(.16)\ 30 \times 10^6\ (.2368)}{9.43\ (3.422)^2}$$

$$\sigma_{pr} = 10{,}200\ \text{psi.}\ \ (A)\ \ 10{,}359\ \text{psi}\ \ (B)$$

where:

σ_{pr} = stress in piston ring due to closing it a distance of (gap closure) inches.

d = radial wall thickness of ring.

2. Small Piston Ring (design B only)

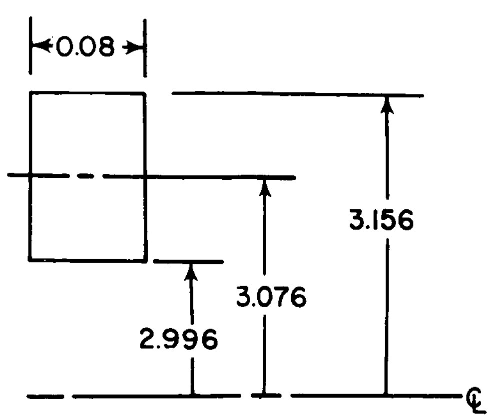

$$I = \frac{1}{12} bh^3 = \frac{1}{12} (.08)(.16)^3 = 2.73 \times 10^{-5} \text{ in}^4$$

$$\text{Gap Closure} = \frac{9.43 (F_{rs}) R_m^4}{EI}$$

$$\text{Gap Closure} = \frac{9.43 (.15)(3.076)^4}{(30 \times 10^6)(2.73 \times 10^{-5})} = .1546 \text{ in}$$

$$I = \frac{d (E) (\text{Gap closure})}{9.43 \; R_m^2}$$

$$\sigma_{pr} = \frac{(.16)(30 \times 10^6)(.1546)}{9.43 \; (3.076)^2} = 8304. \text{ psi}$$

Required Total Loadings (Summary)

Cond. - ΔP, psi	Vel., ft/sec.	F_I	F_{pr}	$F_T = F_I + F_{pr}$	$F_T/0.85$
100	200	.158	.171	.329	.388
200	400	.230	.2988	.5288	.621
300	500	.36	.426	.786	.925

The inertial forces are dependent only upon the rubbing velocity, not on pressure. Since one is interested in $G \geq 1.0$, at the condition of $\Delta P = 100$ psi (vel = 200 ft/sec) F_I will be set equal to $F_I = .158$ (where $G = 1.0$). The same reasoning applies for the bellows secondary face seals.

The factor of 0.85 shown above is a safety factor to overcome the locking-pin friction. The value is based on past experience.

2.1.3.1.3 Geometry Assurance Check (Deflection analysis)

It is required that the center of gravity (C_g) of steel and carbon have the same axial (x) location. Also that $C_p \geq C_g$ so that $\Theta_{fs} \geq \Theta_{col}$.

1. C_g of carbon:

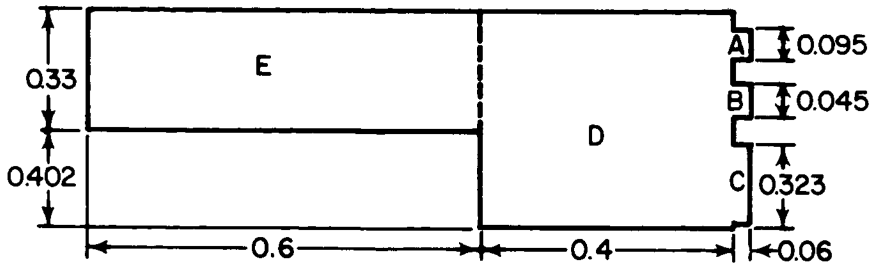

				(Area)	x	$(\bar{x}/2 + \ell)$		
Member	A:	(.060)(.095)	=	.0057	x	(.03)	=	.00017
	B:	(.060)(.045)	=	.0027	x	(.03)	=	.00008
	C:	(.060)(.323)	=	.0193	x	(.03)	=	.00057
	D:	(.40) (.732)	=	.2928	x	(.26)	=	.07612
	E:	(.60) (.33)	=	.1980	x	(.76)	=	.15048
		total area	=	.5185				.22742

$$\therefore \; C_g)_{carbon} = \frac{.22742}{.5185} = .4386\,(A) \qquad .521\,(B)$$

2. Let $C_g)_{steel} = C_g)_{carbon}$

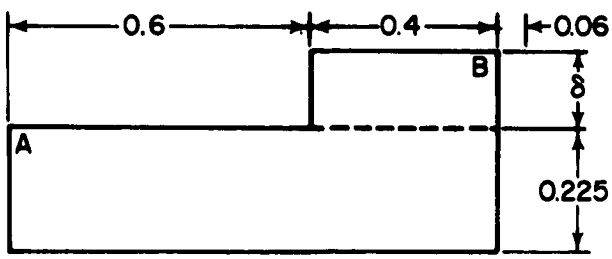

Member	A:	(1.0) (.225)	=	.225	x	(.56)	=	.126
	B:	(.40) δ	=	$.4\,\delta$	x	(.26)	=	$.104\delta$
				$.4\delta + .225$				$.104\,\delta + .126$

If $C_g)_{steel} = C_g)_{carbon}$, then

$$\frac{.104\,\delta + .126}{.4\,\delta + .225} = .4386$$

$$.104\,\delta + .126 = .4386\,(.4\,\delta + .225)$$

$$\delta = .386 \text{ (A)} \qquad .523 \text{ (B)}$$

3. Solving for Θ:

For simplification use only steel since its "E" is so much higher than carbon's.

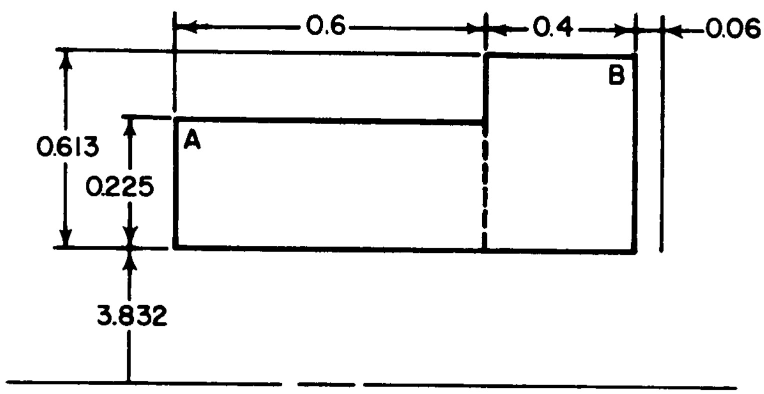

x-direction:

Member	A:	(.6)	(.225)	=	.135	x	(.76)	=	.1026
	B:	(.4)	(.613)	=	.245	x	(.26)	=	.0637
					.380				.1663

$$C_g)_x = \frac{.1663}{.38} = .438$$

Y-direction:

Member	A:	(.6)	(.225)	=	.135	x	(.113)	=	.0153
	B:	(.4)	(.613)	=	.245	x	(.306)	=	.0750
					.380				.0903

$$C_g)_y = \frac{.0903}{.38} = .238$$

$$R_m = 3.832 + .238 = 4.070''$$

Assumed:

1. Plane areas in calculating I

2. Mass conversion has been eliminated for simplification.

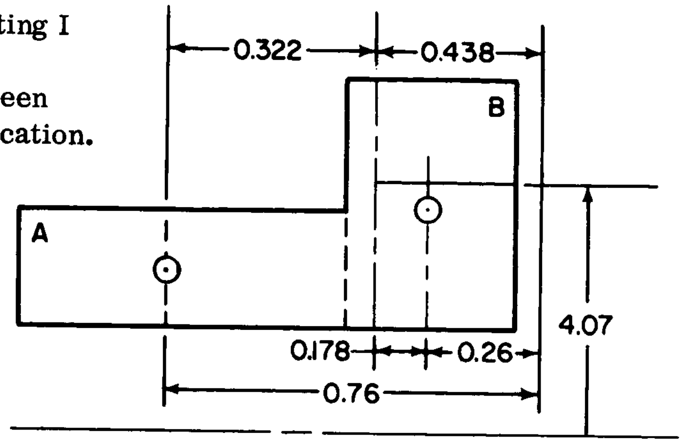

$$I = \frac{bh^3}{12} + A\ell^2$$

Member A: $1/12\,(.225)(.6)^3 + .245\,(.178)^2 = .01181$

B: $1/12\,(.613)(.4)^3 + .135\,(.322)^2 = \underline{.01725}$

$I = .02906\ in^4$

$F_r = \Delta P \ell$ where $\ell \equiv$ distance from face of collar to land face of piston ring

$= 300\ (0.9) = 270$ lb/in. of circ.

$M = F_r\left(\frac{0.9}{2} - .438\right) = 270\ (.012) = 3.24$ lb-in/in. of circ.

$$\theta = \frac{MR^2}{EI} = \frac{(3.24)(4.07)^2}{30 \times 10^6 \times .029} = 61.9 \times 10^{-6}$$

For shrinkage, allow

$\delta_{min} = 18 \times 10^{-3}$ (radial)

$\delta_{max} = 20 \times 10^{-3}$ (radial)

$A_{carbon} = .5186\ in^2$

$A_{steel} = .3802\ in^2$

$$F_{max} = \frac{\delta}{R^2} \times \frac{EA)_{steel} \cdot EA)_{carbon}}{EA)_{steel} + EC)_{carbon}}$$

$$= \frac{20 \times 10^{-3}}{(3.832)^2} \times \frac{30 \times 10^6 \times .3802 \cdot 3 \times 10^6 \times .5186}{30 \times 10^6 \times .3802 + 3 \times 10^6 \times .5186} = 1859 \text{ lb/in.}$$

$$T = F_{max} \times R$$
$$= 1859 \times 3.832 = 7123.68 \text{ lbs.}$$

$$\sigma_{steel} \doteq \frac{T}{A} = \frac{7123.68}{.3802} = 18736.66 \text{ psi.}$$

$$\sigma_{carbon} = \frac{7123.68}{.5186} = 13736.36 \text{ psi}$$

2.1.3.1.4 Collars (Seal Plate Deflection Analysis)

Forces stated in this development are those present during 300 psi condition when the seal is operated with a self-energized face.

Collar, Solid; usage - film riding seals

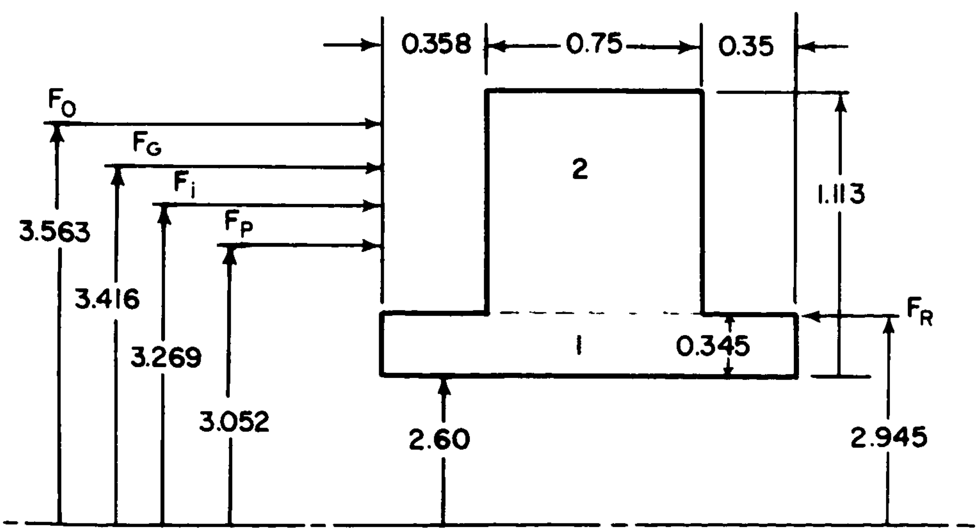

	Area, A	Mean Radius, R	Moment = A x R
Member 1:	(.345) (1.458) = .503	x 2.7725 =	1.394
2:	(.75) (.768) = .576	x 3.329 =	1.92
	1.079		3.314

$$C_g = \frac{3.314}{1.079} = 3.07$$

Location of C_g from side -

	Area, A	Length	Moment = A x L
Member 1:	(.345 (1.458) = .503	x .729 =	.366
2:	(.75) (.768) = .576	x .725 =	.418
	1.079		.784

$$C_g = \frac{.784}{1.079} = .726$$

$$I = \frac{1}{12} (.345)(1.458)^3 + (.345)(1.458)(.726 - .729)^2$$

$$+ \frac{1}{12} (.768)(.75)^3 + (.75)(.768)(.726 - .725)^2 = .1162$$

$\underbrace{\text{Assume these values do not change}}$		Force, F - lb/in	x	R	=	Monent
F_p = 1315 lb. / 2 π (3.07)	=	68.2	x	3.052	=	- 208.
F_i = 1115 lb. / 2 π (3.07)	=	57.9	x	3.269	=	- 189.2
F_G = 490 lb. / 2 π (3.07)	=	25.4	x	3.416	=	- 86.6
F_o = 544 lb. / 2 π (3.07)	=	28.2	x	3.563	=	- 100.6
F_R = 3464 lb. / 2 π (3.07)	=	179.9	x	2.945	=	+ 530.
						- 54.4

where $F_x = (300)\, w \lambda$

$F_R = F_o + F_G + F_i + F_p$

Moment due to pressure:

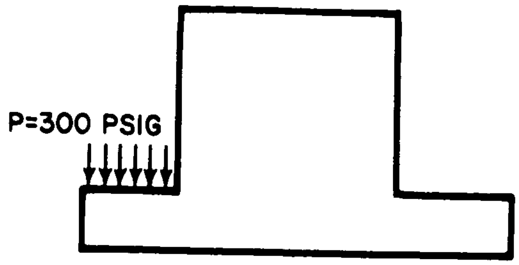

Force per unit length of circ. at R = 3.07

$$\frac{300\ (.358)\ (2.7725)}{3.07} = 97 \text{ lb/in.}$$

This force acts at 0.726 - .358 = 0.368" from the C_g

Moment due to pressure,

$$M_p = 97 \times .368 = 35.7 \text{ lb-in/in.}$$

$$\therefore \text{ the net moment} = M_p + \Sigma M$$

$$= 35.7 - 54.4 = -18.7$$

$$\theta = \frac{-18.7\ (3.07)^2}{30 \times 10^6 \times .1162} = -50.5 \times 10^{-6}$$

Weight of collar,

$$W = \frac{\pi}{4}\ (.278)\ \left[(5.890^2 - 5.2^2)\ (1.458) + (7.426^2 - 5.890^2)\ (.75)\right]$$

$= 5.72$ lb. where sp. wt. of steel $= 0.278 \text{ lb/in}^3$

Weight per inch of circum. at r = 3.07,

$$= 5.72/\pi\, 6.14 = .296 \text{ lb/in.}$$

$$\text{Centrifugal force} = 28.416 \times 10^{-6}\ W R_m\ n^2$$

$$= 28.416 \times 10^{-6}\ (.296)\ (3.07)\ (267 \times 10^6) = 6891.2$$

Deflection due to centrifugal force,

$$E\ \delta_{cf} = \frac{a^2\ (6891.2)\ (3.07)}{(b^2 - a^2)\ (1.458)\ (2.6)\ (3.07)} \left[(1 - \nu)\ 3.07^2 + (1 + \nu)\ b^2\right]$$

where $a^2 = (2.6)^2 = 6.76$

$b^2 = (3.7113)^2 = 13.786$

$\nu = .29 =$ Poisson's ratio

$$E\ \delta_{cf} = 42,834.3$$

Deflection due to pressure,

$$E\ \delta_{cp} = \frac{-b^2\ (97.)\ (2.7725)}{(b^2 - a^2)(1.458)\ (2.945)\ (3.07)} \left[(1 - .29)\ (3.07)^2 + (1.29)\ (6.76)\right] = -616.61$$

$$\therefore E\ \delta_{cg} = E\ \delta_{cf} + E\ \delta_p$$
$$= 42,217.69$$

Deflection at the end Y -

$$E\ \delta_Y = E\ \delta_{cg} + C_g \times E\Theta$$
$$= 42,217.7 + (.726)\ (30 \times 10^6)\ (-50.5 \times 10^{-6})$$
$$= 41,117.8$$

$$\delta_Y = 41,117.8/30 \times 10^6 = 1370.59 \times 10^{-6}$$

$$\epsilon = \frac{1370.59 \times 10^{-6}}{2.7725} = .494 \times 10^{-3} \text{ in/in.}$$

$$\sigma = E\epsilon = 30 \times 10^6 \times .494 \times 10^{-3} = 14,830.5 \text{ psi}$$

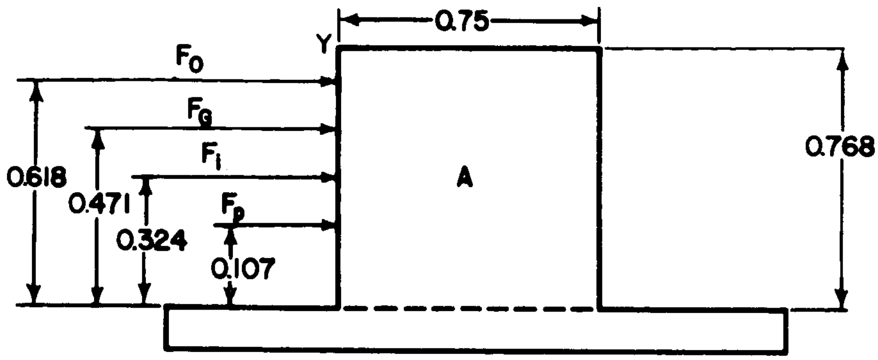

Consider part A to be a cantilever beam fixed at the dashed line as shown, with unit width

$$I = \frac{1}{12} (.768)(.75)^3 = .0269$$

$$F_p = 300 \text{ psi } (.228) \times 1'' = 68.4 \text{ lb/in.}$$

$$F_i = \left(243 + \frac{300 - 243}{2}\right)(.200) = 54.3 \text{ lb/in.}$$

$$F_G = 243 (.094) \times 1 = 22.84 \text{ lb/in.}$$

$$F_o = \frac{243}{2} (.200) = 24.3 \text{ lb/in}$$

Deflection due to force F_p at Y

$$E\,\delta_p = -\frac{1}{6} \frac{F_p}{I} \left[3 (.107)^2 (.768) - (.107)^3\right]$$
$$= -11.66$$

Deflection due to force F_i at Y

$$E\,\delta_i = -\frac{1}{6} \frac{F_i}{I} \left[3 (.324)^2 (.768) - (.324)^3\right]$$
$$= -69.87$$

Deflection due to F_G at Y

$$E\,\delta_G = -\frac{1}{6} \frac{F_G}{I} \left[3 (.471)^2 (.768) - (.471)^3\right]$$
$$= -57.53$$

Deflection due to F_o at Y

$$E\,\delta_o = -\frac{1}{6} \frac{F_o}{I} \left[3 (.618)^2 (.768) - (.618)^3\right]$$
$$= -96.92$$

Total deflection,

$$E\,\delta = E\,\delta_p + E\,\delta_i + E\,\delta_G + E\,\delta_o$$
$$= -\ 235.98$$
$$\delta = -\ 235.98/30 \times 10^6 = -\ 7.866 \times 10^{-6}$$

(All deflection equations taken from Timoshenko)

2.1.3.1.5 Shroud, Windback (Stress Calculations) -

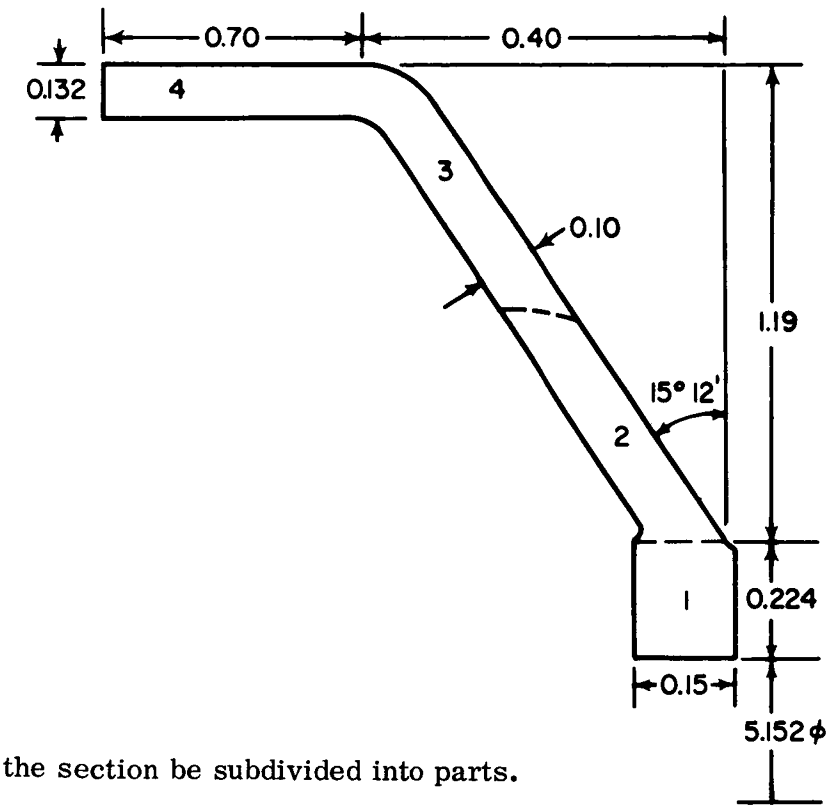

Let the section be subdivided into parts.

Part 1:

$$\text{Volume of ring} = \frac{\pi}{4}\ (5.6^2 - 5.152^2)\ (.15) = .565\ \text{in}^3$$

$$\text{Weight of ring} = .278 \times .565 = .157\ \text{lb.}$$

$$\text{Centrifugal force, } F_1 = 28.416 \times 10^{-6}\ W_1\ R_{m1}\ n^2$$
$$= 28.416 \times 10^{-6}\ .157 \times 2.688\ n^2 = 12.\ \times 10^{-6}\ n^2$$

Part 2:

$$W_2 = \frac{\pi}{4} (6.658^2 - 5.6^2) (.10) (.278) = .2827 \text{ lb.}$$

$$F_2 = 28.416 \times 10^{-6} W_2 R_{m2} n^2$$

$$= 28.416 \times 10^{-6} \times .2827 \times 3.0645 n^2 = 24.61 \times 10^{-6} n^2$$

Part 3:

$$W_3 = \frac{\pi}{4} (7.716^2 - 6.658^2) (.10) (.278) = .3319 \text{ lb.}$$

$$F_3 = 28.416 \times 10^{-6} W_3 R_{m3} n^2$$

$$= 28.416 \times 10^{-6} \times .3319 \times 3.5935 n^2 = 33.89 \times 10^{-6} n^2$$

Part 4:

$$W_4 = \frac{\pi}{4} (7.98^2 - 7.716^2) (.70) (.278) = .6335 \text{ lb.}$$

$$F_4 = 28.416 \times 10^{-6} \times .6335 \times 3.924 n^2 = 70.63 \times 10^{-6} n^2$$

Cond. $-\Delta P$, psi	n	$n^2 \times 10^{-6}$	F_1	F_2	F_3	F_4	ΣF
300	16,350	267.3	3223.6	6516.7	9061.5	18895	37,696.8
250	14,700	216.	2605.	5266.	7322.4	15269	30,462.4
200	13,100	171.6	2069.5	4183.6	5817.	12130	24,200.
100	6,550	42.9	517.4	1046.	1454.3	3032.6	6050.3

$$W = W_1 + W_2 + W_3 + W_4 = 1.405 \text{ lb.}$$

Max. total force = 37,700 lbs.

$$\frac{37,700}{5.376\pi} = 2235 \text{ lb/in}$$

$$\sigma = \frac{F}{A} = \frac{2235}{.1} = 22,350 \text{ psi.}$$

2.1.3.1.6 Compression Springs

Operation of the seal takes place primarily at 200 psi. At this condition $F_T/0.85$ = .621 lb/in., it is assumed that nearly half this force will be taken up by the spring. Consequently, 0.3 lb/in axial spring force will be required.

The total spring force = (0.3 lb/in) (2π 3.502) = 6.6 lb.
Force/spring = 6.6 lb/18 springs = 0.367 lb/spring
δ = 0.367/0.8 = 0.459 in.
Operating Length = 1.336 - .459 = .877 in.

Spring Design -
- Material - Inconel X
- Operating temp. - 900°F (heat treat accordingly)
- Ends to be ground flat & square
- Wire diameter - 0.03 in.
- Mean coil diameter - 0.450 in.
- Total coils - 18
- Active coils - 16
- Scale - 0.8 lb/in.
- Free length - 1.336 in.
- Normal operating length - .877 in.
- Load at operating length - .367 lb/spring
- Stress at operating length - 15,500 psi.

Note: 18 springs required per seal

Force variation (=.015)
Compressed: (.459 + .015) (.8) = .3785 x 18 = 6.813 / 2π 3.502 = .309 lb/in
Normal : .459 (.8) = .3665 x 18 = 6.597 / 2π 3.502 = .300 lb/in
Extended : (.459 - .015) (.8) = .3555 x 18 = 6.391 / 2π 3.502 = .291 lb/in

2.1.3.1.7 Leakage and Restoring Force -

The following is the procedure followed to give curves of face leakage and restoring force vs. face opening for various specified conditions of pressure and temperature (the development below is for seal B).

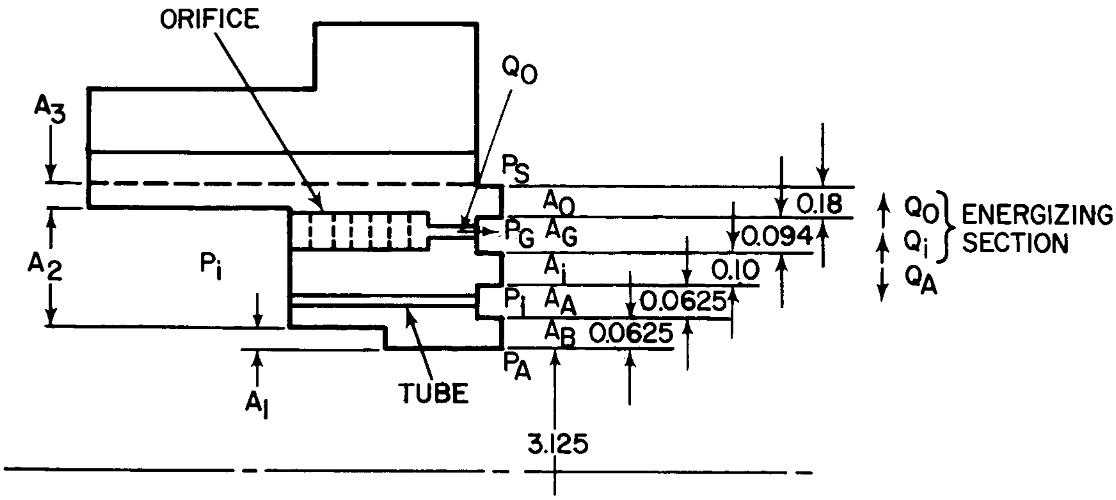

$$A_O = \pi\,(3.624^2 - 3.444^2) = 3.9947$$
$$A_G = \pi\,(3.444^2 - 3.350^2) = 2.0052$$
$$A_i = \pi\,(3.350^2 - 3.250^2) = 2.0724$$
$$A_A = \pi\,(3.250^2 - 3.1875^2) = 1.26353$$
$$A_B = \pi\,(3.1875^2 - 3.125^2) = 1.2390$$
$$A_1 = \pi\,(3.156^2 - 3.125^2) = .6114$$
$$A_2 = \pi\,(3.514^2 - 3.156^2) = 7.4980$$
$$A_3 = \pi\,(3.624^2 - 3.514^2) = 2.4655$$

Energizing Section-

Three orifice assemblies per face (equally-spaced); four orifice plates per assembly (in series); and well-rounded orifice (size - .0225" diameter).

Condition #1 (ref. Figure 1) -

Pressurizing gas pressure P_i = 335 psia, T_i = 300°F
Sump side pressure P_s = 15 psia, T_s = 500°F
Ambient side pressure P_A = 315 psia, T_A = 1300°F
μ = 240 micropoise

Q_{PIT} = leakage flow derived from mass flow (taken from a graph in Keenan) = 16.5 scfm/psia/in^2.

For continuity,

$$Q_{orifice} + Q_{inner\ dam} = Q_{total} = Q_{outer\ dam}$$

where:

$Q_{orifice} = 0.85\ P_i\ A_{orifice}\ \ Q_{PIT}\ K_r$ in scfm

0.85 = orifice coefficient

$A_{orifice}$ = area of orifice

$K_r = f\ (r) = f\ (P_o/P_i)$

$$^{*}Q_{inner\ dam} = 2\ \pi\ R_{m_i}\ \frac{h_o^{\ 3}}{24\mu L_i}\ \frac{(P_i^2 - P_G^2)}{P_{st}}\ \frac{T_{st}}{T}$$

T_{st}, P_{st} = temperature and pressure at standard conditions to convert to proper units

T = absolute operating temperature

$$^{*}Q_{outer\ dam} = 2\ \pi\ R_{m_o}\ \frac{h_o^{\ 3}}{24\mu L_o}\ \frac{(P_G^2 - P_S^2)}{P_{st}}\ \frac{T_{st}}{T}$$

$$5.604\ K_r + 4.0336 \times 10^{+6}\ h_o^{\ 3}\ (P_i^{\ 2} - P_G^{\ 2}) = 2.4 \times 10^{+6}\ h_o^{\ 3}\ (P_G^{\ 2} - P_S^{\ 2})$$

Substituting values of h_o, P_G can be solved.

$$F_{total} = F_o + F_G + F_i$$

where

$F_o = K_o\ A_o\ (P_G - P_o)$

$F_G = A_G\ (P_G - P_o)$

$F_i = K_i\ A_i\ (P_A - P_G)$

K_i, K_o = balancing moduli as discussed under the orifice compensated hydrostatic seal section

*Ref.: "Fluid Throttling Devices" by L. Dodge

$$Q = \pi \frac{d_m\ h_o^{\ 3}\ \Delta P}{12\mu L} \quad \text{(for annular clearance)}$$

Solving for K_o, K_i, and F_{tot}, the results are presented in Table 3.

TABLE 3

LEAKAGE AND RESTORING FORCE RESULTS

$h_o \times 10^{-4}$, in.	P_G, psia	K_o	K_i	F_{tot}, lb.
2	310	0.651	0.5065	1997.3
3	289	0.650	0.512	1874.43
4	275	0.6495	0.516	1798.9
5	271	0.6485	0.5175	1777.1
7	267.5	0.648	0.5185	1756.7

At equilibrium,

$$F_{seat} = F_{total} = F_{lift}$$
$$F_{lift} - F_{seat} = 0$$

At openings other than equilibrium,

$F_{restoring} = F_{lift} - F_{seat}$ where $F_{seat} = P_A A_A$
$F_{restoring}$ is plotted on Figure 5.

Q_{FL} = face leakage to sump = $2.4 \times 10^{+6} h_o^3 (P_G^2 - P_S^2)$. Substitute values of h_o and P_G calculated for face leakage. Face leakage to sump is then plotted in Figure 5.

Q_A = face leakage to ambient = $6.173 \times 10^{+6} h_o^3 (P_i^2 - P_A^2)$. Leakage to ambient side controlled by face opening. These results are plotted as a dotted line in Figure 5.

Results of calculations at other conditions are illustrated by Figures 6 through 8.

Following the same procedure discussed for seal (B), the following curves have been plotted for seal (A).

The curves plotted in Figure 9 are in error due to the value of P_A being (for condition 1, e.g.) 300 psia and not 14.7 + 300 = 314.7 psia. However, since hardware has been designed in reference to these curves, Figures 10 through 13 are submitted for the original geometry and corrected pressures for four specified conditions.

All subsequent hardware will be corrected for the proper pressure differentials. Curves showing trends for correct values of P_A are shown in Figures 14 through 17.

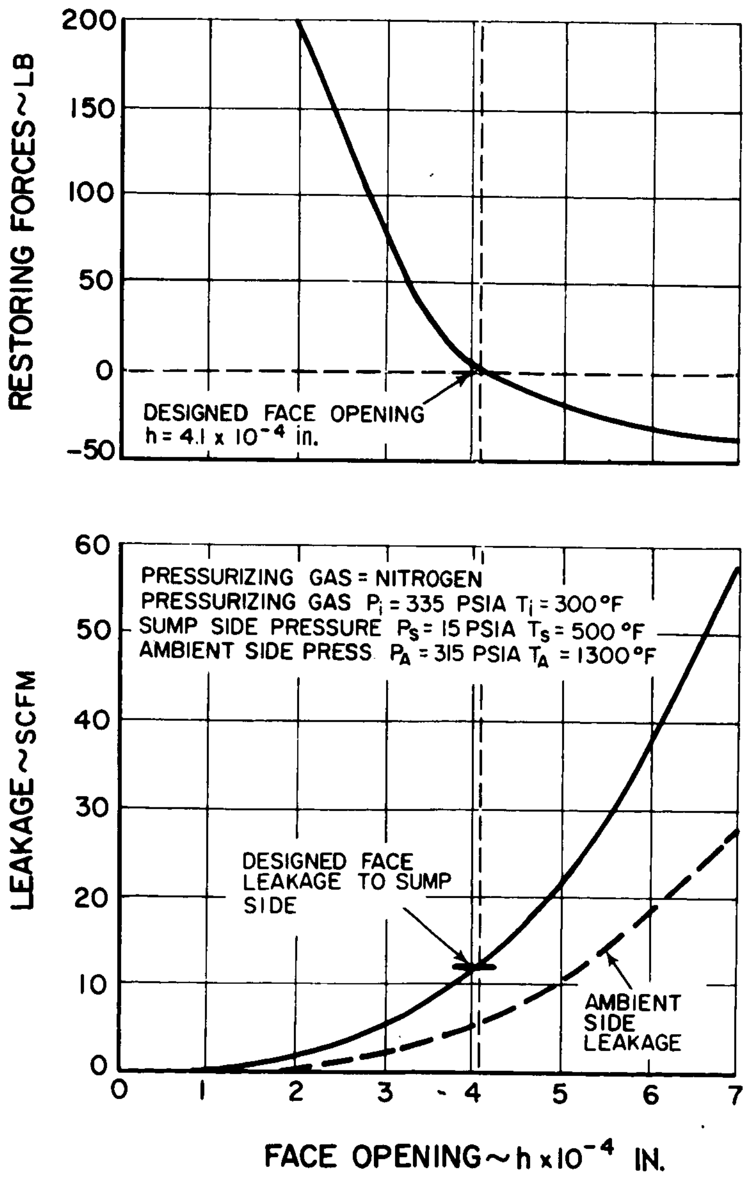

Figure 5 Seal B: Face Leakage to Sump (Pi = 335 psia.)

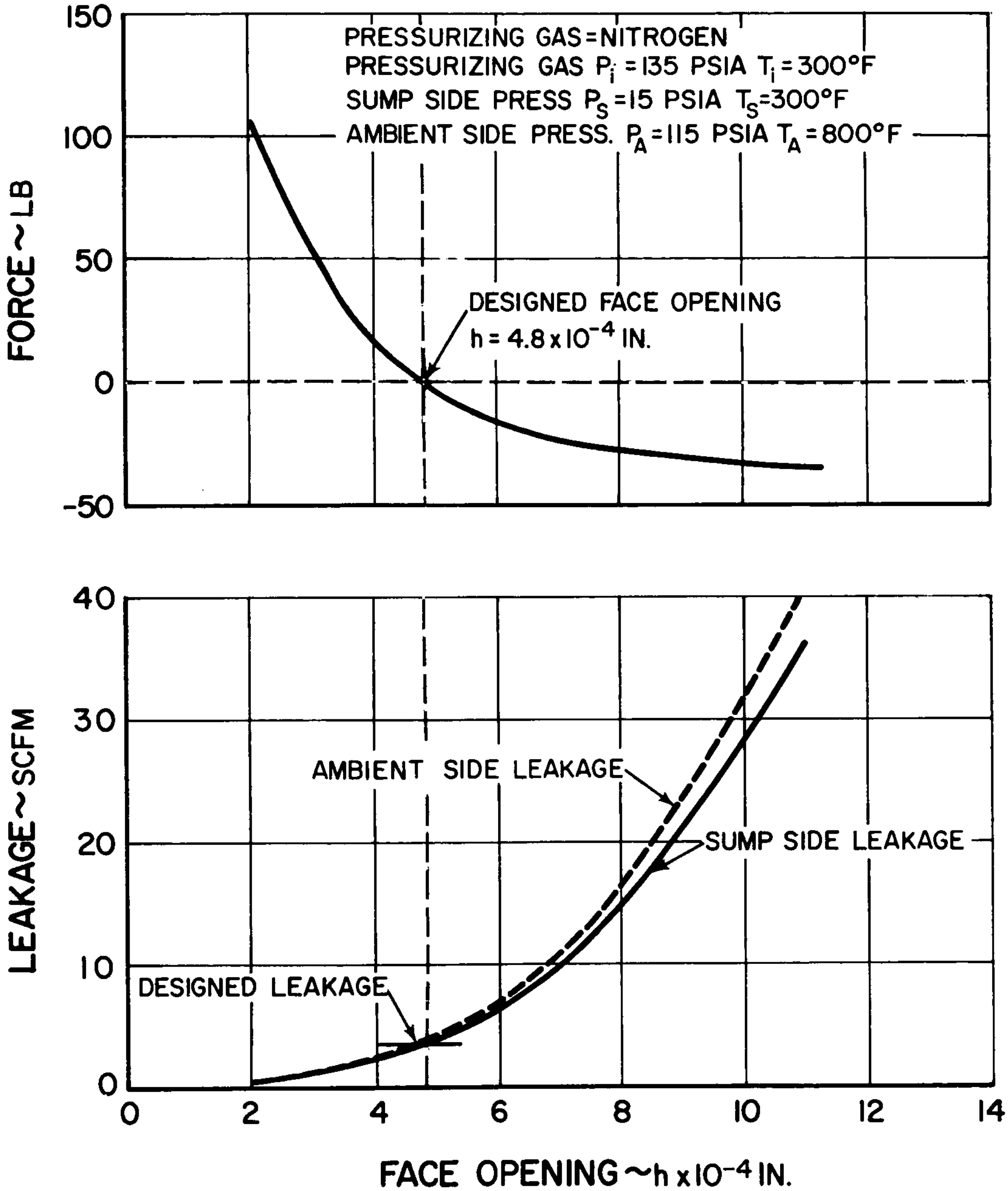

Figure 6 Seal B: Face Leakage to Sump (Pi = 135 psia)

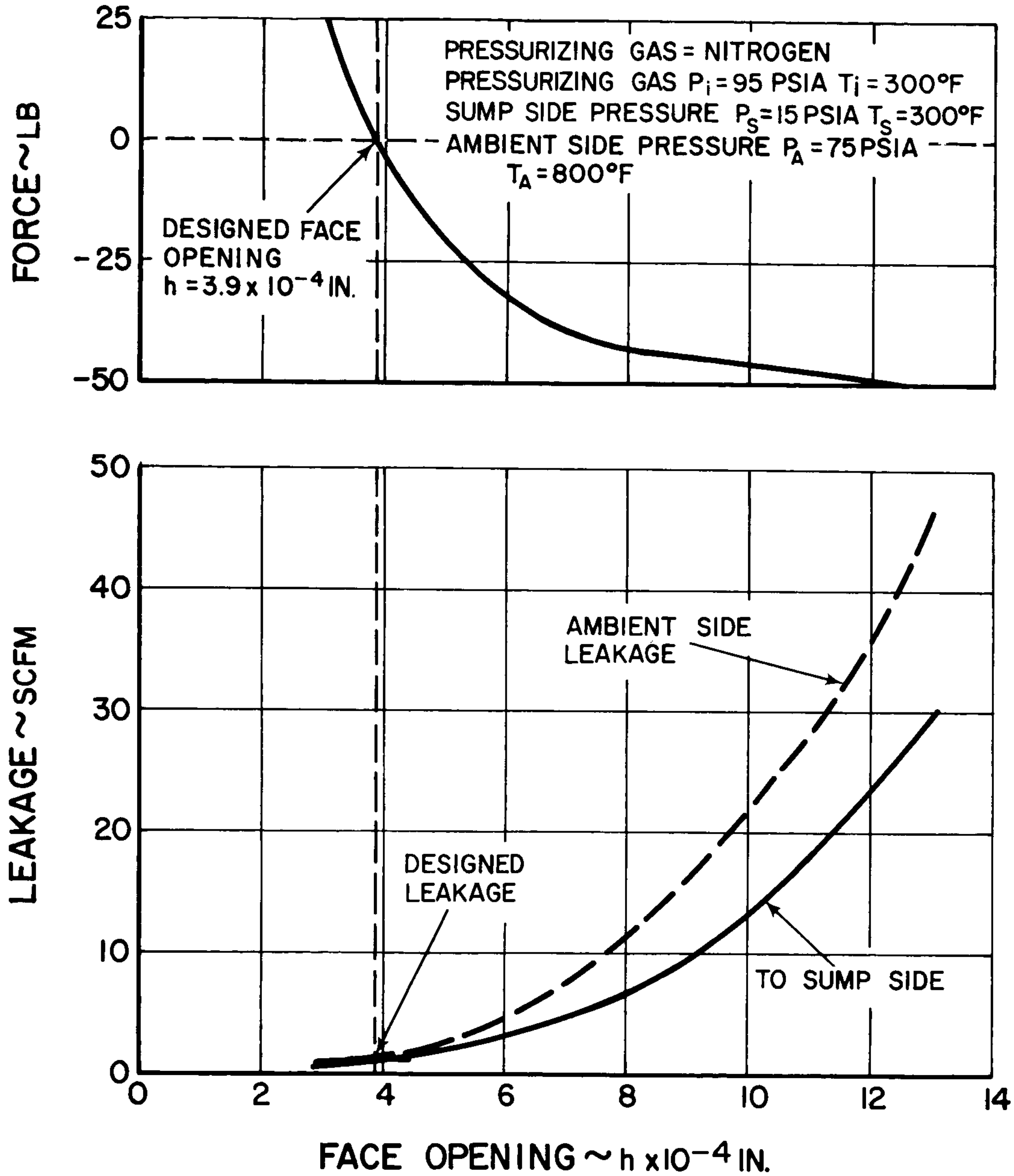

Figure 7 Seal B: Face Leakage to Sump (Pi = 95 psia)

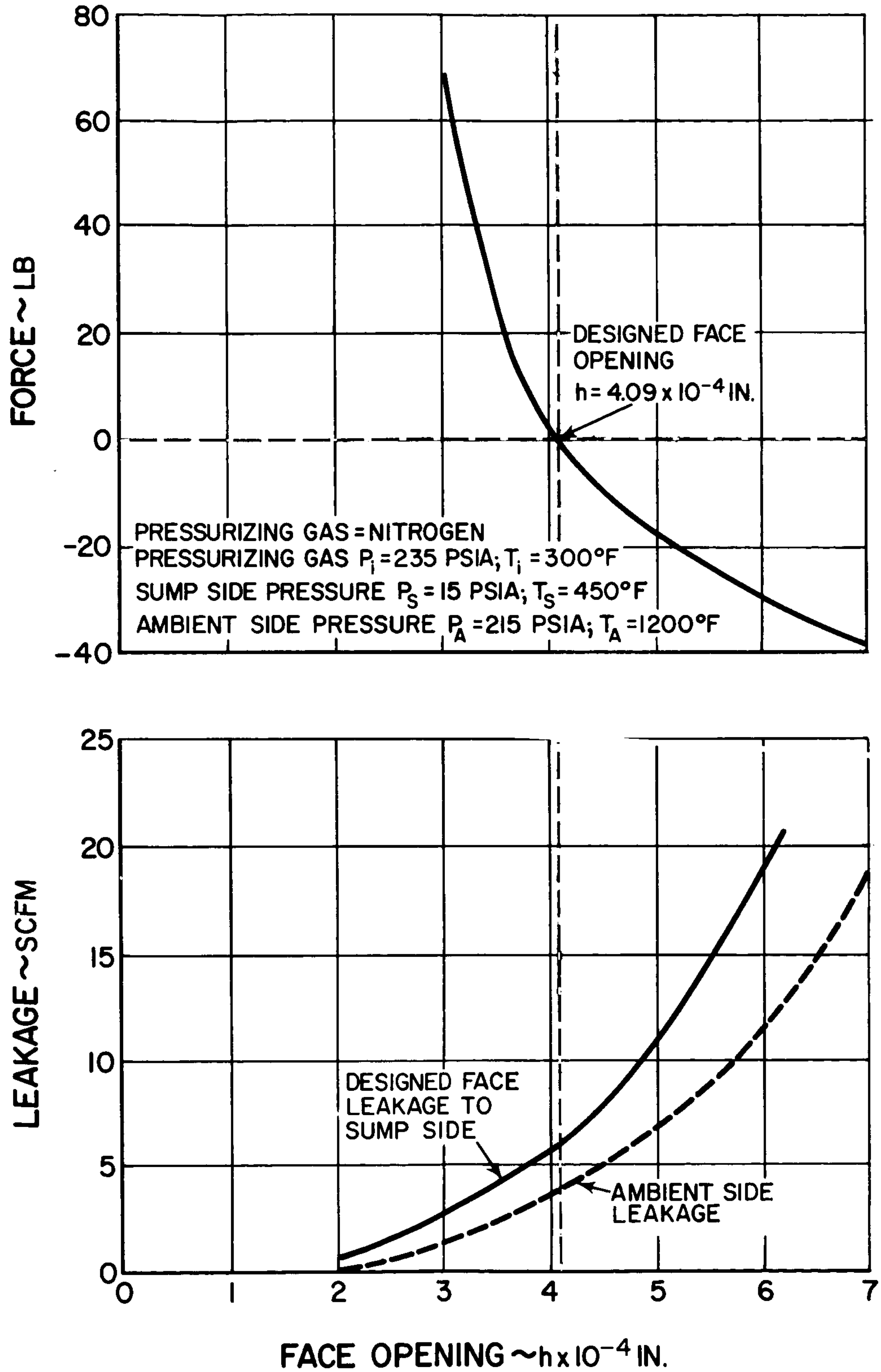

Figure 8 Seal B: Face Leakage to Sump (Pi = 235 psia)

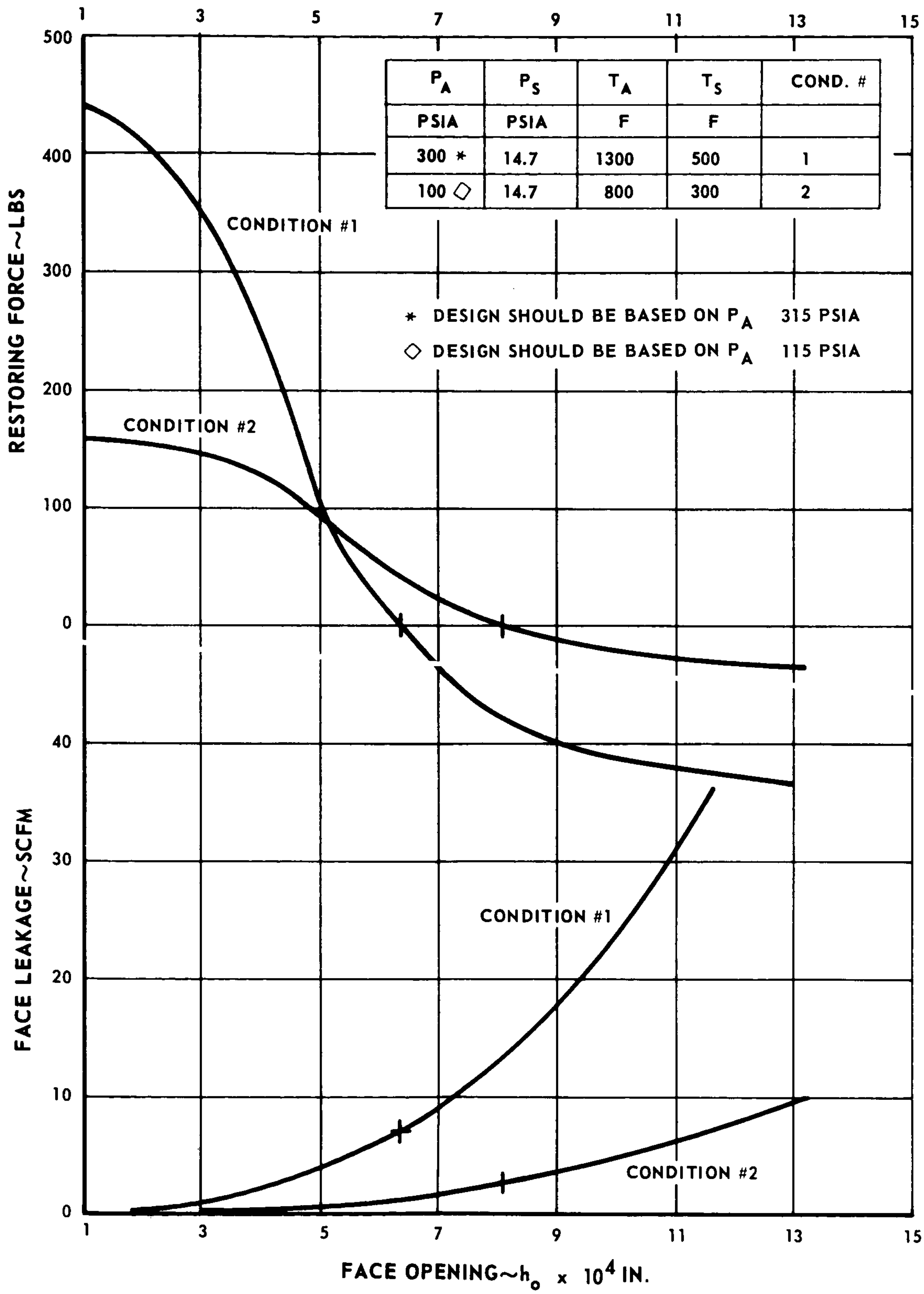

Figure 9 Seal A: Design Characteristics of Self-Energized Face Seal Curves in Error Due to Incorrect P_A Value (P_A = 300; 100 psia)

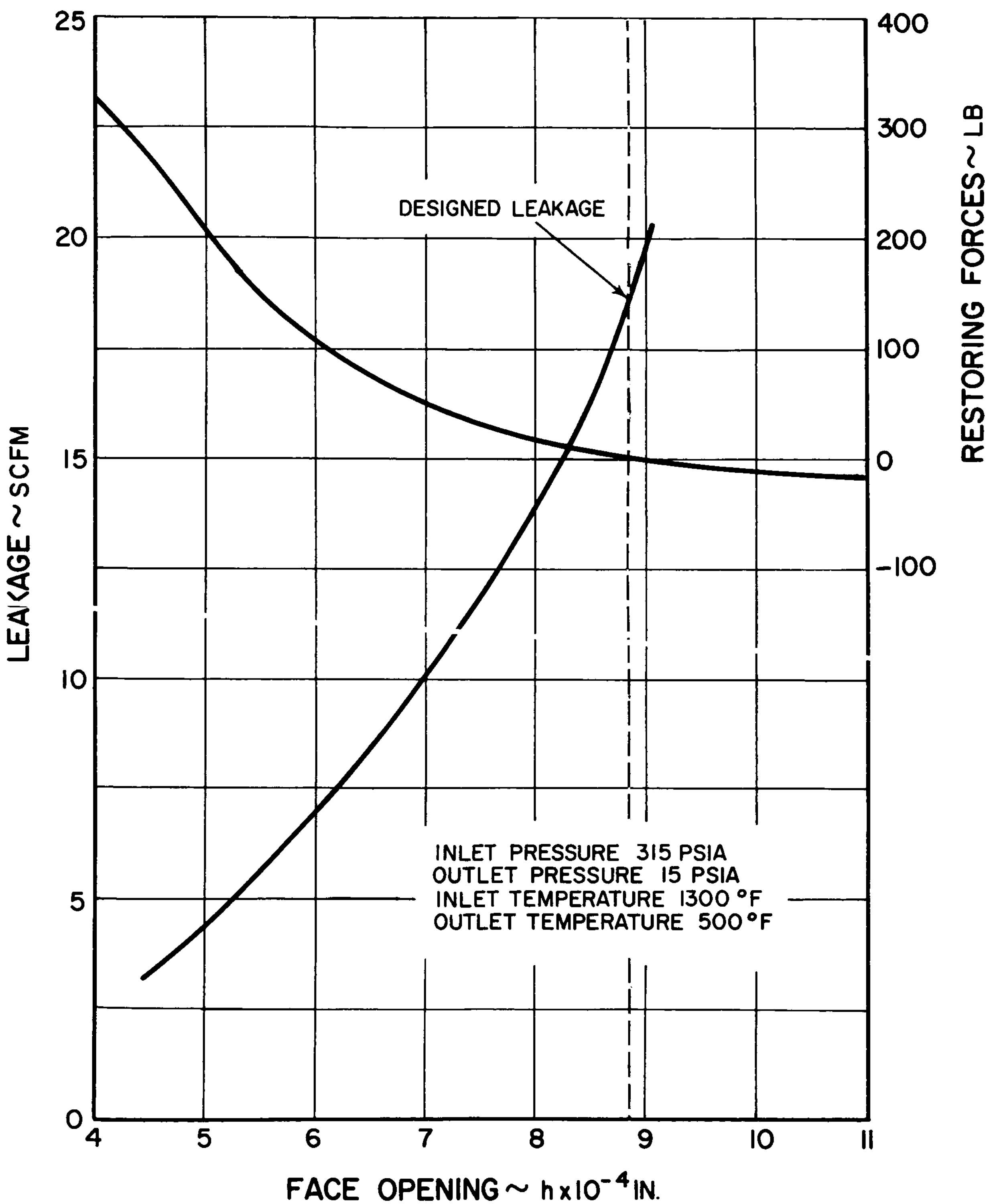

Figure 10 Seal A: Design Characteristics of Self-Energized Face Seal Seal Design Based on Fig. 9 (P_A = 315 psia)

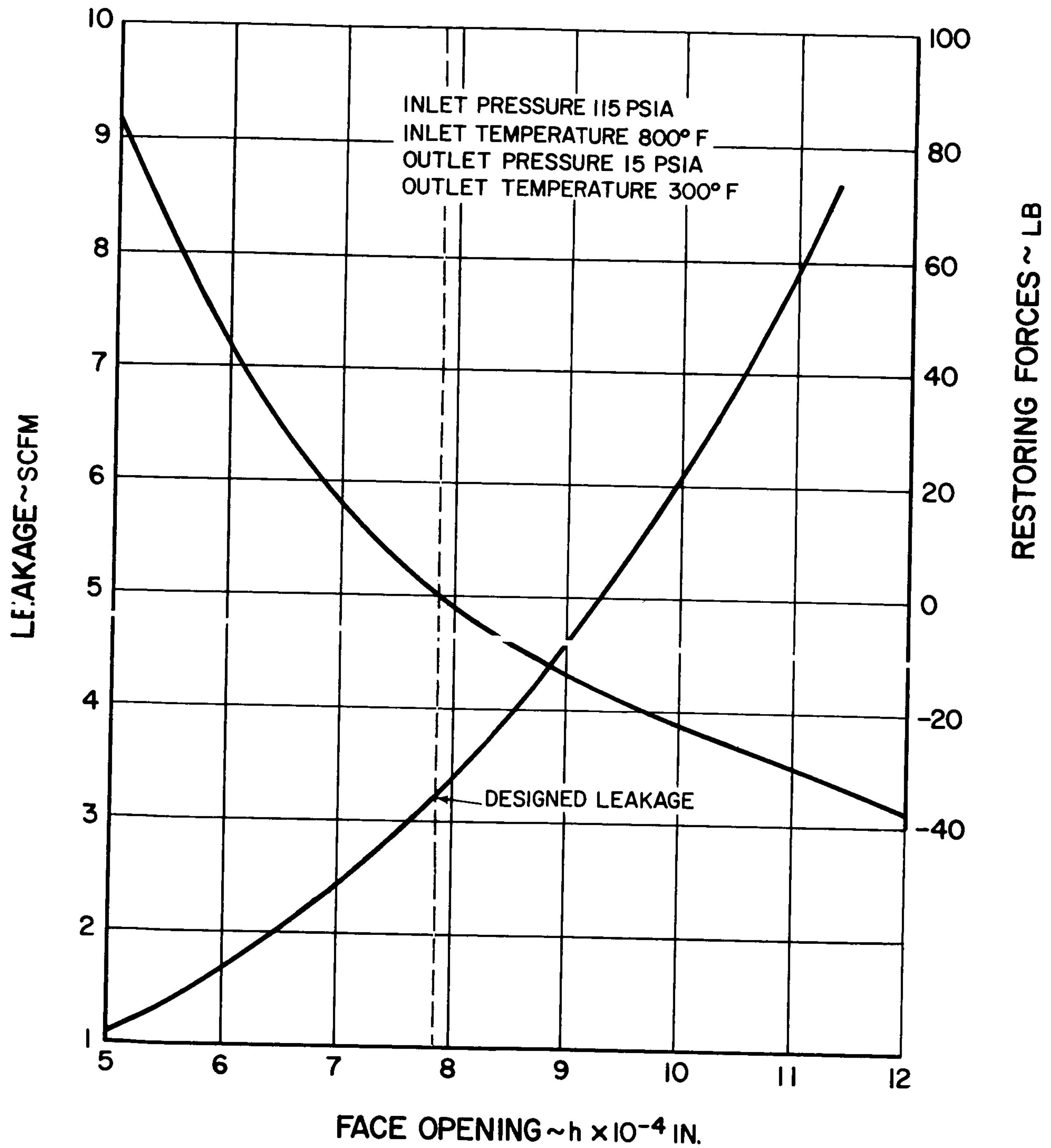

Figure 11 Seal A: Design Characteristics of Self-Energized Face Seal Seal Design Based on Fig. 9 (P_A = 115 psia)

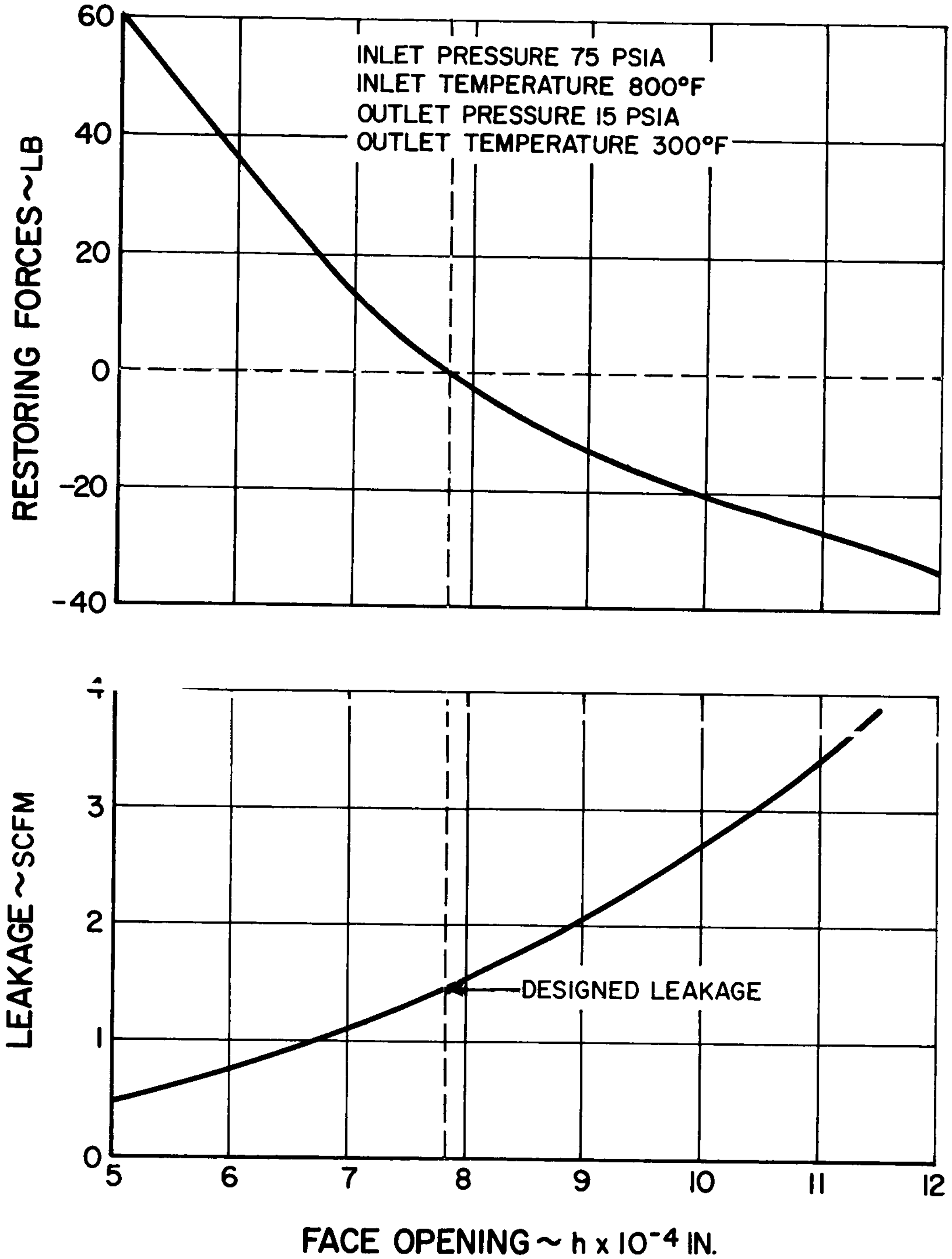

Figure 12 Seal A: Design Characteristics of Self-Energized Face Seal Seal Design Based on Fig. 9 (P_A = 75 psia)

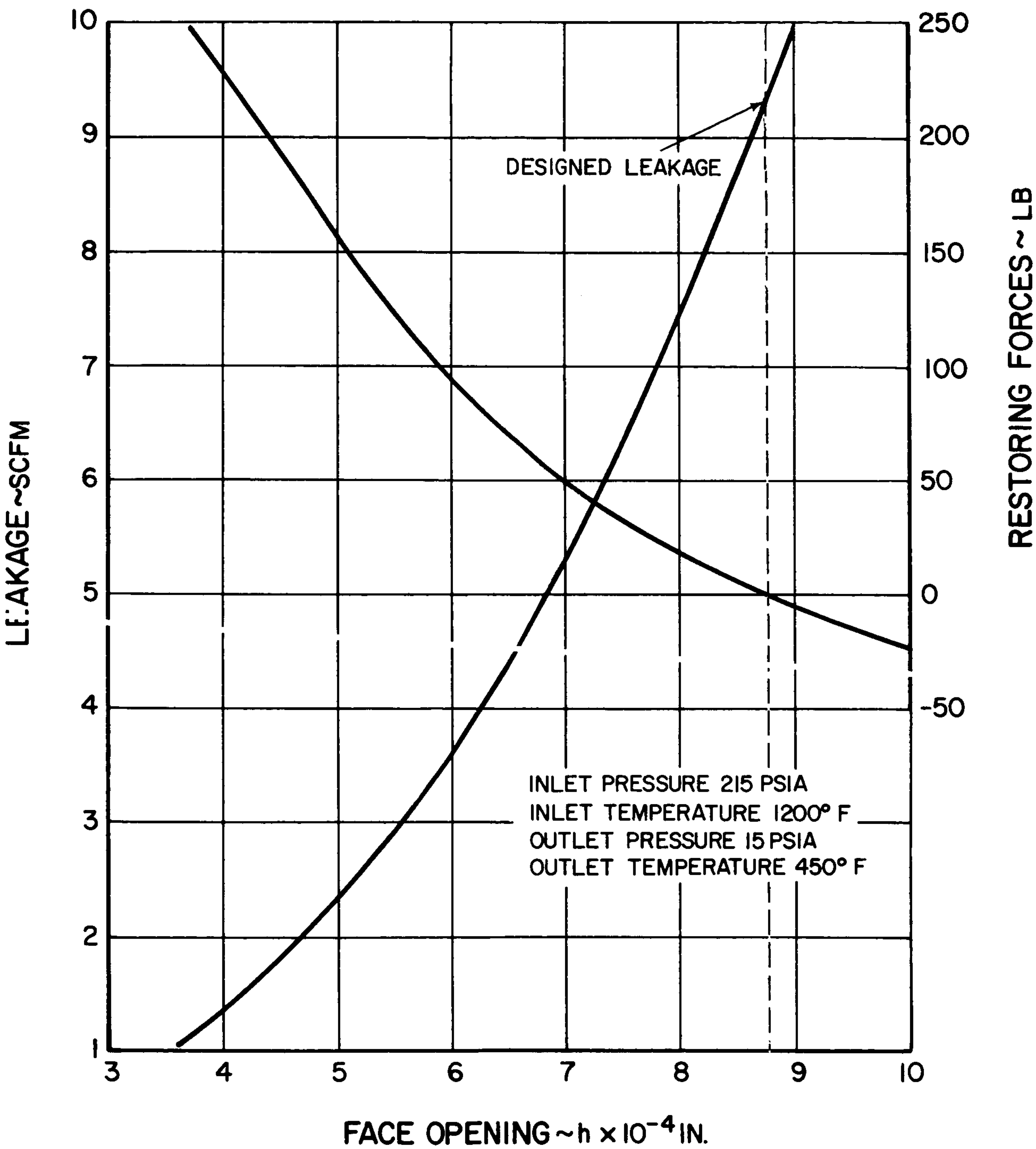

Figure 13 Seal A: Design Characteristics of Self-Energized Face Seal Seal Design Based on Fig. 9 (P_A = 215 psia.)

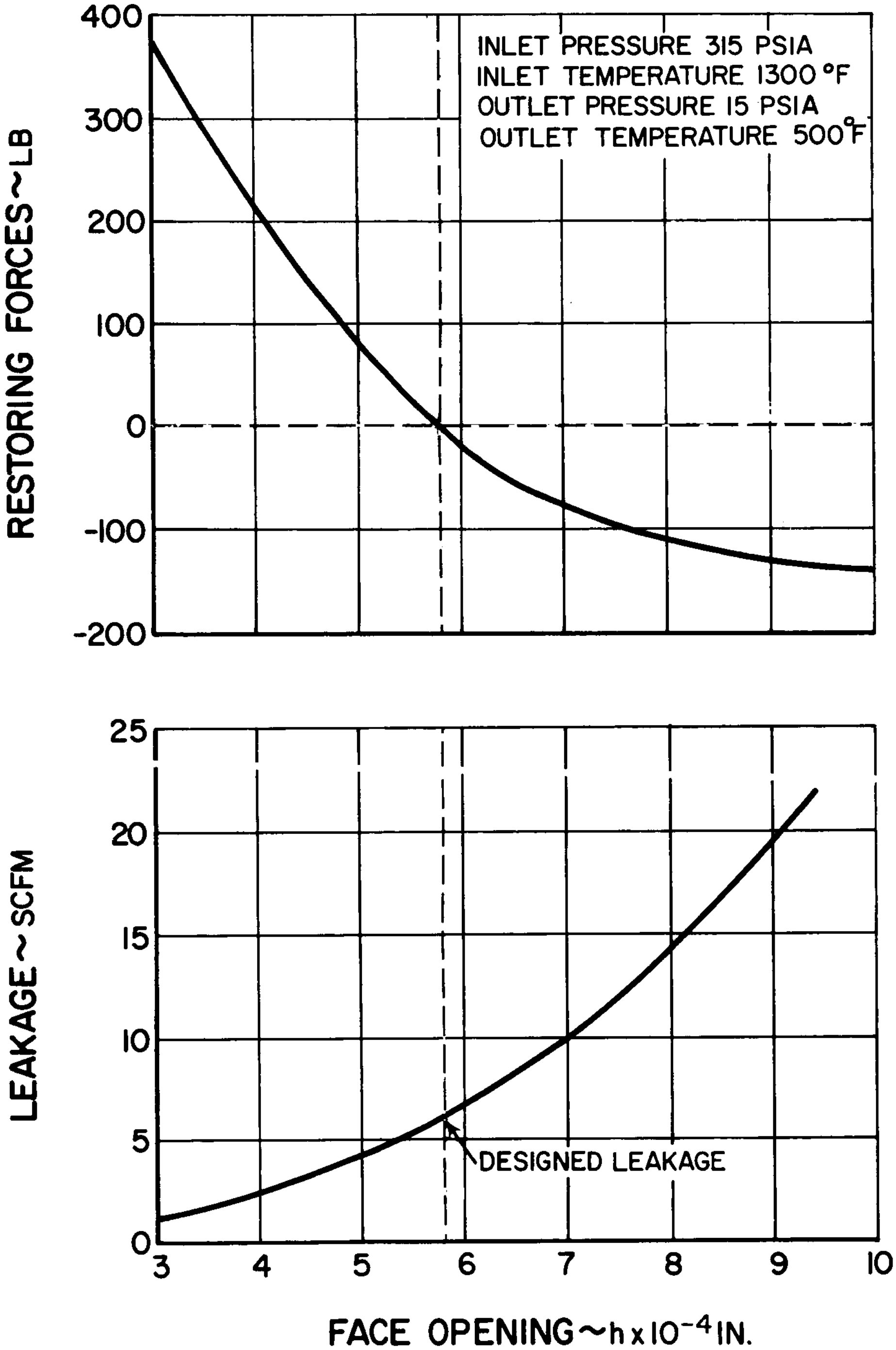

Figure 14 Seal A: Design Characteristics of Self-Energized Face Seal Using Correct Value of P_A (P_A = 315 psia)

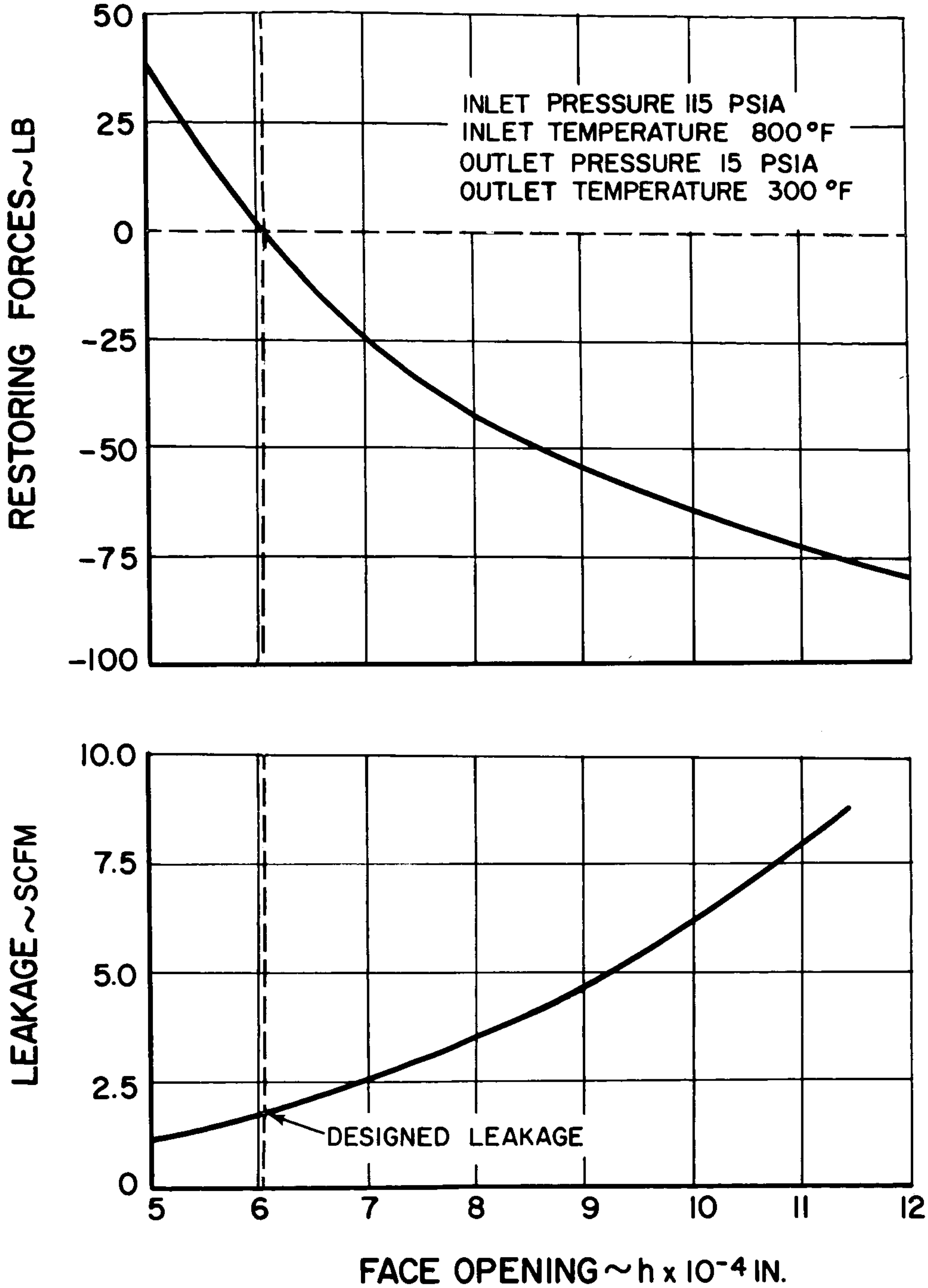

Figure 15 Seal A: Design Characteristics of Self-Energized Face Seal Using Correct Value of P_A (P_A = 115 psia)

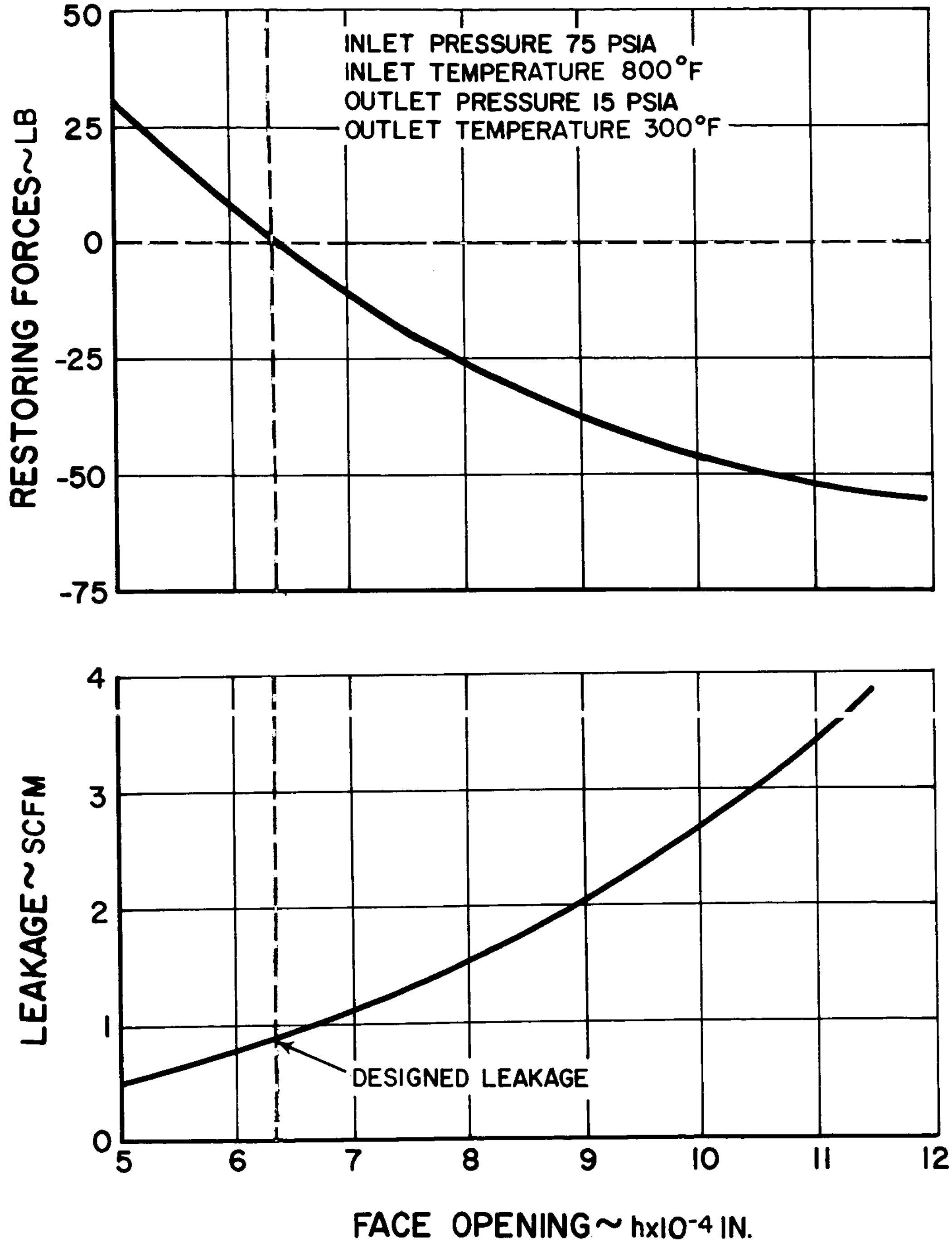

Figure 16 Seal A: Design Characteristics of Self-Energized Face Seal Using Correct Value of P_A (P_A = 75 psia)

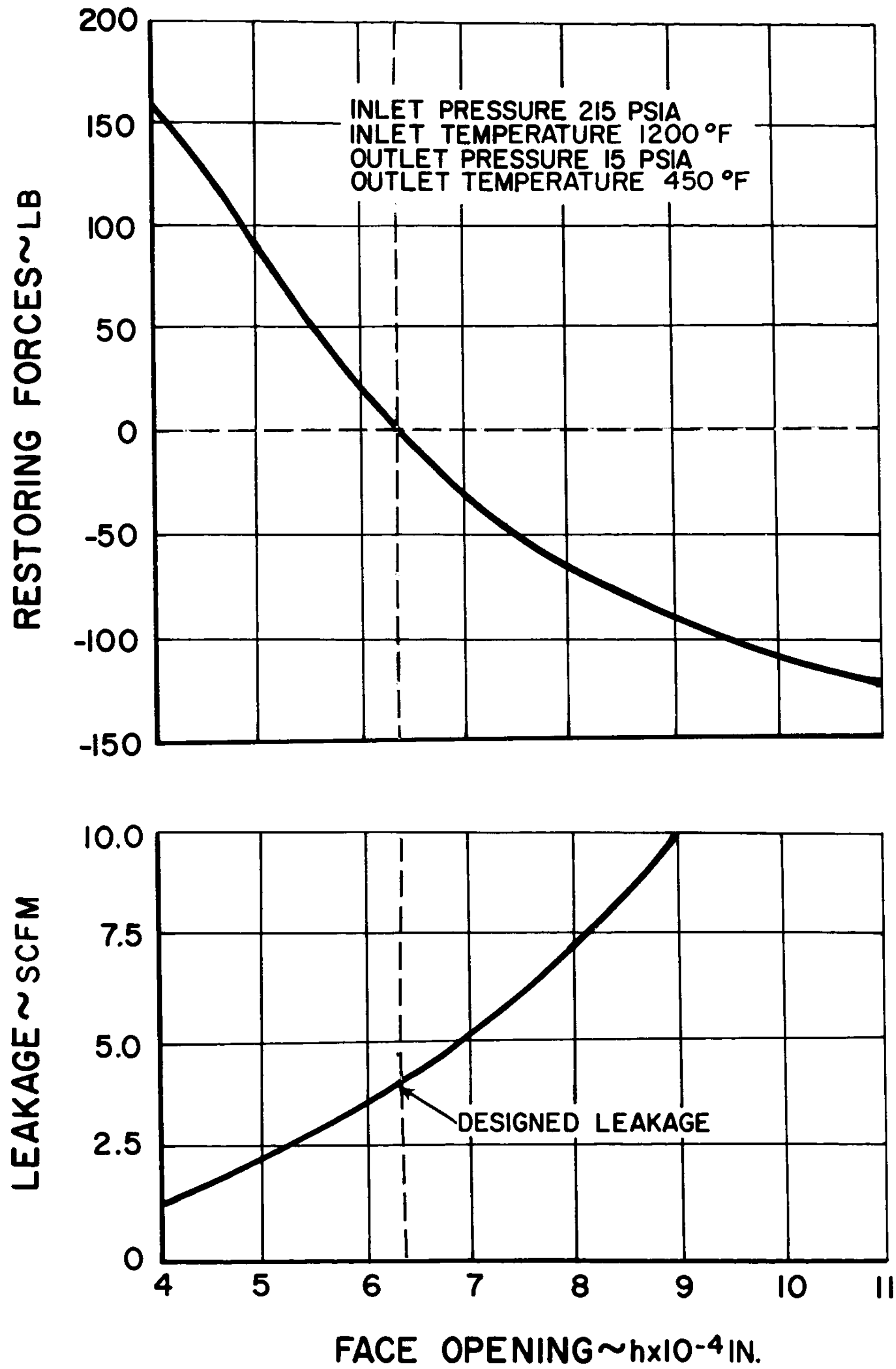

Figure 17 Seal A: Design Characteristics of Self-Energized Face Seal Using Correct Value of P_A (P_A = 215 psia)

2.1.3.2 Carbon Face Contact Seal with Bellows Secondary Seal (C)

2.1.3.2.1 Inertial Loadings - Following the procedure given under the orifice compensated hydrostatic seal, the equivalent face forces are calculated.

1. Bellows front, end fitting (steel)

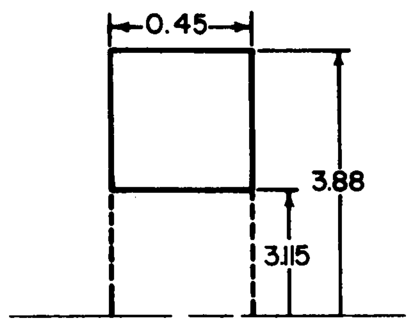

wt. = .28 π $(3.88^2 - 3.115^2)$ (.45) = 2.116 lb.

2. Bellows wafer

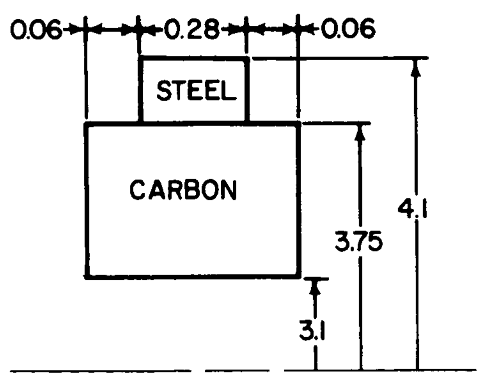

wt. of steel	= .28 π $(4.1^2 - 3.75^2)$ (.28)	=	.6893 lb.
wt. of carbon	= .065 π $(3.75^2 - 3.1^2)$ (.40)	=	.4000 lb.
total weight of wafer		=	1.0893 lb.
+ front, end fitting		=	2.116 lb.
total weight		=	3.2053 lb.

$$\text{wt./in. of circum} = \frac{3.2053 \text{ lb.}}{2\pi\,(3.502)} = .1457 \text{ lb/in.}$$

Table of Resulting Inertial Loads:

Cond. - ΔP, psi	Vel., ft/sec.	Vel. ratio	$(\text{Vel. ratio})^2$	G	F_I, equiv. face force, lb/in.
100	200	2/5	4/25	.3646	.0531
calc.	332			1.003	.146
200	400	4/5	16/25	1.458	.2124
300	500	1	1	2.28	.3321

2.1.3.2.2 Required Total Loadings (Summary) -

Cond. - ΔP, psi	Vel., ft/sec.	F_I
100	200	.146
200	400	.2124
300	500	.3321

2.1.3.2.3 Face Pressure Forces

Cond. - ΔP, psia	Force Required lb/in.	Pressure Force Required lb/in.	Pi, psia	λ	Pressure Seat Force (lb/in) Supply	Excess
100	.146	-.1861	114.7	.629	.115	.3011
200	.2124	-.1197	214.7	.646	.06	.1797
300	.3321	0	314.7	.652	0	0

$F_{300} = (.652 - .652)\,(.05)\,(300) = 0$

$F_{200} = (.652 - .646)\,(.05)\,(200) = .06$ lb/in.

$F_{100} = (.652 - .629)\,(.05)\,(100) = .115$ lb/in.

where 0.05 is the amount the seals are damped; the value is based on experience and has been checked out.

2.1.3.2.4 Collars (Deflection Analysis)

Collar, Oil Holes (Deflection Analysis); usage - contact seals

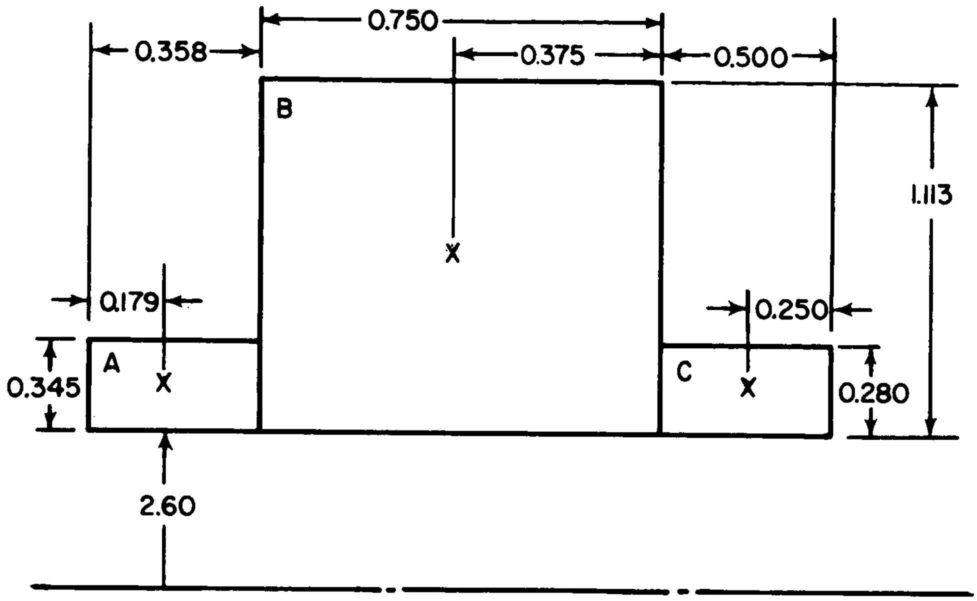

x - axis:

Member A: (.358) (.345) (.179) = .02215
B: (.750) (1.113) (.733) = .612
C: (.500) (.280) (1.358) = .190
1.0987 .82415

$$C_g)_x = \frac{.82415}{1.0987} = .75$$

Y - axis

Member A: .1237 x .172 = .02125
B: .835 x .557 = .465
C: .140 x .140 = .0196
1.0987 .50585

$$C_g)_y = \frac{.50585}{1.0987} = .461$$

$R_m = 2.60 + .461 = 3.061$

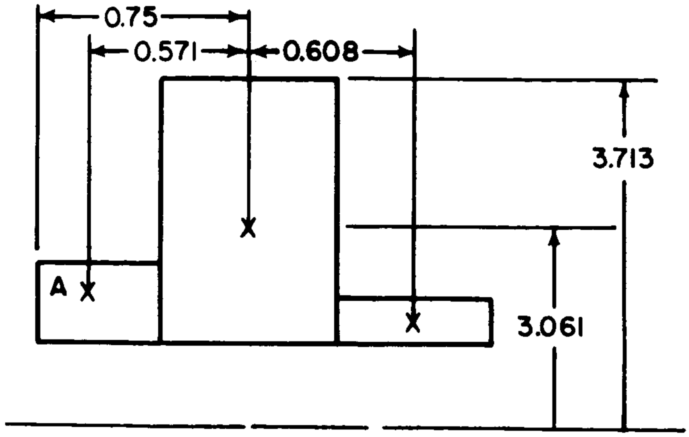

Moments of Inertia of -

$$\text{Member A: } \frac{1}{12} (.345)(.358)^3 + .1238 (.571)^2 = .0416$$

$$\text{B: } \frac{1}{12} (1.113)(.750)^3 = .0391$$

$$\text{C: } \frac{1}{12} (.38)(.500)^3 + .140 (.608)^2 = \underline{.0546}$$

$$I = .1353 \text{ in}^4$$

$$F_F = \Delta P\, A_F / 2\pi (3.061)$$

$$= 300\cancel{\pi} \left[(3.713)^2 - (2.6)^2\right] \Big/ 6.122\cancel{\pi} = 344 \text{ lb/in. of circ.}$$

$$M_F = 344 (.211'') = 72.5 \text{ lb-in/in.}$$

$$F_A = (300)(.358) = 107.4 \text{ lb/in.}$$

$$M_A = (107.4)(.571) = 61.5 \text{ lb-in/in.}$$

$$M_R = 72.5 - 61.5 = 11. \text{ lb-in/in.}$$

$$\Theta = \frac{MR^2}{EI}$$

$$= \frac{11.\ (3.061)^2}{30 \times 10^6 \times .1353} = .2544 \times 10^{-4}$$

Face Seal Rolls: $\Theta = 61.9 \times 10^{-6}$ (from page 16 - Orifice Compensated Hydrostatic Face Seal)

$61.9 \times 10^{-6} > 25.44 \times 10^{-6}$ $\therefore$ O.K.

2.1.4 Seal-Housing Deflection Analysis (PWA design)

It is desired to be able to determine the deflections of the seal-housing assembly. A detailed analysis has been performed yielding eight equations with eight unknowns. These equations are solved simultaneously on the IBM 1620 computer. The equations are arrived at by equating the slopes and deflections of contiguous members to ensure continuity of structure. For example, referring to the sketch below, the deflection of cylinder (3) at A is equal to the deflection of cylinder (2) at A, and the slope of (3) is equal to the slope of (2) at A.

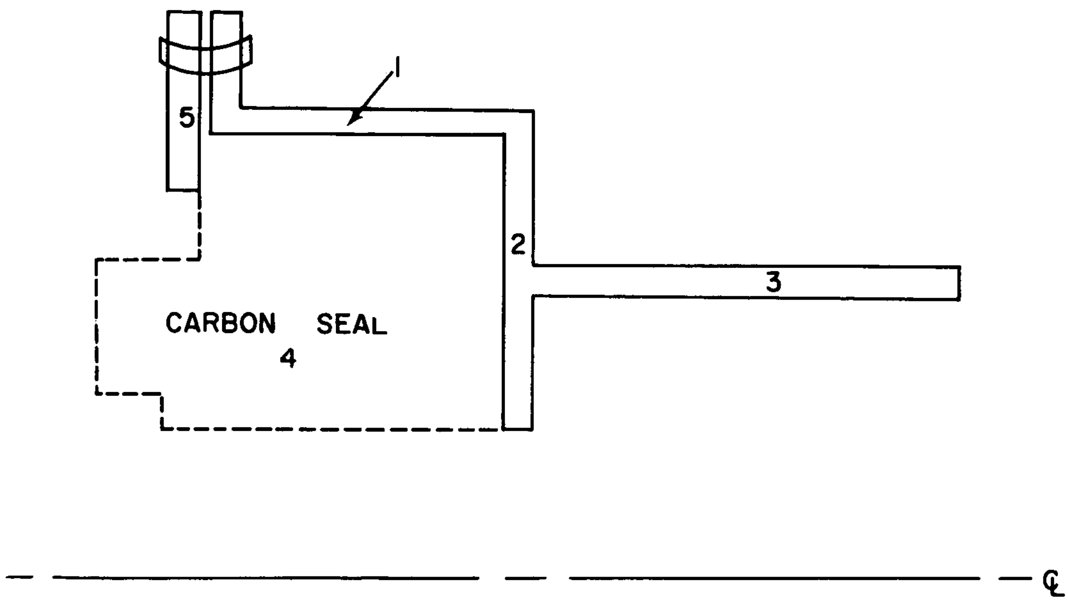

The following is a detailed description of the analysis. The equations are based on material given in Roark's "Formulas for Stress and Strain". A free body diagram of the PWA seal design is sketched below. Bodies 1, 2, 3 comprise the carrier; body 4 the seal; body 5 the carbon retention ring; P refers to pressure; M refers to moment; V refers to shear; L refers to horizontal length; h refers to vertical length; and R refers to radius.

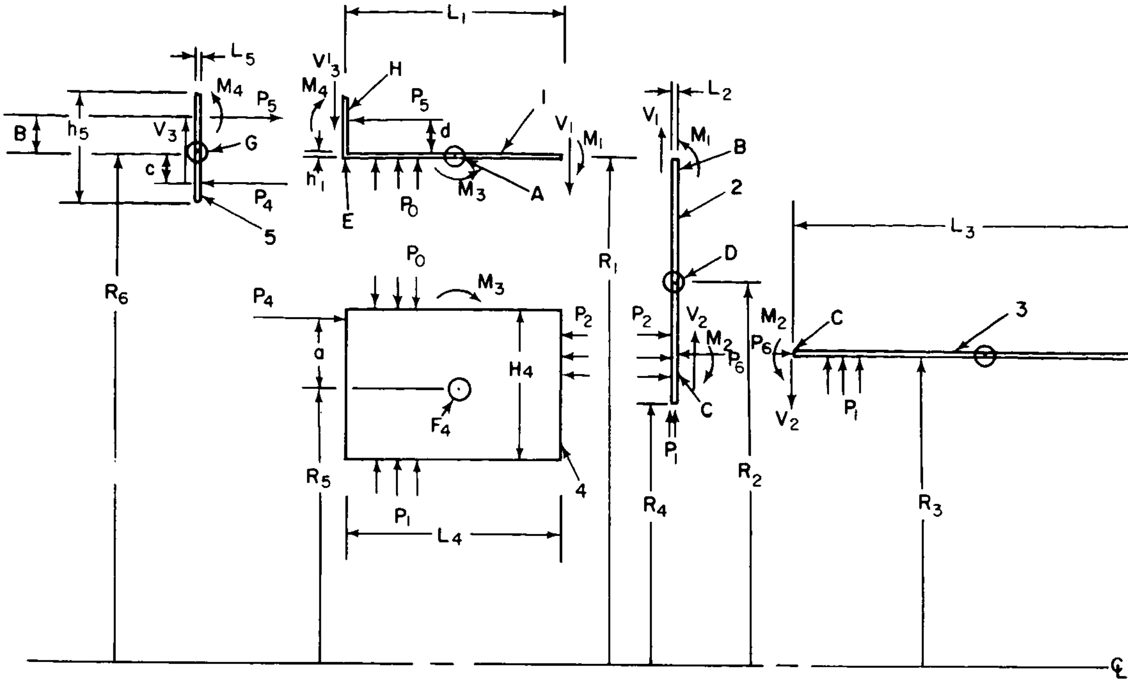

2.1.4.1 Deflection and Rotation Equations

2.1.4.1.1 For Body (1) -

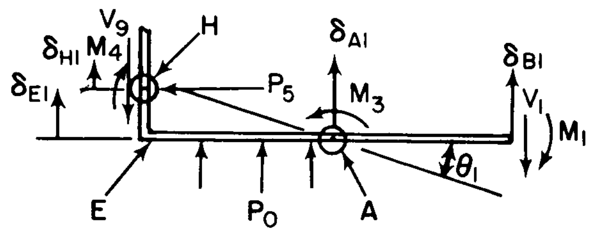

The radial displacement of body (1) at point A (δ_{A_1}) and the corresponding angular displacement Θ_1 are given by the following equations -

$$\delta_{A_1} = \frac{P_0 R_1^{\,2}}{E\,h_1} - \frac{V_1 R_1^{\,2}}{E L_1 h_1} - \frac{V_3 (R_1 + d) R_1}{E L_1 h_1}$$

$$\Theta_1 = \frac{R_1^{\,2}}{E I_1}\left[M_1 - M_3 + 1/2\, L_1 V_1 - 1/2\, L_1 V_3 \left(\frac{R_1 + d}{R_1}\right) - P_5 d \left(\frac{R_1 + d}{R_1}\right) + M_4 \left(\frac{R_1 + d}{R_1}\right)\right]$$

The radial displacements of body (1) with respect to points B, E, and H are represented below:

$$\delta_{B1} = \delta_{A1} - 1/2\ L_1\ \Theta_1$$
$$\delta_{E_1} = \delta_{A1} + 1/2\ L_1\ \Theta_1$$
$$\delta_{H_1} = \delta_{A1} + 1/2\ L_1\ \Theta_1$$

where E = modulus of elasticity
(Flange contribution is insignificant to torsional stiffness since it is scalloped.)

2.1.4.1.2 For Body (2) -

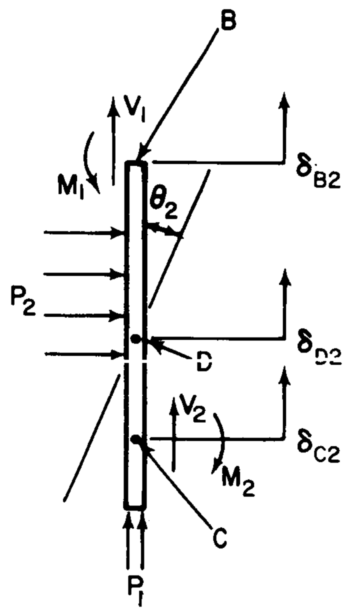

The radial displacement of body (2) with respect to point D (δ_{D2}) and the corresponding angular displacement Θ_2 are given below.

$$\delta_{D2} = \frac{P_1R_4R_2}{Eh_2} + \frac{V_1R_1R_2}{Eh_2L_2} + \frac{V_2R_2R_3}{Eh_2L_2}$$

$$\Theta_2 = \frac{R_2^{\ 2}}{EI_2}\ (M_2 - M_1)$$

The radial displacement of (2) at point B, $\delta_{B2} = \delta_{D2}$
The radial displacement of (2) at point C, $\delta_{C2} = \delta_{D2}$
(Moment due to pressure P_2 is assumed negligible)

2.1.4.1.3 For Body (3) -

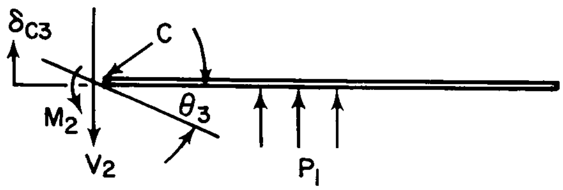

The radial displacement of body (3) at points C(δ_{C3}) and the corresponding angular displacement Θ_3 are given below -

$$\delta_{C3} = \frac{P_1 R_3^2}{E h_3} - V_2 \left(\frac{C_3}{2D\lambda^3} \right) - M_2 \left(\frac{C_5}{2D\lambda^2} \right)$$

$$\Theta_3 = - V_2 \left(\frac{C_4}{2D\lambda^2} \right) - M_2 \left(\frac{C_6}{\lambda D} \right)$$

where $D = \frac{E h_3^3}{12(1-\nu^2)}$; $\lambda = \left(\frac{3(1-\nu^2)}{R_3^2 h_3^2} \right)^{1/4}$

and C_3, C_4, C_5, C_6 are constants dependent on λL_3 and are given in Roark, p. 297.

2.1.4.1.4 For Body (4) -

The radial displacement of body (4) at point F(δ_{F4}) and the corresponding angular displacement Θ_4 are given below -

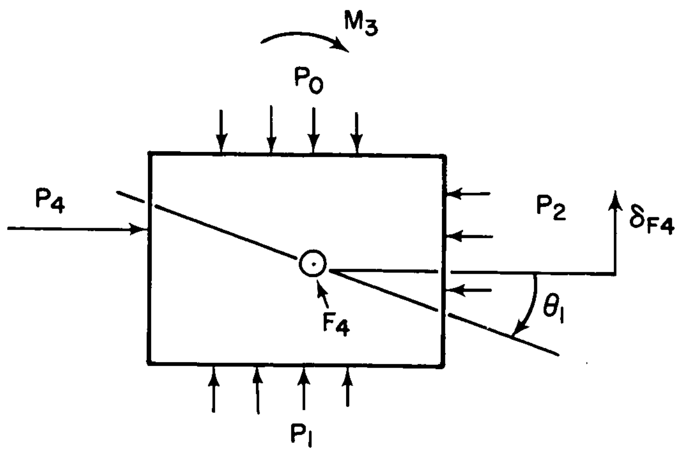

$$\delta_{F_4} = \frac{P_1 R_5 (R_5 - 1/2\, h_4)}{E_1 h_4} - \frac{P_o R_5 (R_5 + 1/2\, h_4)}{E_1 h_4} + R_5 \beta \Delta T$$

$$\Theta_4 = \frac{R_5^2}{E_1 I_4} (M_3 + P_4 a)$$

where

$\beta = (\alpha_1 - \alpha)$

α_1 = coefficient of thermal expansion of carbon

α = coefficient of thermal expansion of housing material

E_1 = Young's modulus of carbon

ΔT = operating temp. - room temp.

2.1.4.1.5 For Body (5) -

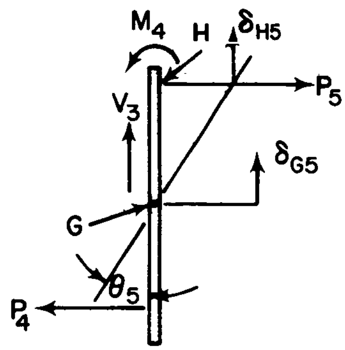

The radial displacement of body (5) at point G(δ_{G_5}) and the corresponding angular displacement Θ_5 are given below -

$$\delta_{G_5} = \frac{R_6 (R_6 + b)}{E L_5 h_5} V_3 \qquad (V_3 \text{ acts at bolt circle radius})$$

$$\Theta_5 = \frac{R_6^2}{E I_5} \left[P_5 \left(\frac{R_6 + b}{R_6} \right) b + P_4 \left(\frac{R_6 - C}{R_6} \right) C - M_4 \left(\frac{R_6 + b}{R_6} \right) \right]$$

The radial displacement of (5) at point H, $\delta_{H_5} = \delta_{G_5}$

2.1.4.1.6 Relations between P_2, P_4, and P_5

From lateral equilibrium,

$$P_2 R_5 h_4 = P_4 (R_5 + a)$$

$$P_4 (R_5 + a) = P_5 (R_6 + b)$$

$$P_4 = \frac{P_2 R_5 h_4}{R_5 + a} \quad , \quad P_5 = \frac{P_2 R_5 h_4}{R_6 + b}$$

2.1.4.1.7 Slopes and Deflections -

Slopes and deflections are equated to insure continuity of structure:

$$\delta_{B_1} = \delta_{B_2} \qquad \Theta_1 = \Theta_2$$

$$\delta_{C_2} = \delta_{C_3} \qquad \Theta_2 = \Theta_3$$

$$\delta_{F_4} = \delta_{A_1} \qquad \Theta_1 = \Theta_4$$

$$\delta_{H_5} = \delta_{H_1} \qquad \Theta_1 = \Theta_5$$

There exist 8 unknowns (P_o, V_1, M_1, V_2, M_2, V_3, M_3, M_4) and 8 simultaneous equations. Consequently, the problem is solveable. The desired results are δE_1, Θ_1, which represent the radial displacement and rotation of point E.

The moments of inertia are approximated for this analysis to be

$$I_n = 1/12\ h_n L_n^3 \text{ where } n = 1, 2, \ldots 5$$

The simultaneous equations that are solved on the IBM 1620 computer are as follows -

$$\delta_{B_1} = \delta_{B_2} : P_o \frac{R_1^2}{h_1} - V_1 \frac{R_1^2}{L_1 h_1} - V_3 \frac{R_1 (R_1 + d)}{L_1 h_1} - \frac{R_1^2 L_1}{2 I_1}$$

$$\left\{ M_1 - M_3 + 1/2\, V_1 L_1 - 1/2\, V_3 L_1 \left(\frac{R_1 + d}{R_1} \right) - P_5 \left(\frac{R_1 + d}{R_1} \right) d + M_4 \left(\frac{R_1 + d}{R_1} \right) \right\}$$

$$= P_1 \frac{R_2 R_4}{h_2} + V_1 \frac{R_1 R_2}{h_2 L_2} + V_2 \frac{R_2 R_3}{h_2 L_2}$$

$$\delta_{C_2} = \delta_{C_3} : \; P_1 \frac{R_3^{\,2}}{h_3} - V_2 \frac{C_3 E}{2D \lambda^3} - M_2 \frac{C_5 E}{2D \lambda^2} = P_1 \frac{R_2 R_4}{h_2} + V_1 \frac{R_1 R_2}{L_2 h_2}$$

$$+ V_2 \frac{R_2 R_3}{L_2 h_2}$$

$$\delta_{F_4} = \delta_{A_1} : P_o \frac{R_1^{\,2}}{h_1} - V_1 \frac{R_1^{\,2}}{L_1 h_1} - V_3 \frac{R_1 (R_1 + d)}{L_1 h_1} = P_1 \frac{E R_5 (R_5 - 1/2\, h_4)}{E_1 h_4}$$

$$- P_o \frac{E R_5 (R_5 + 1/2\, h_4)}{E_1 h_4} + R_5 E \beta \Delta T$$

$$\delta_{H_5} = \delta_{H_1} : V_3 \frac{R_6 (R_6 + b)}{L_5 h_5} = P_o \frac{R_1^{\,2}}{h_1} - V_1 \frac{R_1^{\,2}}{L_1 h_1} - V_3 \frac{R_1 (R_1 + d)}{L_1 h_1}$$

$$+ \frac{R_1^{\,2} L_1}{2 I_1} \left\{ M_1 - M_3 + 1/2\, V_1 L_1 - 1/2\, V_3 L_1 \left(\frac{R_1 + d}{R_1} \right) - P_5 \left(\frac{R_1 + d}{R_1} \right) d \right.$$

$$\left. + M_4 \left(\frac{R_1 + d}{R_1} \right) \right\}$$

$$\Theta_1 = \Theta_2 : \frac{R_1^{\,2}}{I_1} \left\{ M_1 - M_3 + 1/2\, V_1 L_1 - 1/2\, V_3 L_1 \left(\frac{R_1 + d}{R_1} \right) - P_5 d \right.$$

$$\left. \left(\frac{R_1 + d}{R_1} \right) + M_4 \left(\frac{R_1 + d}{R_1} \right) \right\} = \frac{R_2^{\,2}}{I_2} (M_2 - M_1)$$

$$\Theta_2 = \Theta_3 : \frac{R_2^{\ 2}}{I_2} \left(M_2 - M_1\right) = - V_2 \frac{C_4 E}{2D\lambda^2} - M_2 \frac{C_6 E}{D\lambda}$$

$$\Theta_1 = \Theta_4 : \frac{R_1^{\ 2}}{I_1} \left\{ M_1 - M_3 + 1/2\ V_1 L_1 - 1/2\ V_3 L_1 \frac{R_1 + d}{R_1} - P_5 d \frac{R_1 + d}{R_1} + M_4 \left(\frac{R_1 + d}{R_1}\right)\right\} = \frac{E}{E_1} \frac{R_5^{\ 2}}{I_4} \left(M_3 + P_4 a\right)$$

$$\Theta_1 = \Theta_5 : \frac{R_1^{\ 2}}{I_1} \left\{ M_1 - M_3 + 1/2\ V_1 L_1 - 1/2\ V_3 L_1 \left(\frac{R_1 + d}{R_1}\right) - P_5 d \left(\frac{R_1 + d}{R_1}\right) \right.$$

$$\left. + M_4 \left(\frac{R_1 + d}{R_1}\right)\right\} = \frac{R_6^{\ 2}}{I_5} \left\{ P_5 \left(\frac{R_6 + b}{R_6}\right) b + P_4 \left(\frac{R_6 - C}{R_6}\right) C - M_4 \left(\frac{R_6 + b}{R_6}\right)\right\}$$

For the Pratt & Whitney Aircraft carbon face contact seal, the analysis by means of computer solution yielded the following results:

1. For the press fit (seal pressed into carrier; no pressure applied on seal $\rightarrow$ $P_1 = 0$):

   The algebraic addition of the deflections of body (1) at points E and B yields the required radial deflection of body (1):

   $$\delta_{E_1} + (-\delta_{B_1}) = 0.00431 \text{ in.}$$

   The desired deflection is at the carbon seal face.
   Consequently, the radial deflection of body (1) will be transposed by the ratio of carbon face width to the length of body (1) -
   Deflection on the carbon face $= \frac{\text{face width}}{L_1} (0.00431) = \underline{\underline{.00262}}$ in.

2. Relaxing the press fit (applying temperature) -
   Thermal relief:

   $$\delta_T = \frac{\text{fit} - \Delta\text{fit due to thermals}}{\text{fit}} (.00262) = .00219$$

   Deflectionon the carbon face = .00262 - .00219 = - $\underline{\underline{.00043}}$ in.

3. Pressurization of the seal (applying a pressure P_1 of 300 psi to the seal) -

$$\delta_{E_1} - \delta_{B_1} = .00154 \text{ in.}$$

$$\text{Deflection of the carbon face} = \frac{\text{face width}}{L_1}(.00154) + (-.00043) = \underline{\underline{.000505}} \text{ in.}$$

2.1.5 Thermal Analysis

The TOSS Computer Program from the SHARE General Program Library was utilized for the thermal analysis of the critical components of the mainshaft seal rig. The TOSS program employs a method whereby an initial guess for the temperature distribution is "relaxed" in a cyclic order and a new temperature distribution is obtained after each cycle or iteration. The seal which was analyzed is the Pratt & Whitney Aircraft rubbing contact seal. Several cases were run with the objective of determining the temperature variation of the carbon seal relative to a variation in the values of the input parameters. Table 4 demonstrates this variation.

TABLE 4

NECK SEAL TEMPERATURE AS AFFECTED BY INPUT PARAMETERS

	Heat Transfer Coefficients Btu/hr ft^{2}F°				Btu/Min		
	Rotating Surfaces To Air				Heat Generation		
Case No.	High Pressure	Low Pressure	Oil Through Seal Plate	Heatloss by Radiation °F	Seal Interface	Bearings	Seal Temp °F
1	1000.	1.0	865.	NONE	420.	135.	1640.
2	1000.	1.0	865.	NONE	210	135	1400.
3	1000.	1.0	865.	600. SINK	210.	135.	1385.
4	1000.	1.0	865.	300. SINK	NONE	NONE	1150.
5	1.0	1.0	865.	600. SINK	210.	135.	1240.
6	1.0	1.0	260.	600. SINK	210	135.	1665.
7	202.	242.	3770.	300. SINK	210.	67.5	1220.
8	202.	242.	865.	300. SINK	210.	67.5	1282.

Heat transfer coefficient of oil in bearing race = 260. Btu/hr ft^{2}F

Heat transfer coefficient of stationary surfaces to air ≐ 1.0 $\frac{\text{Btu}}{\text{hr ft}^2\text{F}}$

The thermal map, Figure 18, is the result of inputing the best estimates of the input parameters at the design conditions. The critical parameter was found to be the heat generated at the seal-seal plate interface. The heat generation is a function of the coefficient of friction at the interface, the rpm of the seal-plate, the seal face loading and the presence of an interface air film. It was assumed that no air film existed at the interface to remove any heat generation. The seal temperature was found to vary (dependent on the input heat generation at the interface) from the oil sump temperature to a temperature greater than that of the high pressure air. It is intended to determine the heat generation at the interface by instrumenting the seal with thermocouples. Knowledge of the seal temperature will then make it possible to determine the heat generation by use of the analytical model. Reference to cases 1, 2, 3 and 4 listed in Table 4 illustrates the dependence of the seal temperature on the heat generated at the interface.

The coefficient of heat transfer of the rotating surfaces was obtained from

$$Nu = 0.11\,(.5\,Re^{2.}\,Pr)^{.35} \qquad (1)$$

$$\text{where } Re = \frac{60.\ \pi\ D^2\ (RPM)}{\mu / \rho} \qquad (2)$$

D = diameter of rotation, feet

μ = viscosity of air $\frac{\text{lbs mass}}{\text{ft hour}}$

ρ = air density $\frac{\text{lbs mass}}{\text{ft}^3}$

Equations 1 and 2 were obtained from Reference 1. At the design rpm of 17,000 and for air at 1300°F and 300 psi, the equations reduce to h = 147 $R^{\circ 4}$ Btu hr ft^2 F° where R is the radius of revolution, inches. The values of the coefficient of heat transfer for the rotating surfaces were input into the analytical model according to this equation for cases 7 and 8 (See Table 4). Case numbers 1, 2, 3 and 4 demonstrate the seal temperature variation relative to the interface heat generation at the seal. Case numbers 5 and 6 demonstrate the seal temperature dependence on the heat transfer coefficient of the oil in the plate passage. Cases 7 and 8 demonstrate the reduction in seal temperature by design of the oil passage so that the heat transfer coefficient (h = 3770) is in the turbulent regime. Cases 3 and 5 illustrate the effect of the two extreme values of the heat transfer coefficient on the seal temperature. The extremes referred to are for very high shaft rotation and for a stationary shaft.

Reference 1: Trans ASME Vol. 77, 1955, p. 1283-1289. G. A. Etemad, "Free Convection Heat Transfer from a Rotating Horizontal Cylinder with Interferometer Study of Flow"

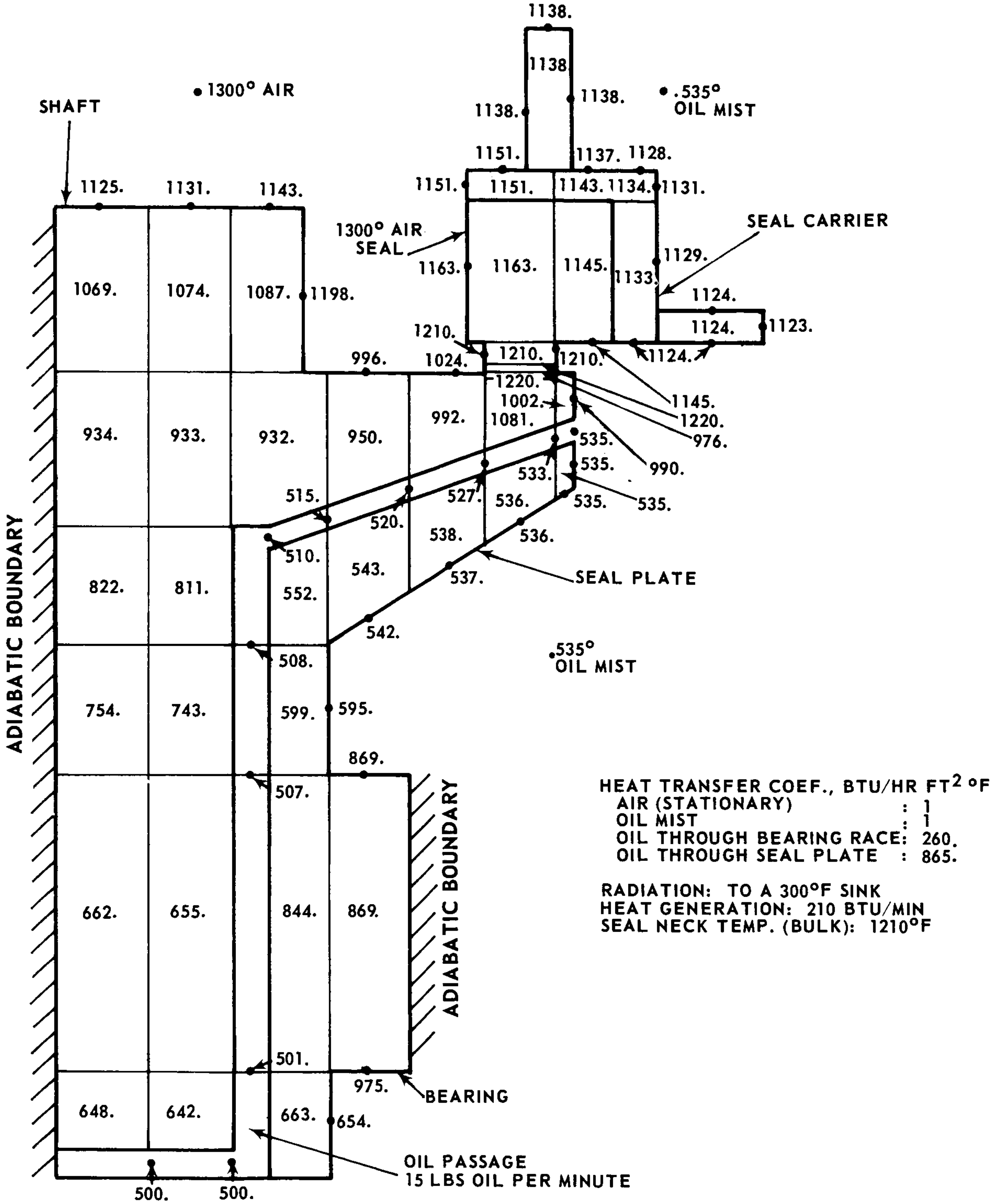

Figure 18 Temperature Map of Carbon Seal For Design Conditions

Figure 18 is a thermal map of the conditions of case 7, Table 4. Figures 19 and 20 are design graphs for the oil passage in the seal plate. Figure 19 shows the variation of the frictional pressure drop per unit length of passage with the mass flow rate of oil coolant. Figure 20 shows the variation of the heat transfer rate with the mass flow rate. Both graphs are derived with passage diameter as parameter (the equations, on which the two graphs are based, were derived assuming the oil filled the flow passages.) The dotted lines indicate the boundaries between the laminar, transition, and turbulent regimes. In the laminar flow regime, the Sieder and Tate empirical equation was used for Reynolds numbers less than 2100.

$$Nu_d = 1.86 \left[Re\ Pr \frac{D}{L}\right]^{.33} \left[\frac{\mu\ b}{\mu\ s}\right]^{.14} \qquad (3)$$

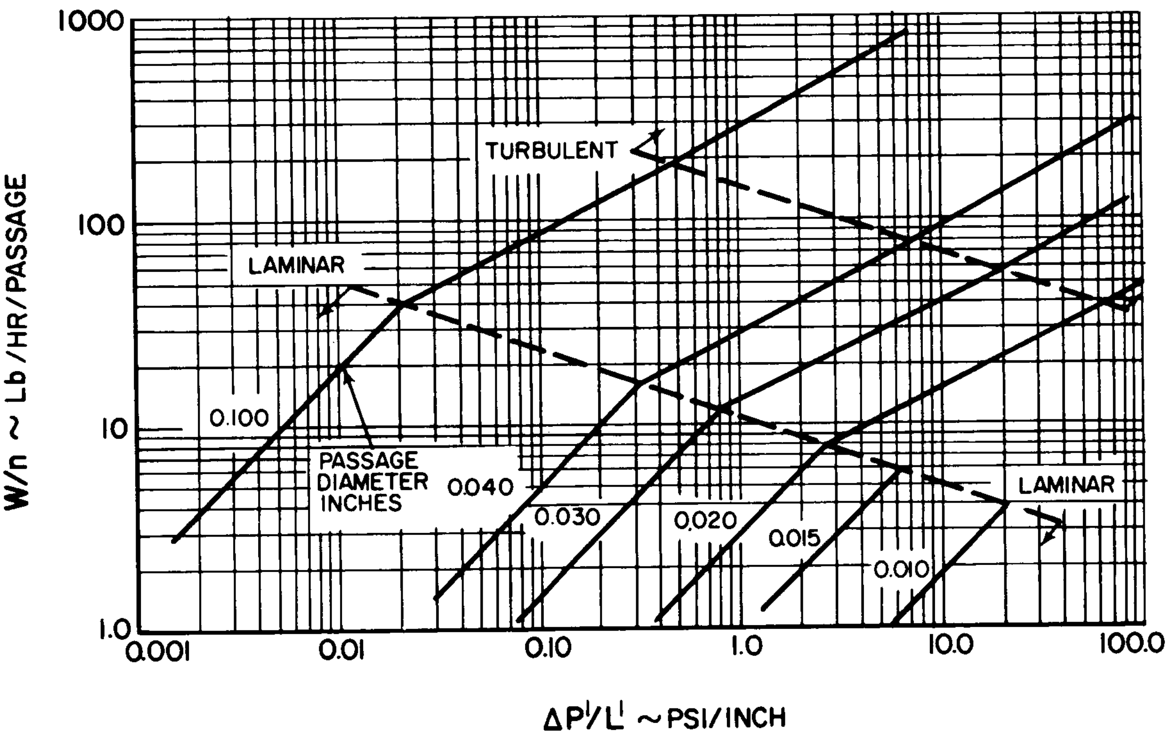

Figure 19 Pressure Drop Per Unit Length (psi/in) as a Function of Oil Flow - Rate Per Passage (lb/hr) With Passage Diameter as Parameter

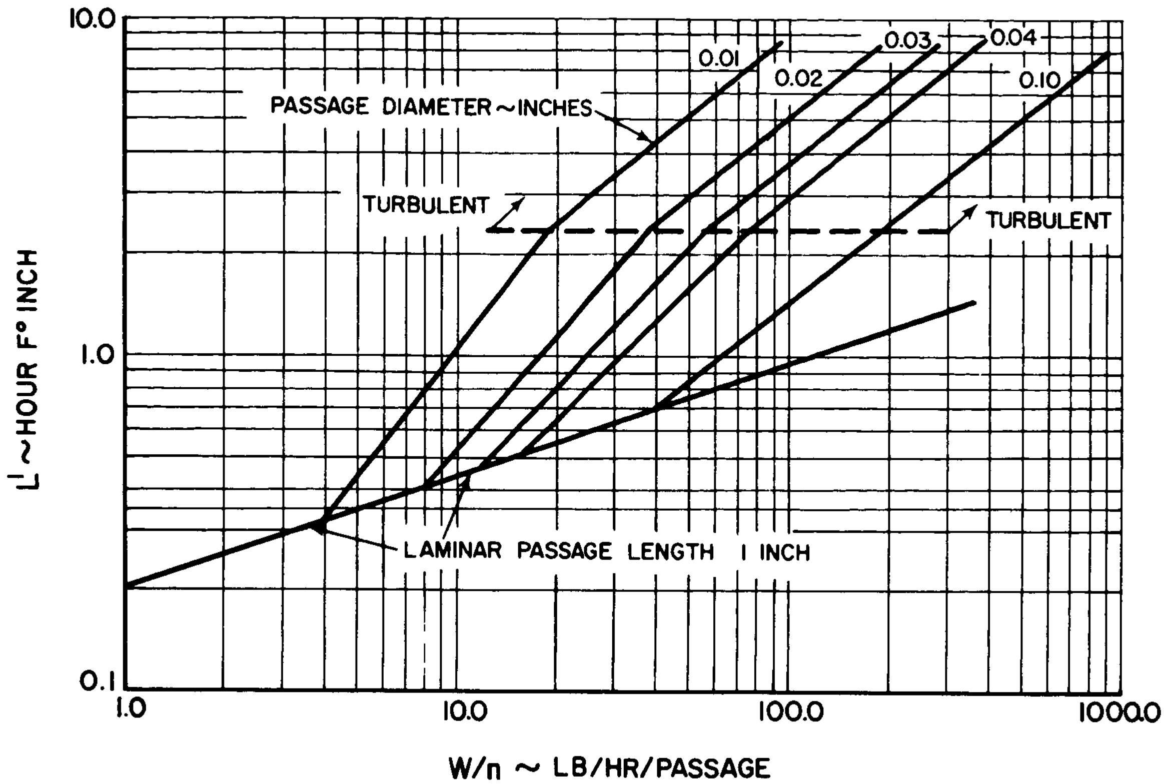

Figure 20 Heat Transfer As a Function of Oil Flow Rate Per Passage With Passage Diameter as Parameter

The friction factor used to determine pressure drop was given by $f = 16/Re$. In the turbulent regime, the Dittus-Boelter equation was used for Reynolds numbers greater than 10,000.

$$Nu = 0.023\ Re^{.8}\ Pr^{.4} \tag{4}$$

The friction factor employed for turbulent flow was $f = 0.046\ Re^{-.2}$. The pressure drop was calculated by substitution of the above friction factors into

$$\Delta P = 4f\left(\frac{L}{D}\right) \rho \frac{V^2}{2g} \tag{5}$$

The transition regime on Figures 19 and 20 was denoted by connecting the laminar and turbulent lines at constant passage diameter.

Substitution of f = 16/Re into equation (5) and evaluating the physical properties results in

$$\frac{W}{n} = 0.1885 \left(\frac{\Delta P'}{L'}\right)_{\text{laminar}} (D')^4 \times 10^8 \qquad (6)$$

where $\frac{W}{n}$ = lbs oil per hour per passage

D' = passage diameter, inches

$\frac{\Delta P'}{L'}$ = psi pressure drop per inch of passage length

Equation (6) is plotted in Figure 19 for the laminar regime.

Substitution of $f = 0.046\ Re^{-.2}$ into equation (5) and again evaluating the physical properties results in

$$\left(\frac{\Delta P'}{L'}\right)_{\text{turbulent}} = \frac{58.0}{(D')^{4.8}} \left(\frac{W}{n}\right)^{1.8} \times 10^{-11} \qquad (7)$$

Equation (7) is also plotted in Figure 19.

Equation (3) may be rewritten in terms of the parameter $\frac{hA}{L'}$ as follows

$$\frac{hA}{L'} = 1.86 \frac{K}{D} \left(Re\ Pr \frac{D}{L}\right)^{.33} \left(\frac{\mu\ \text{bulk}}{\mu\ \text{surface}}\right)^{.14} \left(\frac{\pi DL}{L'}\right) \qquad (8)$$

Evaluation of the physical properties and rearrangement for a one-inch passage length, yields

$$\frac{hA}{L'} = 0.205 \left(\frac{W}{n}\right)^{.33} \text{Btu/hr F}^\circ \text{ inch} \qquad (9)$$

Equation (9) is plotted as one line for the laminar regime in Figure 20.

Repetition of the preceding process for equation (4) yields for the turbulent regime.

$$\frac{hA}{L'} = \frac{0.00561}{(D')^{.8}} \left(\frac{W}{n}\right)^{.8} \qquad (10)$$

Equation (10) is plotted in Figure 20 for the turbulent regime.

The turbulent and transition regimes are assumed to intersect at Re = 10,000 where $\frac{W}{n} = 1895\ D'$. Therefore $\left(\frac{hA}{L'}\right)_{\text{Turbulent Transition}} = \frac{.00561}{(D')^{.8}} (1895\ D')^{.8}$

$$= 2.36 \qquad (11)$$

The laminar and transition regimes are assumed to intersect at Re = 2100 where $\frac{W}{n} = 398\ D'$.

$$\text{Therefore,} \left(\frac{hA}{L'}\right)_{\text{Transition Laminar}} = 0.205\ (398\ D')^{.33} \qquad (12)$$

For specific values of passage diameter, D', the transition regime was drawn on Figure 20 so that both values of $\left(\frac{hA}{L'}\right)$ as indicated by equations (11) and (12) were satisfied.

To determine where the laminar lines on Figure 19 ended, $\frac{W}{n} = 398\ D'$ was solved for each passage diameter.

The result was the lower dotted line indicated by arrows. Likewise, to determine where the turbulent lines on Figure 19 began, $\frac{W}{n} = 1895\ D'$ was solved for each passage diameter. The upper dotted line indicated by arrows was the result. The transition regime was then indicated by connection of the two dotted lines.

2.2 TASK II - MAINSHAFT SEAL EVALUATION

2.2.1 Statement of Objective

The work to be accomplished under this task is: (1) the procurement of four seal assemblies of each of four seal designs after approval by NASA project manager, (2) the design and procurement of test equipment capable of testing these seals at the design conditions stated in Task I, and (3) an experimental evaluation program, to be carried out on each seal design.

2.2.2 Progress

2.2.2.1 NASA Approval of Seal Designs

To date, NASA has approved three of the four designs submitted:

1. Face contact seal with piston ring secondary seal. (PWA)
2. Face contact seal with bellows secondary seal. (Stein)
3. Orifice compensating hydrostatic face seal with piston ring secondary. (Stein)

The fourth and final design, consisting of an externally pressurized hydrostatic face seal (Stein) has been submitted to NASA for concept approval.

Detail drawings of the face contact seal with piston ring secondary were included in the Semiannual Progress Report No. 1 (PWA-2683). Detail drawings of the face contact seal with the bellows secondary and the orifice compensating hydrostatic face seal with piston ring secondary are included in Appendix A.

2.2.2.2 Seal Procurement

Procurement of the approved seal designs stands as follows:

1. Face contact with piston ring secondary seal - in-house
2. Face contact with bellows secondary seal - Due July 1966
3. Orifice compensating hydrostatic face seal with piston ring secondary - in-house

2.2.2.3 Test Stand and Facilities

The seal tests are being run in test stand X-81, which is a completely enclosed cell with the control panel and instrumentation outside the test area. The rig is bed-plate mounted and driven by a Ford industrial engine through a truck 4 speed transmission and a 12 to 1 ratio gearbox. Facilities for heating the oil required for the test are located in the test cell and the heated test air is piped through the wall from the adjacent cell where the electrical air heater is located.

A schematic diagram of the test stand and facilities is presented in Figure 21. An overall view of the interior of the stand is shown in Figure 22 and a close-up of the rig is shown in Figure 23. Rig instrumentation readout is located outside the cell and is shown in Figure 24,the right half of the picture. Rig temperatures are recorded here as are rig and seal vibration. The hydraulic unloading and seal wear measurement readouts are also located here. The stand control panel is shown on the left.

2.2.2.4 Test Rig A

Rig design and procurement was carried out with the express intention that all seals would be compatible with the test rig and would be capable of being tested without the use of special adapters. In this respect, all seal designs to be tested will have the same bolt circle and the same axial length. The rig is capable of withstanding the maximum temperatures and pressures needed to fulfill the contract requirement.

Each seal assembly of each type seal will be identified by type name and build number.

2.2.2.4.1 Rig Procurement and Assembly - Parts procurement for the main-shaft seal test rig (reference Figure 25) is complete and all parts are in-house. Initial rig assembly was completed during March 1966.

2.2.2.4.2 Rubbing Contact Face Seal with Piston Ring Secondary - Build 1 - Assembly of Build 1 was accomplished April 5, 1966, and rig installation in the test cell was completed April 21, 1966.

The preliminary checkout of Build 1 was terminated due to high air leakage through the seal (above 50 scfm).

The curve of air leakage vs. seal pressure is shown in Figure 26.

Analysis of the force transducer output of the two torque arms indicated that the torque pin sleeves were restraining the seal from rotating and that the torque arms were not transmitting the load to the transducers.

Figures 27 through 36 show the seal rig components prior to Build 1 testing, Figures 37 through 41 show the seal rig components after 16 hours of preliminary dynamic checkout.

2.2.2.4.3 Rubbing Contact Face Seal with Piston Ring Secondary - Build 2 - Assembly of Build 2 was completed on May 25, 1966 and mounting completed on May 26, 1966. Figure 42 shows the enlarged inlets of the seal plate oil holes to reduce local sludge buildup.

Preliminary dynamic checkout was completed during June 1966. The curve of seal leakage vs. seal pressure is shown in Figure 43.

A comparison of Figures 26 and 43 will show a decrease in air leakage from Build 1 to Build 2. This decrease was brought about by increasing the spring load from 19 to 30 pounds. At 10,230 rpm, an air leakage of 10 scfm occurred at a ΔP of 42 psi for Build 1 and at 132 psi ΔP for Build 2. The increased spring load also enabled readings of ΔP up to 250 psi, all readings being within the stand capability. Further running is required before any pertinent conclusions can be made.

A total of 40 hours have been logged on Build 2.

2.2.2.5 Test Rig B

In an effort to accelerate the testing of the approved seals, Pratt & Whitney Aircraft initiated the construction of a second test rig. This rig is identical to the NASA rig in every respect. The major intent of the second rig is to reduce the time required for the test programs.

Parts procurement for the mainshaft seal test Rig B is complete. Assembly of this rig is approximately 95 percent complete. This rig will be assembled with the orifice compensating hydrostatic face seal (Stein). References to photographs, Figures 44 through 49 will show the seal assembly prior to installation in the rig. Rig assembly should be complete by July 15, 1966.

2.2.2.6 Inert Gas Test Rig

This rig will be a modification, as shown in Figure 50, of either Rig A or Rig B and will allow the best seal to be operated in a nitrogen atmosphere as specified in the contract.

Procurement of parts necessary to convert the mainshaft seal test rig in the inert gas configuration is continuing with approximately 95 percent of the parts received. This rig will be assembled after the endurance testing phase of the program has been completed.

2.2.2.7 Instrumentation Validation Rig

A current Pratt & Whitney Aircraft seal test rig (see Figure 51) has been modified to develop the instrumentation techniques necessary to measure the seal-face-generated torque and seal axial forces.

Procurement of all parts necessary to build this rig is complete. All parts were available during June 1966. The rig was assembled in June and is now mounted on a test stand and is being readied to run. Initial testing will commence during July 1966.

Photographs of this rig prior to complete assembly are shown in Figures 52 through 54.

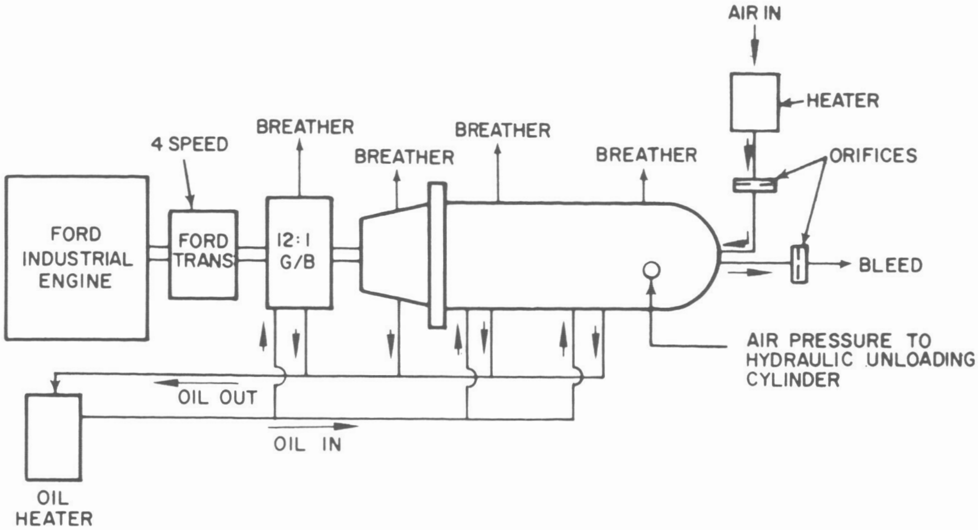

Figure 21 Schematic Diagram of Test Facilities X-81 Stand

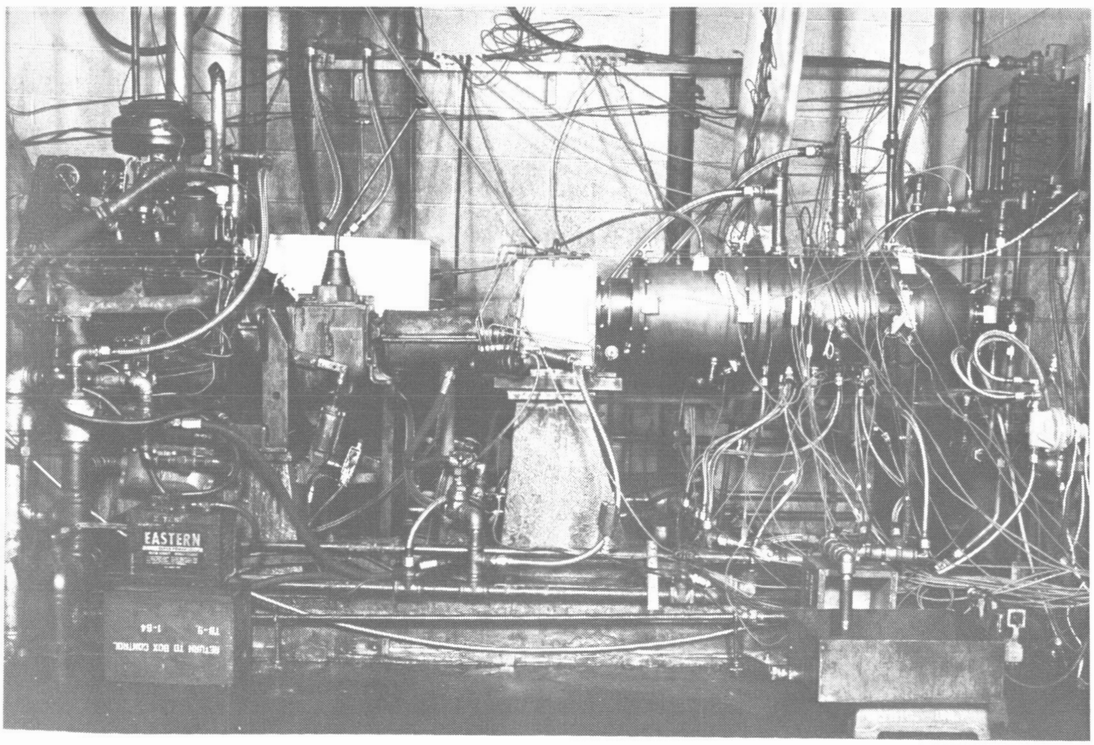

Figure 22 Mainshaft Seal Rig 29360 - Overall View of Interior of X-81 Stand Showing Test Rig, Gear Box and Drive Engine CN-5980

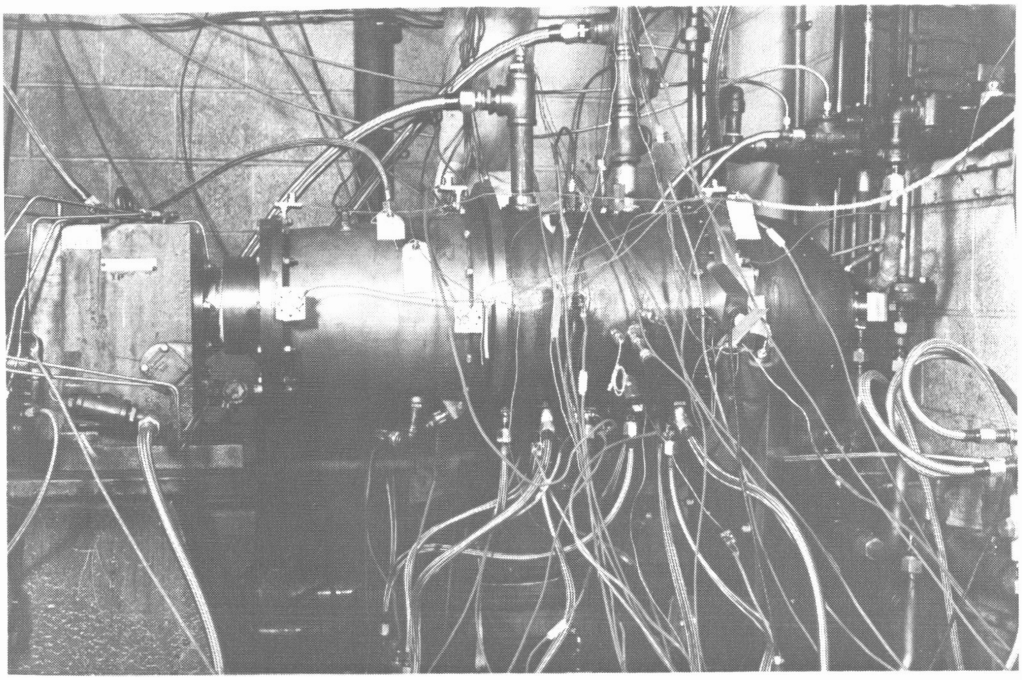

Figure 23 Mainshaft Seal Rig 29360 - Close-Up of Test Rig and Gear Box As Mounted in X-81 Test-Stand CN-5982

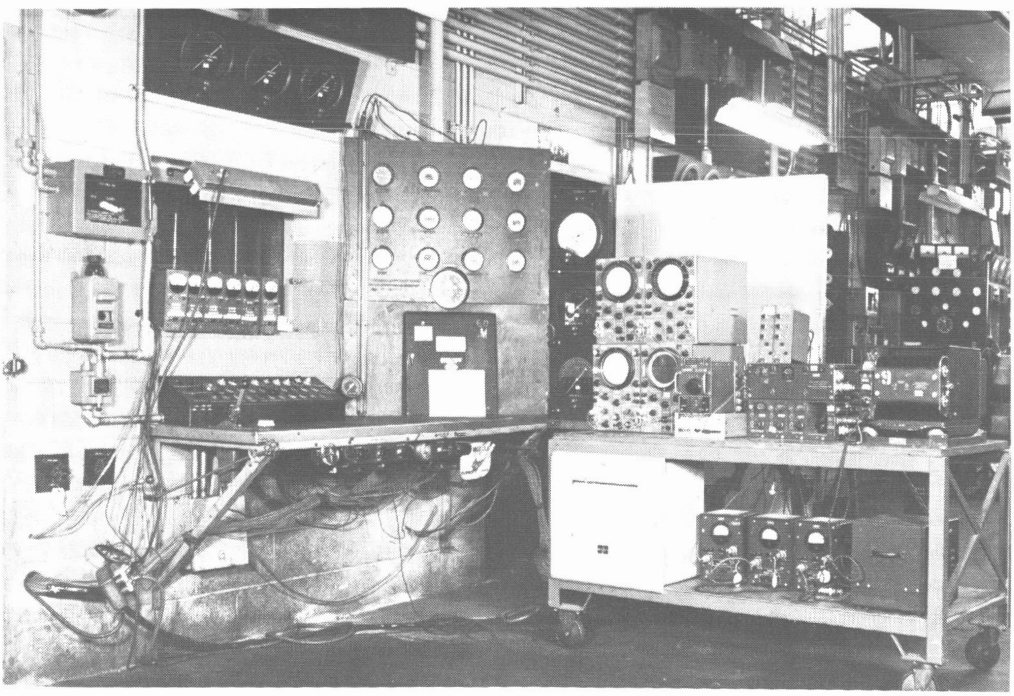

Figure 24 Mainshaft Seal Rig 29360 - View of X-81 Stand Control Panel and Specialized Instrumentation Required for NASA Contract. CN-5981

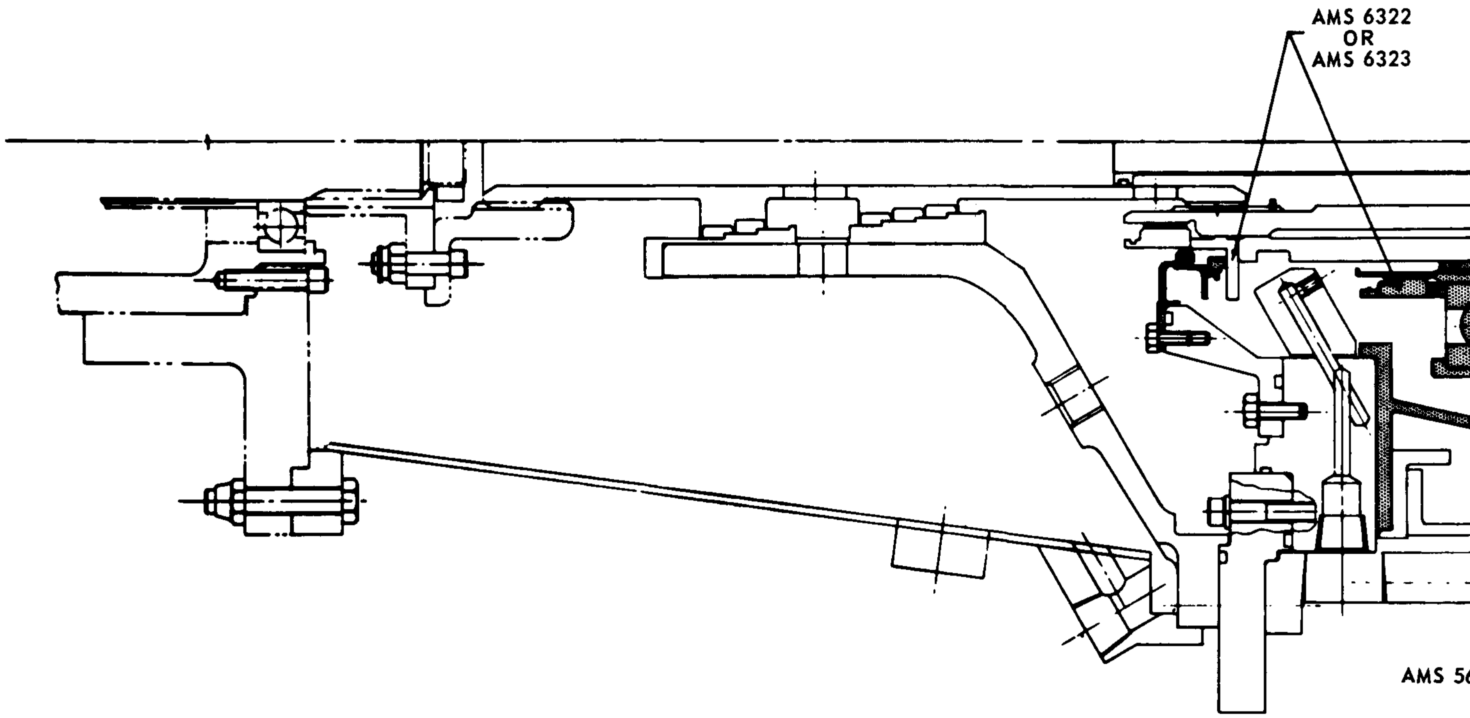
AMS 6322
OR
AMS 6323
AMS 56

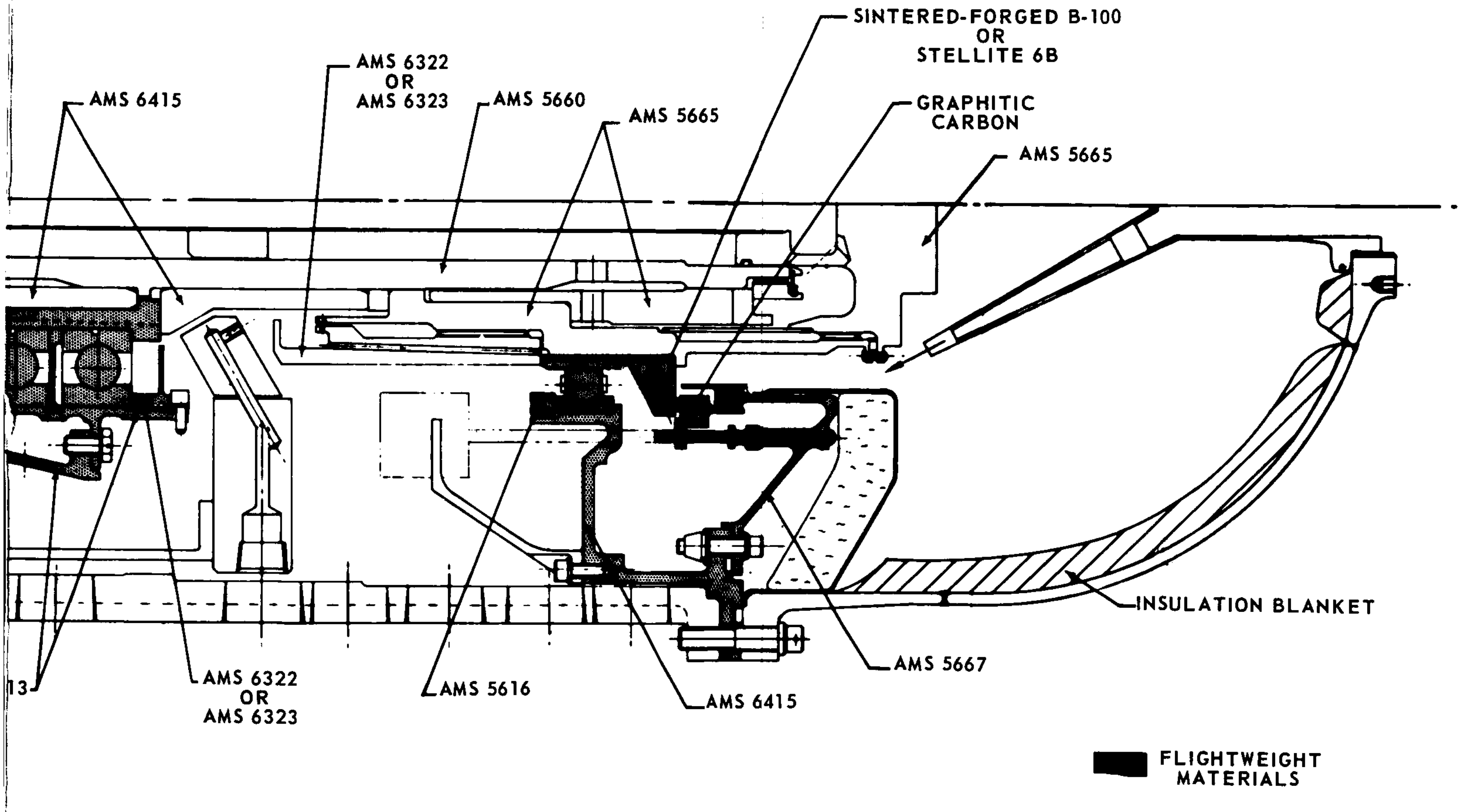

Figure 25 Rig Layout Showing Materials Used

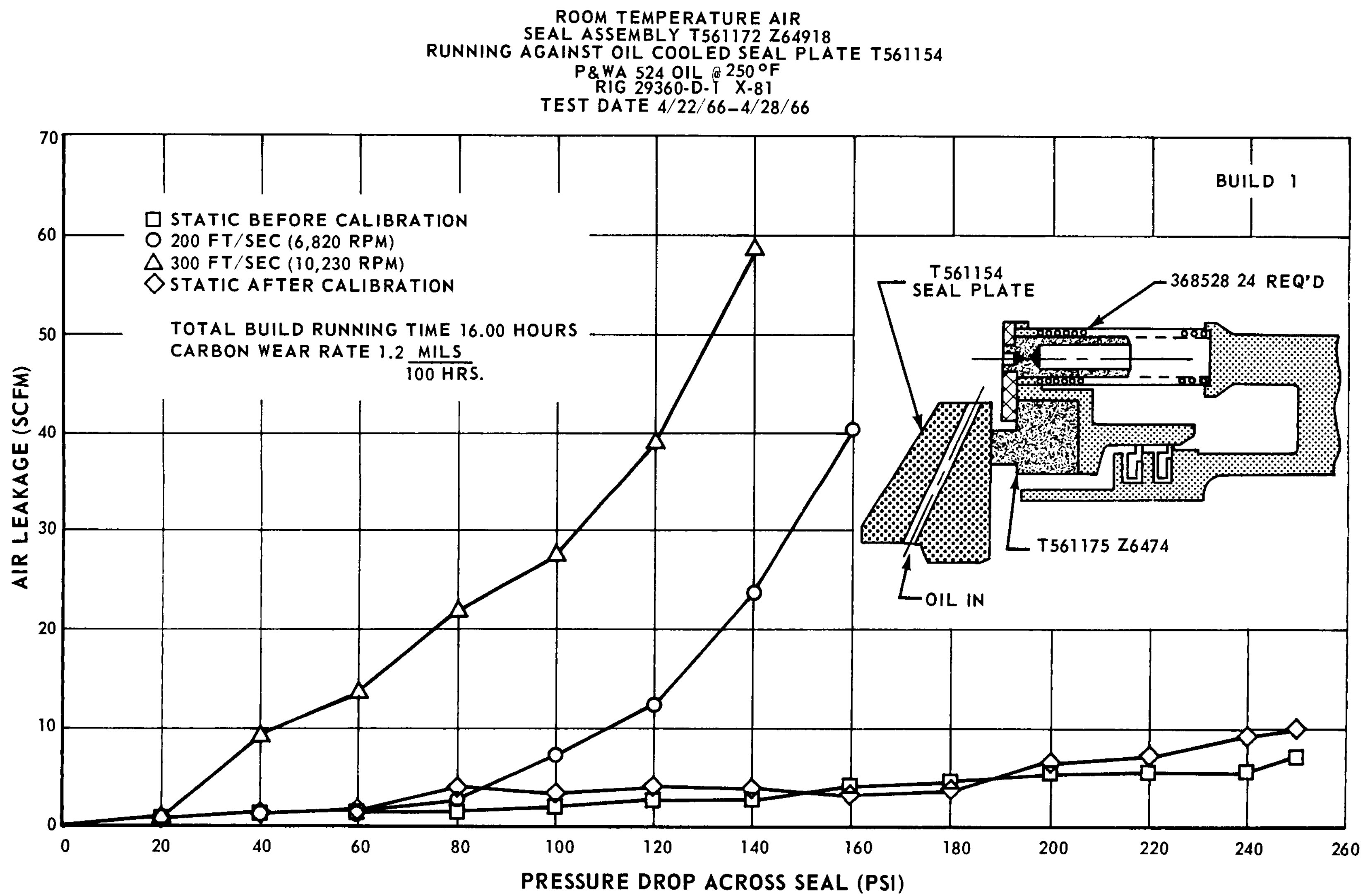

Figure 26 Preliminary Dynamic Checkout Program P&WA Rubbing Contact Seal With Piston Ring Secondary Leakage Calibration - Build 1

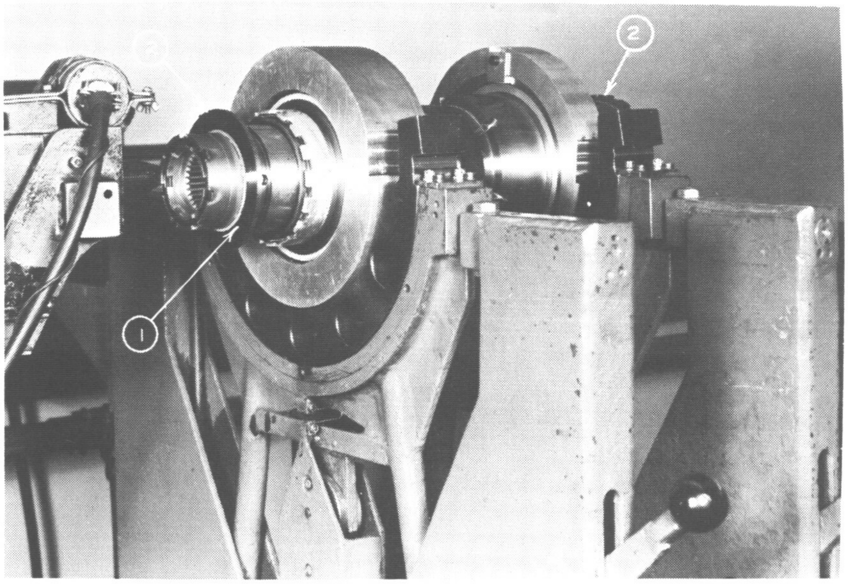

Figure 27 Mainshaft Seal Rig 29360 - Shaft Assembly in Gisholt Dynetric Balance Machine Supports During Balance Operation. Note: 1. Speed Indication Band. 2. Balancing Planes.

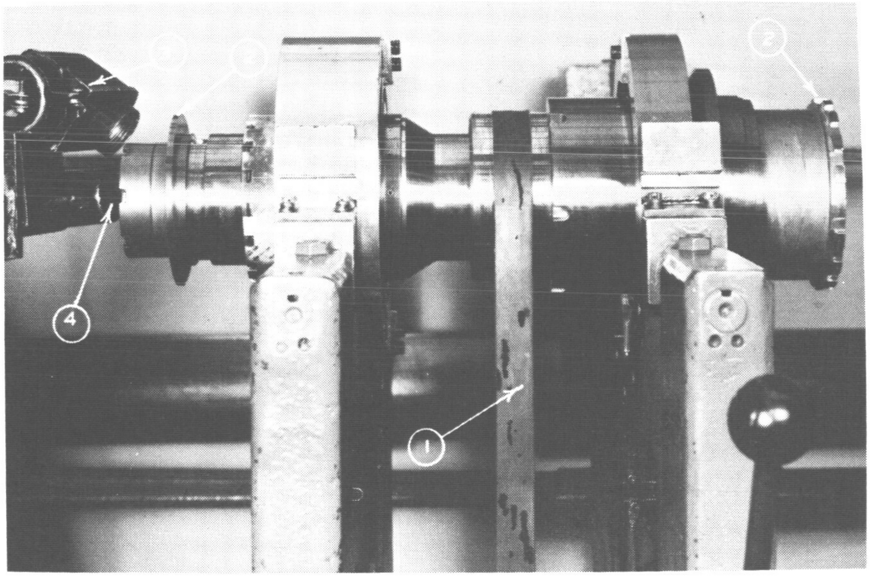

Figure 28 Mainshaft Seal Rig 29, 360 - Shaft Assembly in Gisholt Dynetric Balance Machine Supports During Balance Operation. Note: 1. Belt Drive. 2. Correction Planes. 3. Photo-Cell Compensator. 4. Speed Pickup

XP-62916

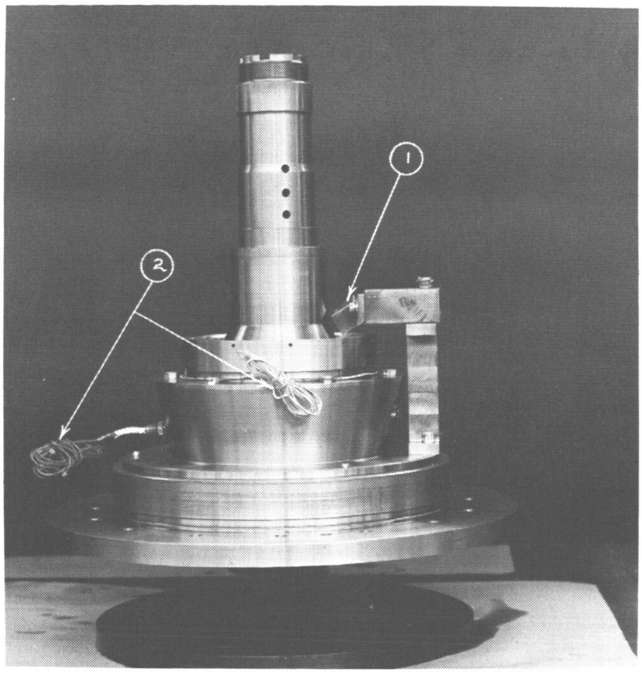

Figure 29 Mainshaft Seal Rig 29,360 - View of Shaft and Rear Bearing Support Assembly. Note: 1. Jet to Front Hub Axial Scoop Supplying Roller Bearing Under Race and Seal Plate Cooling Oil. 2. Bearing Outer Race T/C's. XP-63612

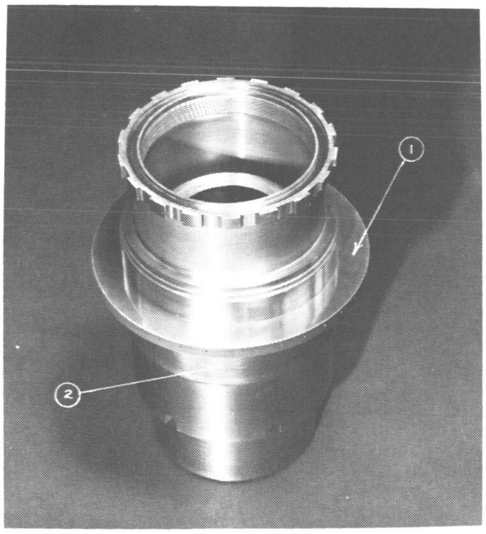

Figure 30 Mainshaft Seal Rig 29,360 - Front Hub Assembly Prior to Final Assembly of Rig. Note: 1. PWA 771 Seal Plate With LCIC Hardface. 2. Roller Bearing Inner Race. XP-63613

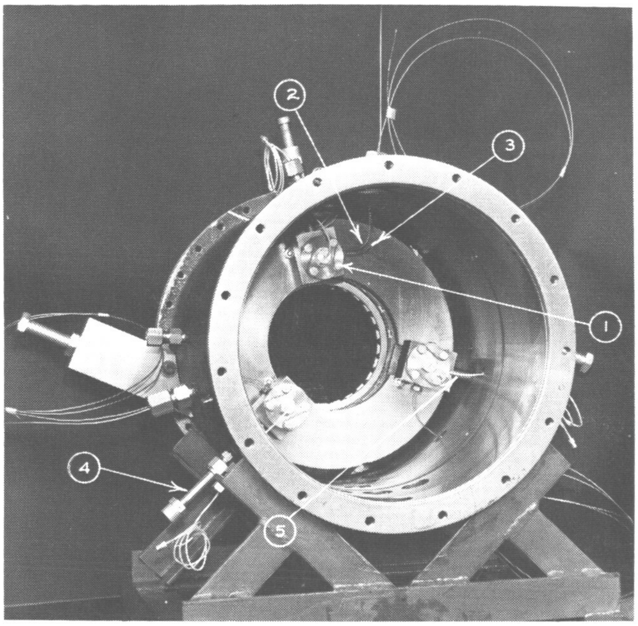

Figure 31 Mainshaft Seal Rig 29,360 - Rear View of Instrumentation Support Assembly in Rig Housing. Note: 1. Hydraulic Load Cylinder. 2. Cylinder T/C Lead. 3. Cylinder Pressure Tap. 4. Pressurizing Tube. 5. Proximity Probe Lead. XP-63614

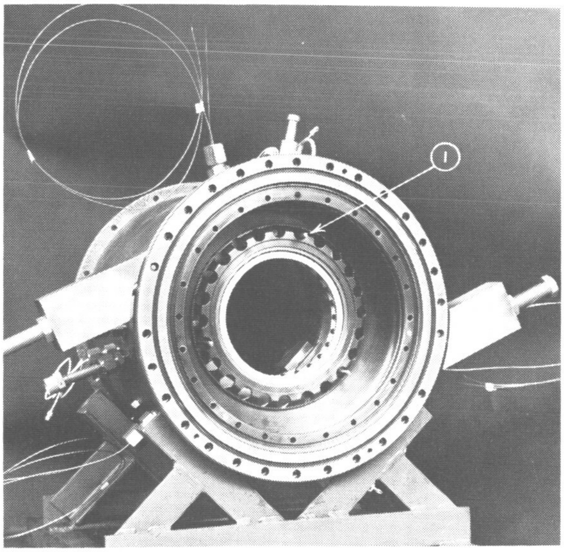

Figure 32 Mainshaft Seal Rig 29,360 - Front View of Outer Case Showing Roller Bearing Support. Note: 1. Hydraulic Loading Piston Push Rods. XP-63616

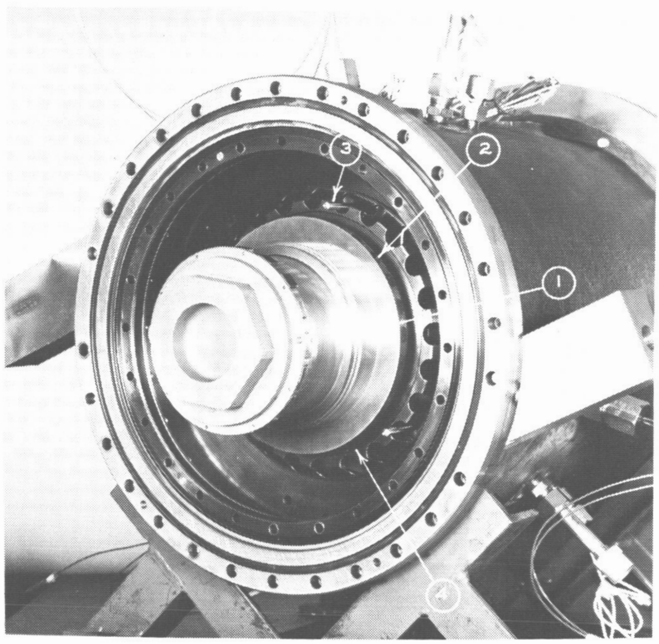

Figure 33 Mainshaft Seal Rig 29,360 - Rig Hub Assembly Prior to Installation of the Test Seal Assembly. Note: 1. PWA 771 Seal Plate With LCIC Hardface. 2. Oil Cooling Holes. 3. Hydraulic Loading Piston Push Rod. 4. Roller Bearing Support. XP-63733

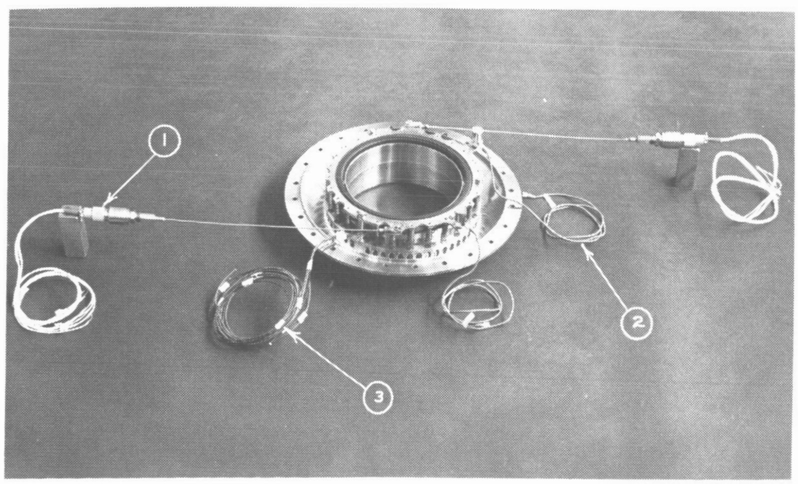

Figure 34 Mainshaft Seal Rig 29,360 - P&WA Rubbing Contact Seal With Piston Ring Secondary Assembly Shown With Instrumentation Installed. Note: 1. Transducers to Measure Generated Torque at Seal Interface. 2. Accelerometers. 3. Seal Housing and Carbon T/C's. XP-63615

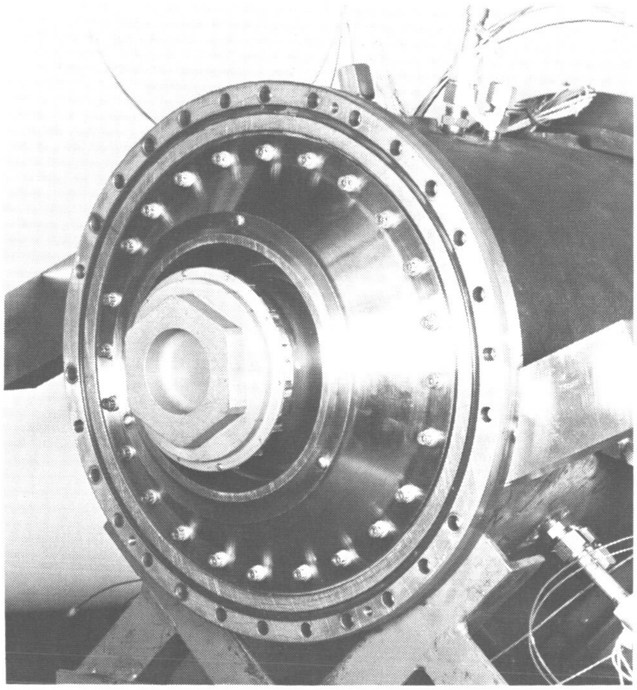

Figure 35 Mainshaft Seal Rig 29, 360 - Front View of Rig With the Seal Assembly Installed XP-63731

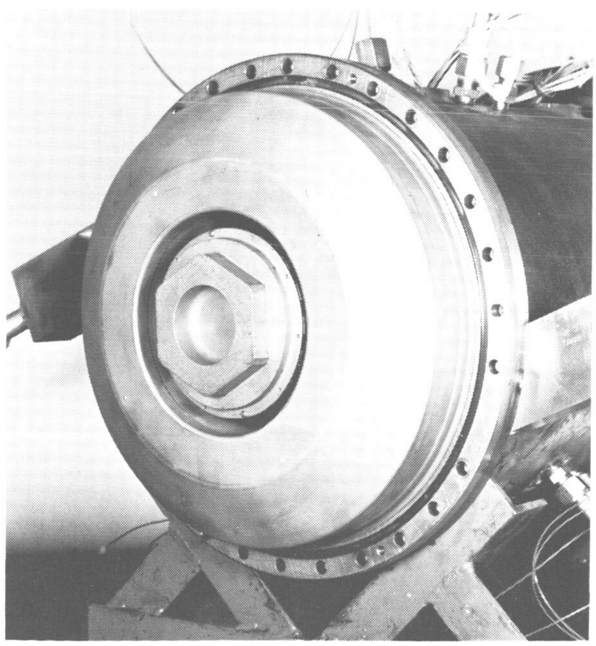

Figure 36 Mainshaft Seal Rig 29, 360 - Front View of Rig With The Insulation Shield Installed Over the Seal Assembly Support. XP-63732

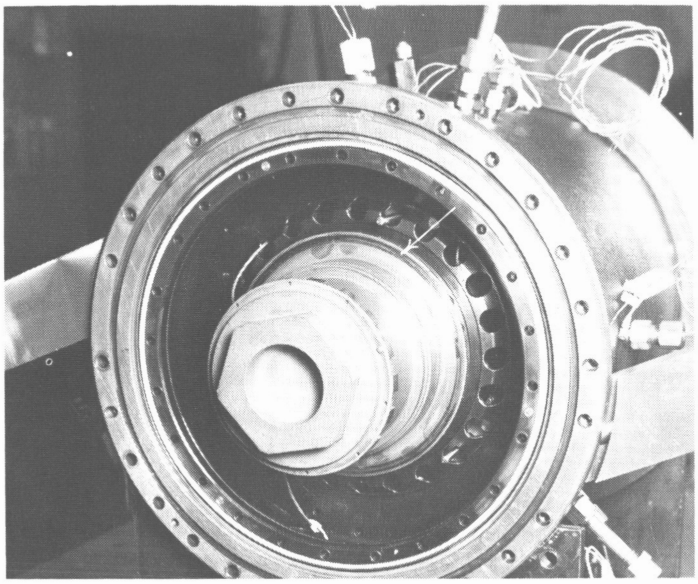

Figure 37 Mainshaft Seal Rig 29,360 - Rig Hub Assembly After 16.0 Hours Running of the Preliminary Dynamic Checkout Program on the P&WA Rubbing Contact Seal With Piston Ring Secondary. Note: Carbon Wear Path on Seal Plate XP-64577

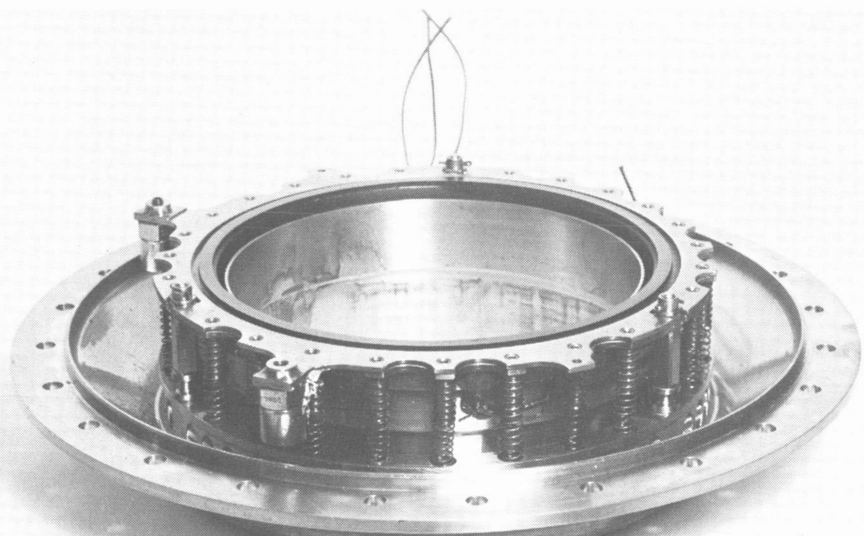

Figure 38 Mainshaft Seal Rig 29,360 - P&WA Rubbing Contact Seal With Piston Ring Secondary After 16.0 Hours Running of the Preliminary Dynamic Checkout Program. XP-64578

Figure 39 Mainshaft Seal Rig 29,360 - PWA 771 Seal Plate With LCIC Hardface After 16.0 Hours Running of the Preliminary Dynamic Checkout Program against the P&WA Rubbing Contact Seal With Piston Ring Secondary. Note: Carbon Lip Wear Path on the Seal Plate.

XP-64666

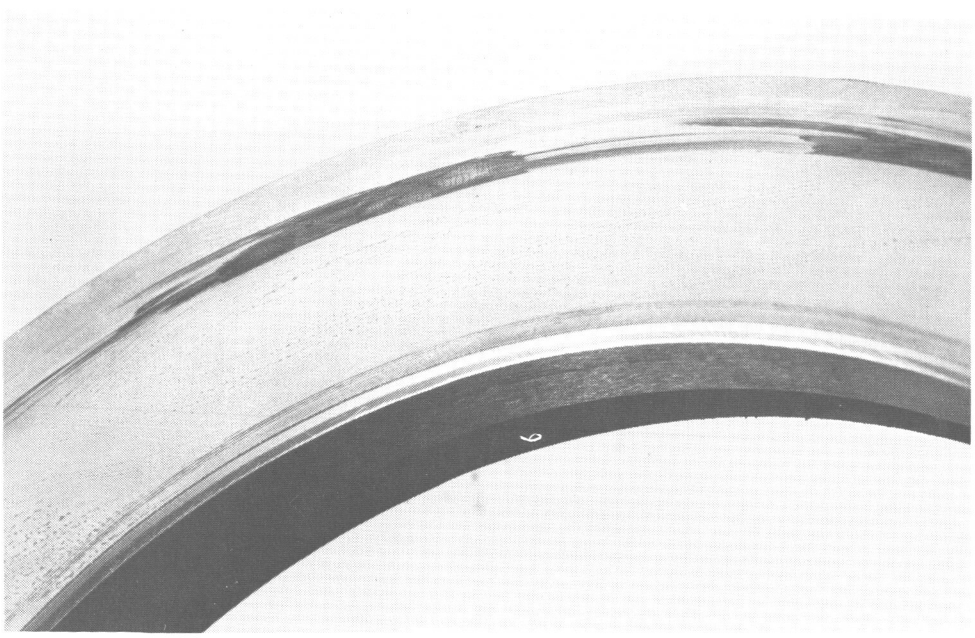

Figure 40 Mainshaft Seal Rig 29,360 - Close-Up View of Carbon Lip Wear Path on the PWA 771 Seal Plate with LCIC Hardface.

XP-64668

Figure 41 Mainshaft Seal Rig 29, 360 - Rear View of the Oil Cooled Seal Plate Showing Oil Scoop With Oil Inlet Holes. Note: Deposits on O. D. of Scoop After 16. 0 Hours of Running. XP-64667

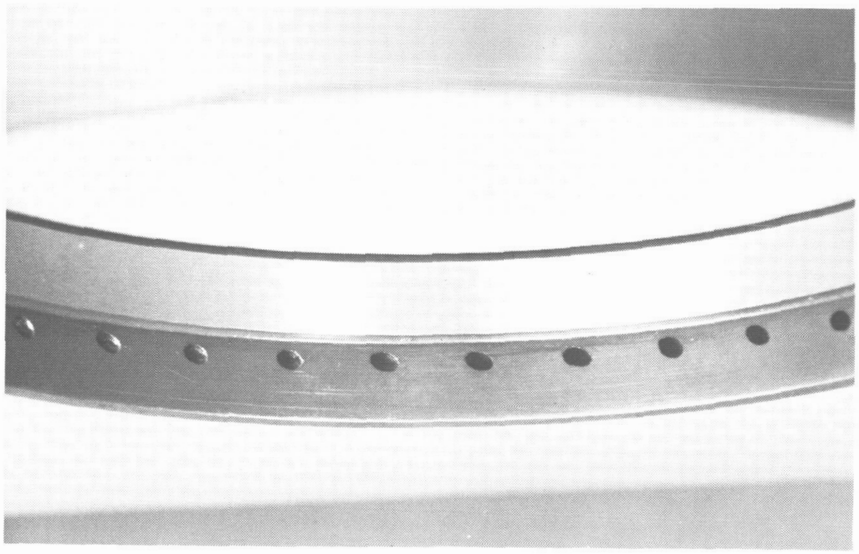

Figure 42 Mainshaft Seal Rig 29360 - Rear View of the Oil Cooled Seal Plate Showing Oil Scoop With the Enlarged Oil Inlet Holes. XP-65050

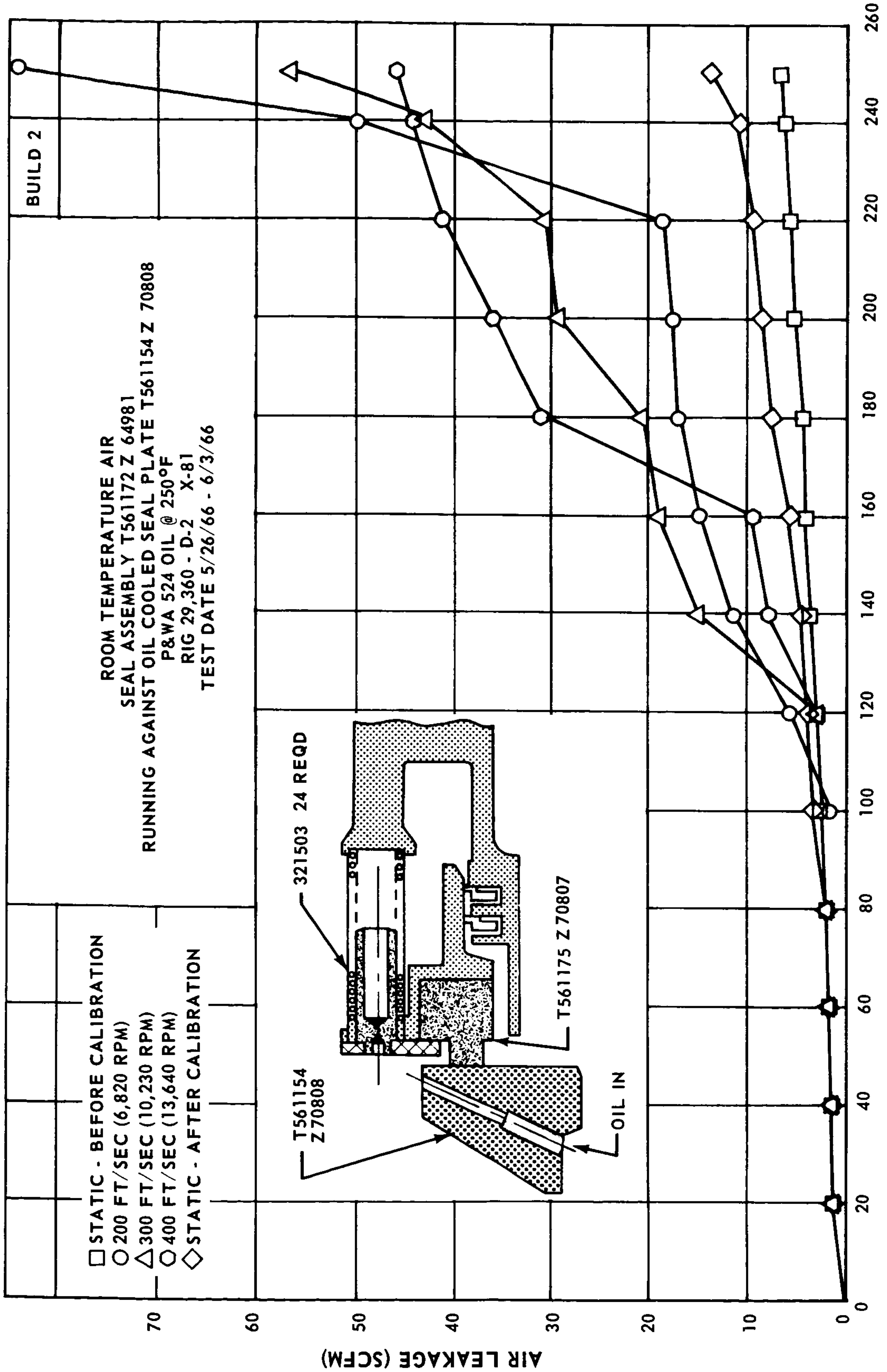

Figure 43 Preliminary Dynamic Checkout Program P&WA Rubbing Contact Seal With Piston Ring Secondary Leakage Calibration - Build 2

Figure 44 Mainshaft Seal Rig 29360 B Build 1. Front Hub Assembly Prior to Final Assembly. Note: 1. AMS 6322 Seal Plate With LF-2 Hardface. 2. Windback Shroud. XP-66911

Figure 45 Mainshaft Seal Rig 29360 B. Build 1. Front Hub Assembly Prior to Final Assembly. Note: 1. Solid Collar AMS 6322 Seal Plate With LF-2 Hardface. 2. Windback Shroud. 3. Windback Screw Threads. 4. Oil Scoop Outlet Holes. 5. Roller Bearing Inner Race. XP-66912

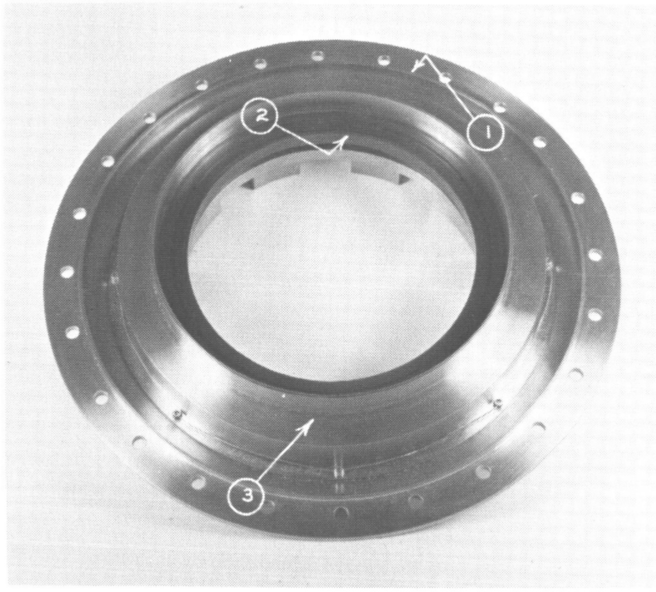

Figure 46 Mainshaft Seal Rig 29360 B. Build 1. Stein Seal Company Orifice Compensating Hydrostatic Face Seal With Piston Rig Secondary. Note: 1. Carrier. 2. Seal Ring Assembly. 3. Assembly Guard.
XP-66913

Figure 47 Mainshaft Seal Rig 29360 B - Build 1. Component Parts of the Stein Seal Company Orifice Compensating Hydrostatic Face Seal with Piston Rig Secondary. Note: 1. Carrier. 2. 18 Springs. 3. Piston Ring. 4. 3 Anti-Rotation Lock Pins. 5. Carbon Carrier Band. 6. Carbon Seal Ring. 7. Assembly Guard.
XP-66914

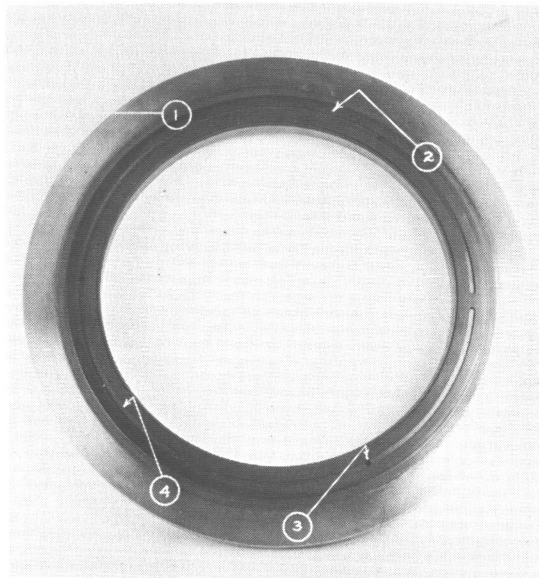

Figure 48 Mainshaft Seal Rig 29360 B - Build 1. Stein Seal Company Orifice Compensating Hydrostatic Carbon Seal Ring Assembly. Note: 1. Carbon Carrier Band. 2. Carbon Seal Ring. 3. Orifice Vent to Seal Face. 4. Annulus. XP-66915

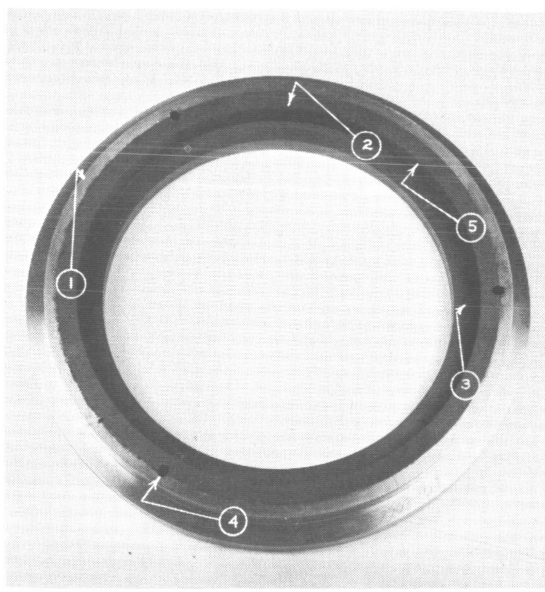

Figure 49 Mainshaft Seal Rig 29360 B - Build 1. Rear Side of Stein Seal Company Orifice Compensating Hydrostatic Carbon Seal Ring Assembly. Note: 1. Carbon Carrier Band. 2. Carbon Seal Ring. 3. Orifice. 4. Hole for Lock Pin. 5. Piston Ring Bore XP-66916

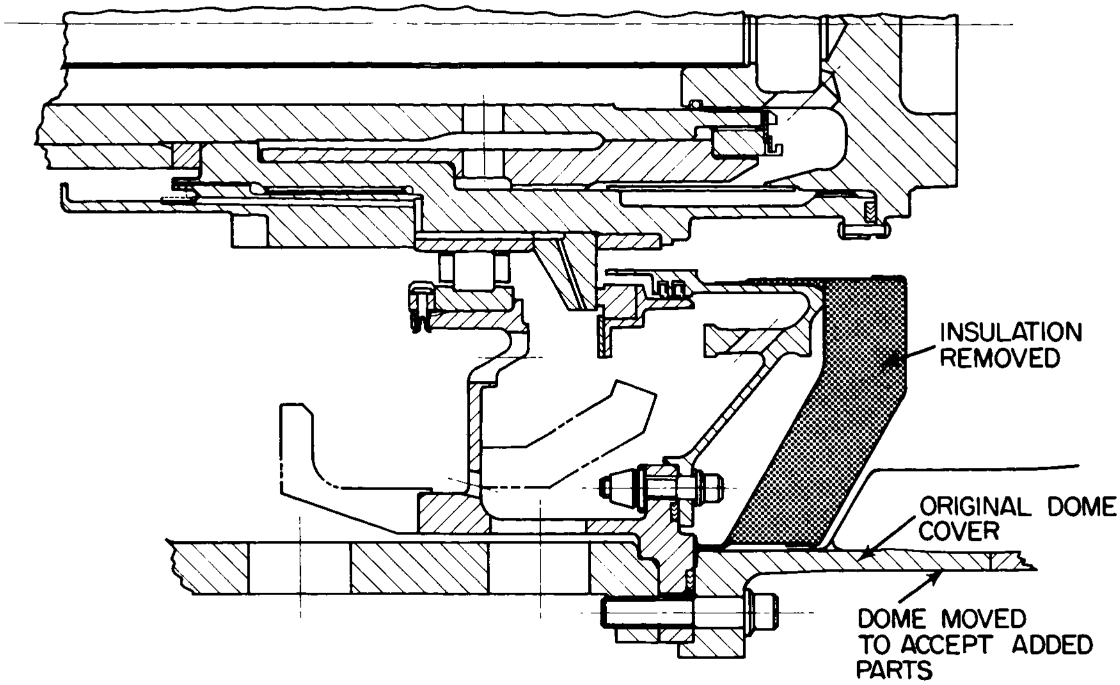

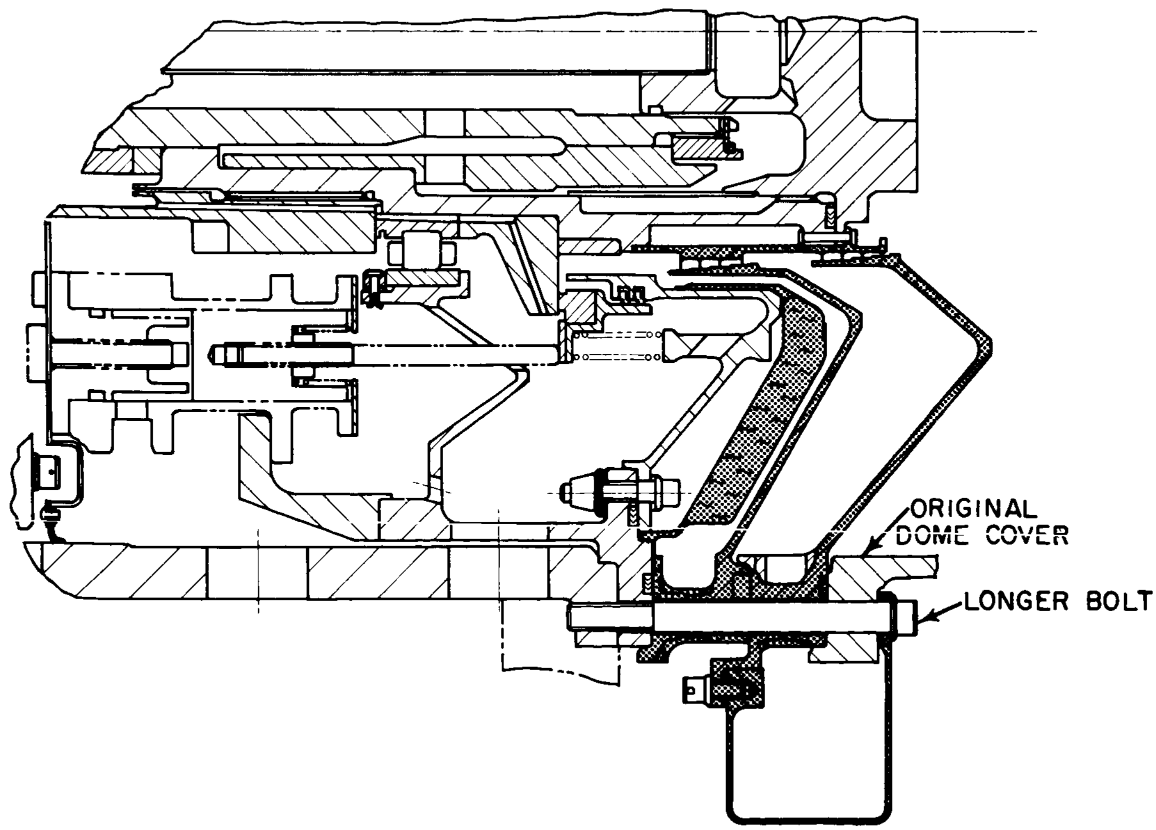

Figure 50 The Shaded Areas of These Two Layouts Illustrates the Changes Made to the Rig to Permit Testing of Seals Using an Inert Gas Blanket on the Oil Sump.

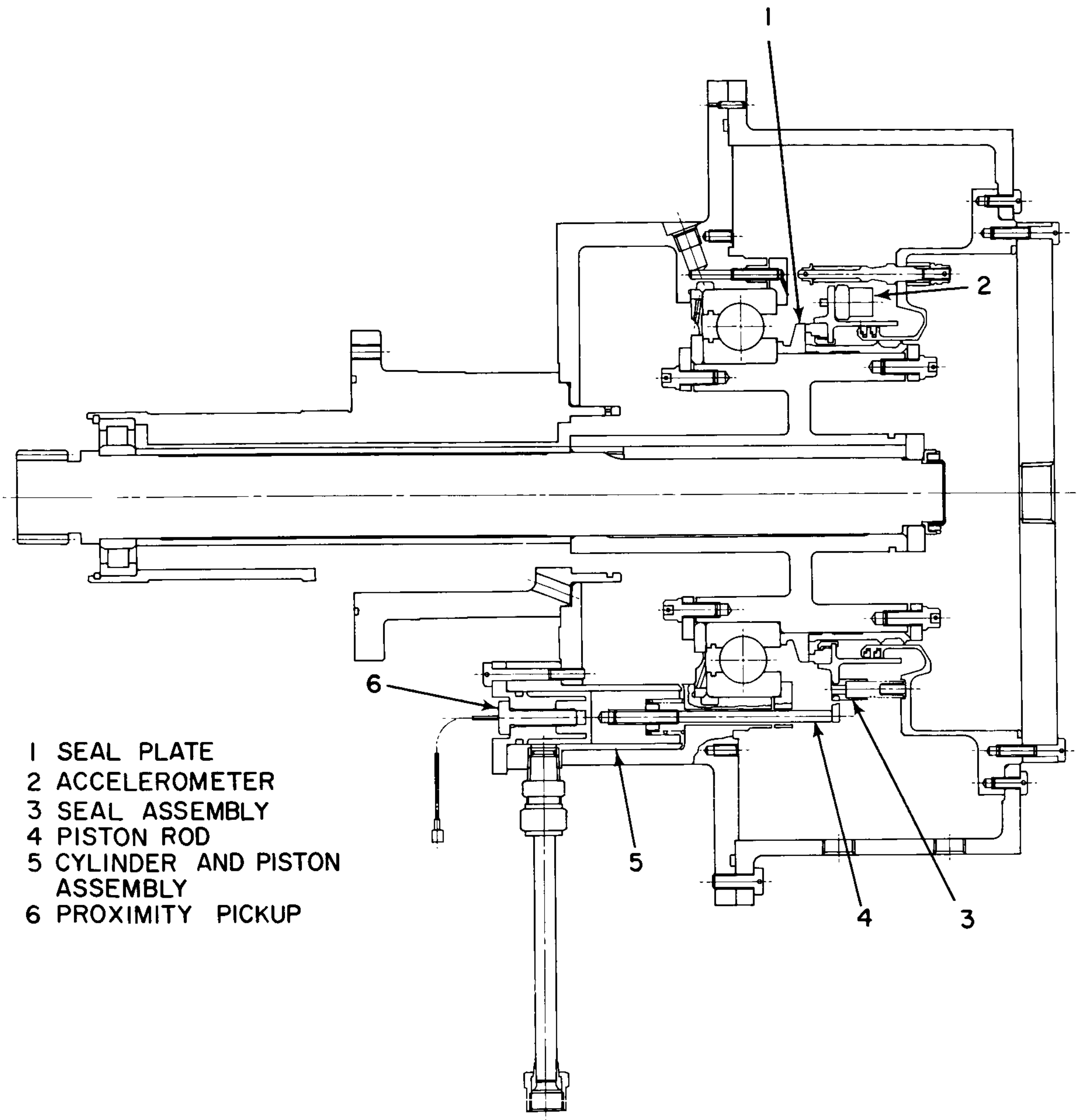

Figure 51 Instrumentation Validation Rig (TL-67996) (Torque Measuring Not Shown) X-4752

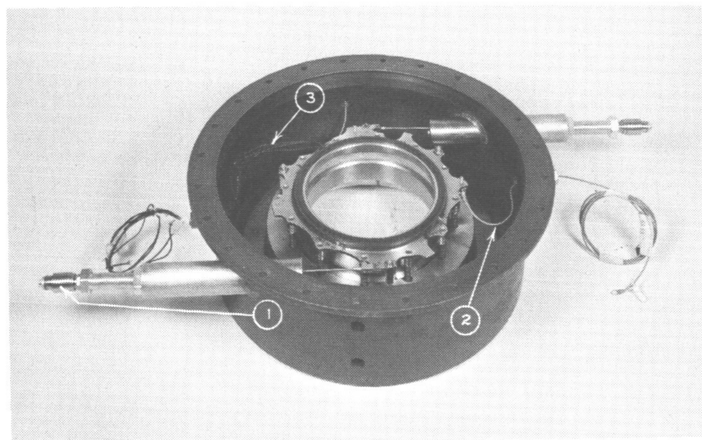

Figure 52 Instrumentation Validation Rig 29401 - Build 1. Test Seal Assembly Installed in Rig Cover. Note: 1. Transducers to Measure Generated Torque at Seal Interface. 2. Accelerometers. 3. Seal Housing and Carbon T/C's. XP-66908

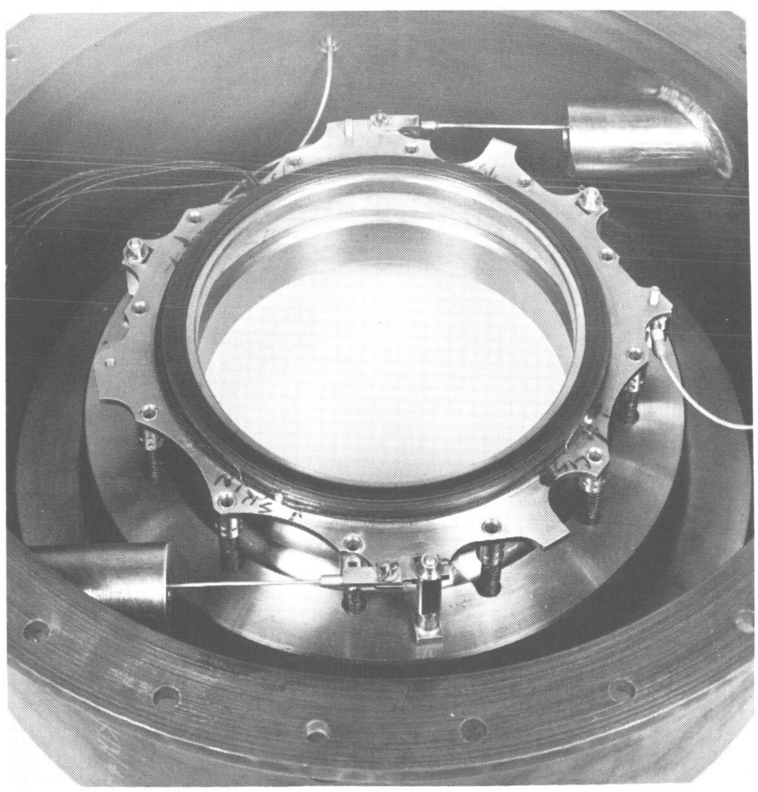

Figure 53 Instrumentation Validation Rig 29401 Build 1. Close-Up of Test Seal Assembly Installed in Rig Cover. XP-66909

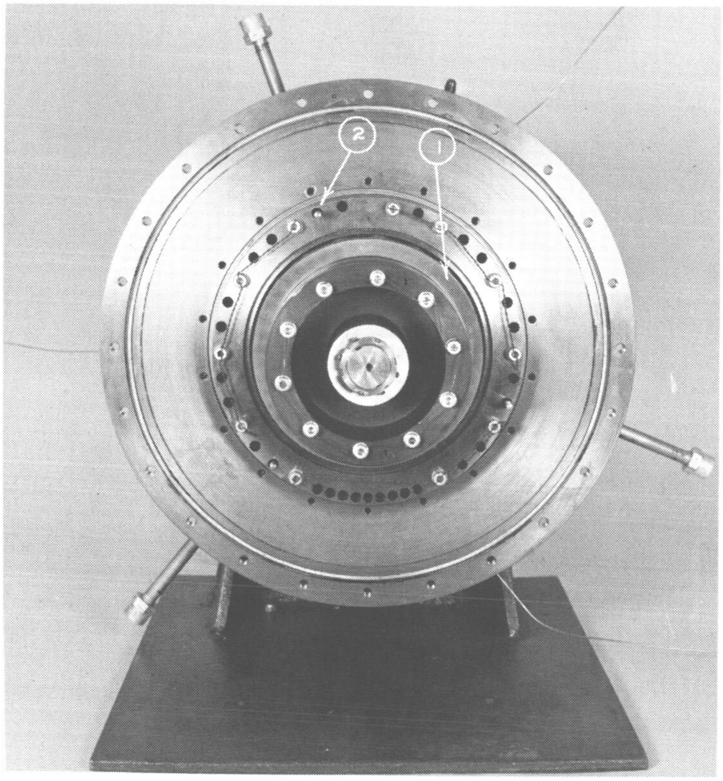

Figure 54 Instrumentation Validation Rig 29401 Build 1. Rig Hub Assembly Prior to Installation of the Test Seal Assembly. Note: 1. AMS 6322 Seal Plate With LCIC Hardface. 2. Hydraulic Loading Piston Push Rod. XP-66910

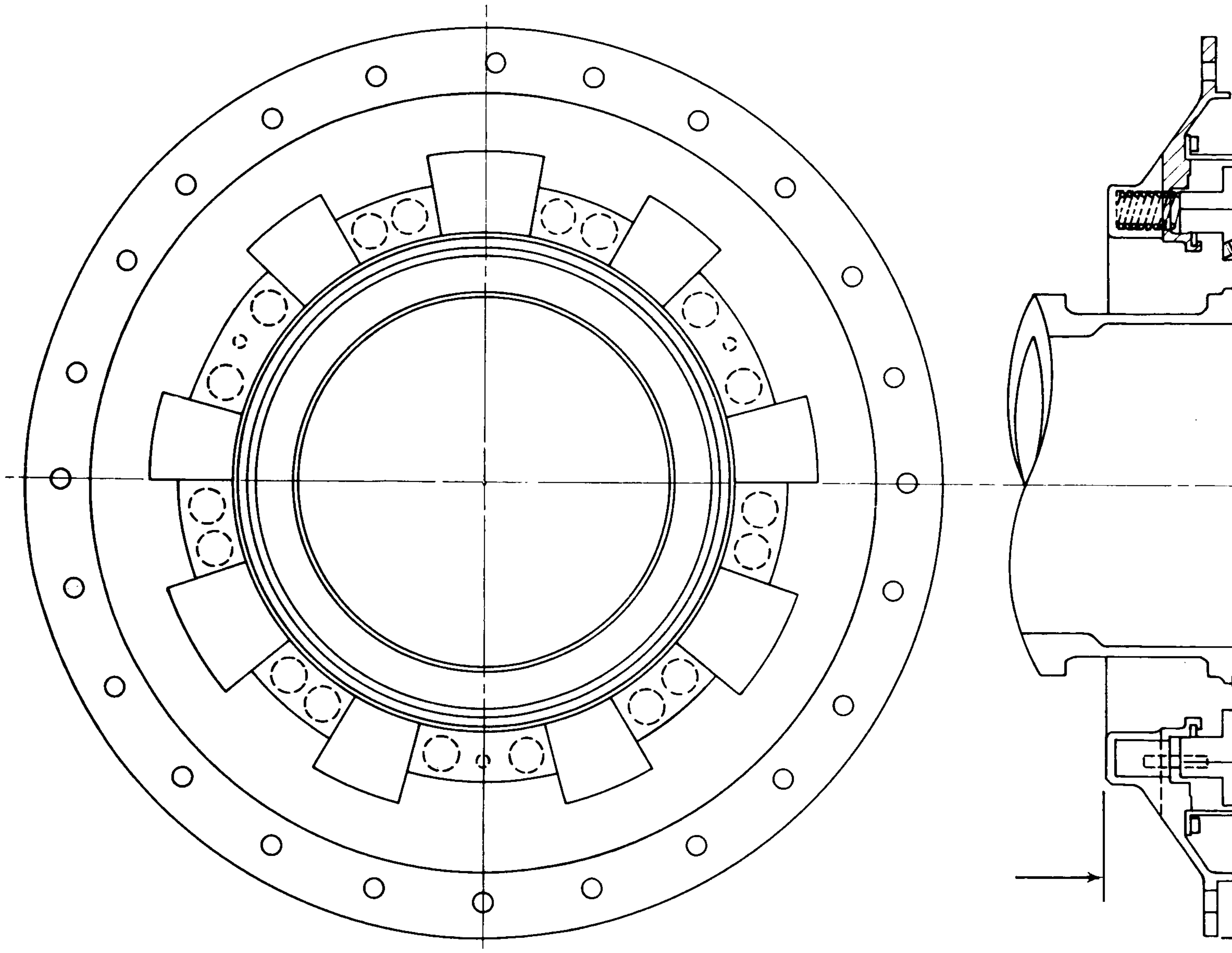

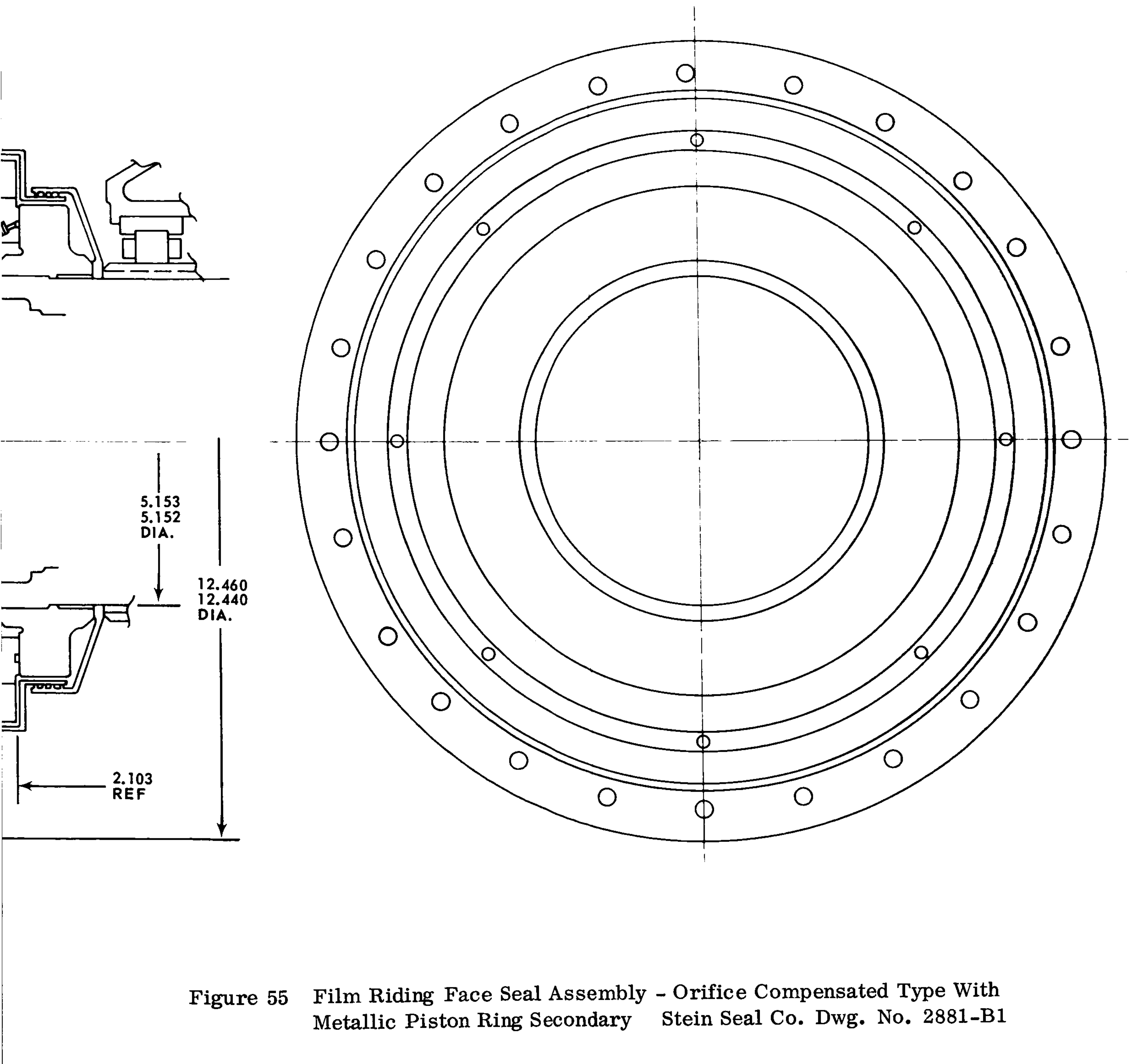

Figure 55 Film Riding Face Seal Assembly - Orifice Compensated Type With Metallic Piston Ring Secondary Stein Seal Co. Dwg. No. 2881-B1

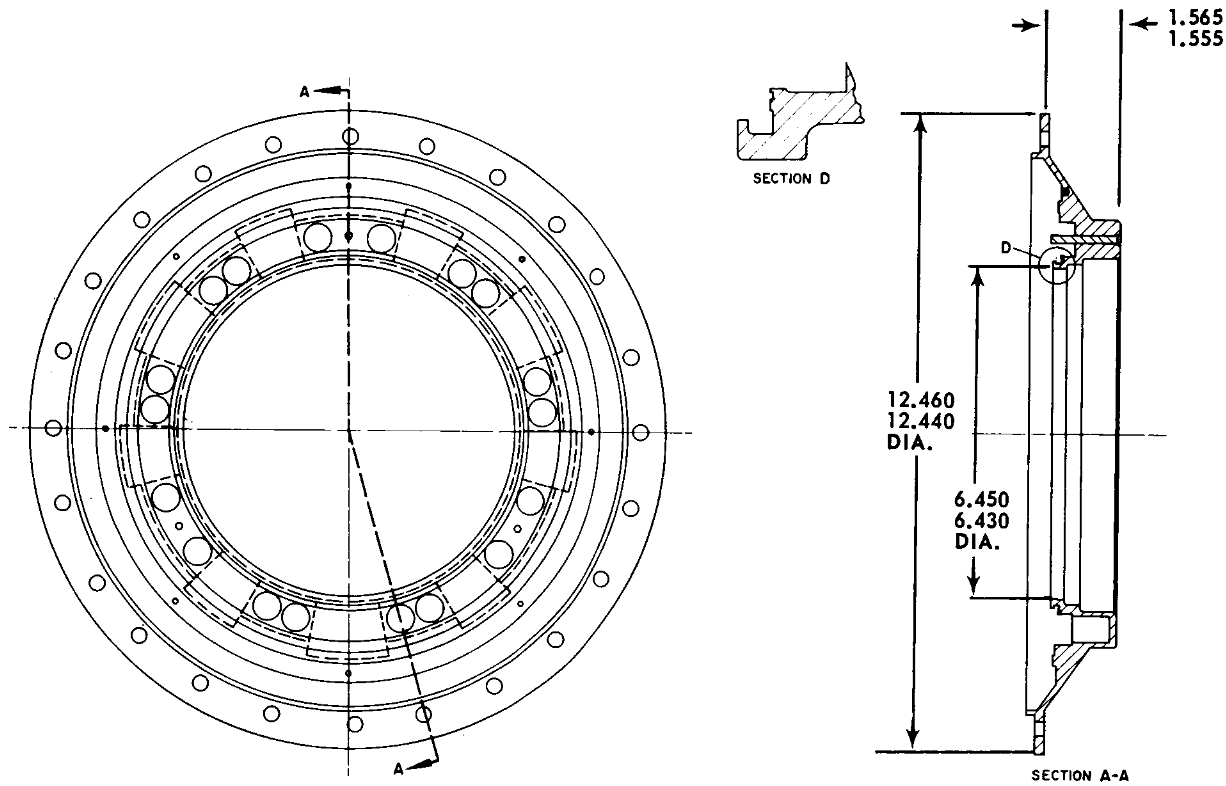

Figure 56 Seal Carrier For Orifice Compensated Seal
PWA Dwg. No. SKZ-70722-C

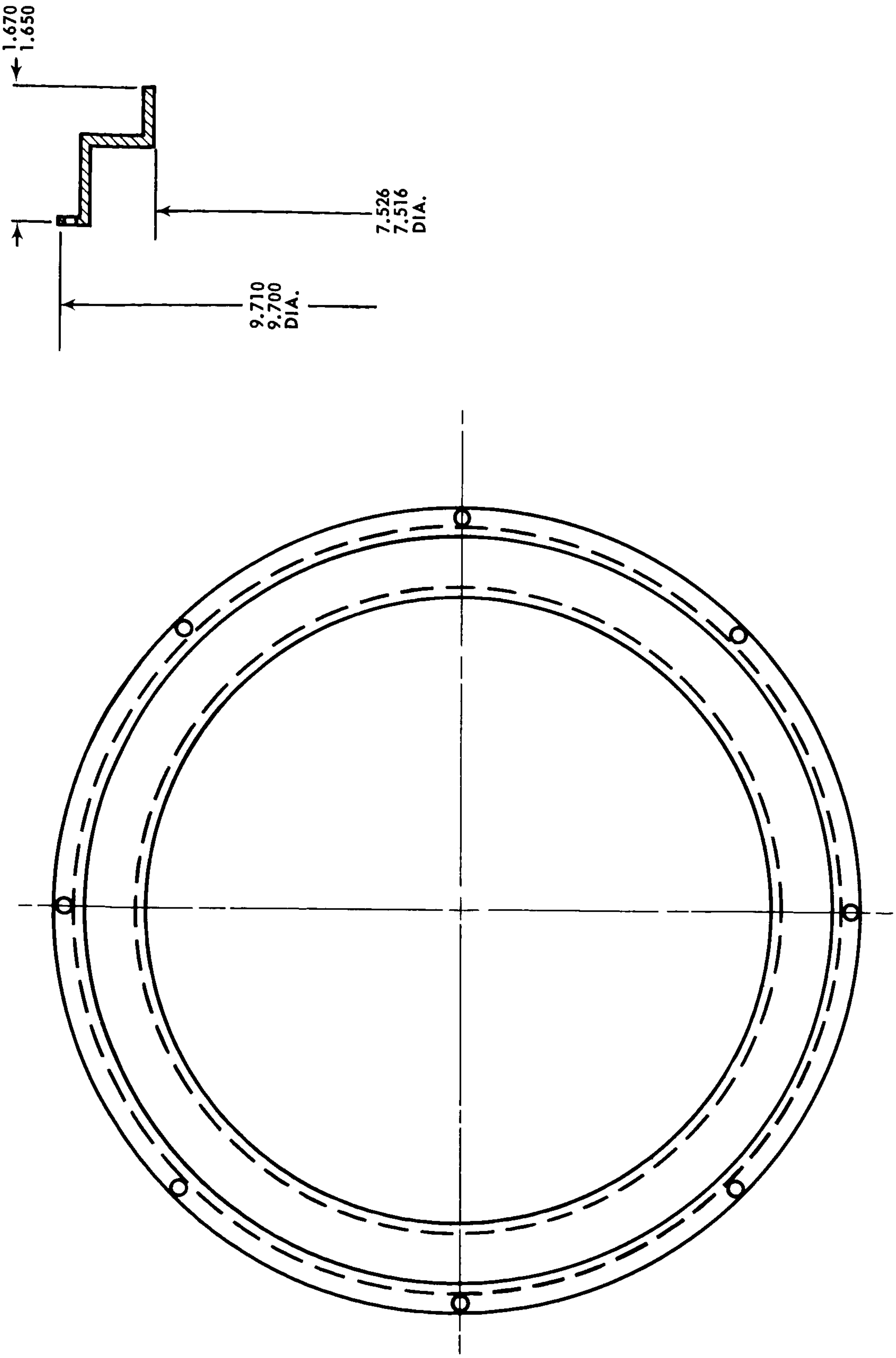

Figure 57 Assembly Guard For Orifice Compensated Seal
PWA Dwg No. SKZ-70716-C

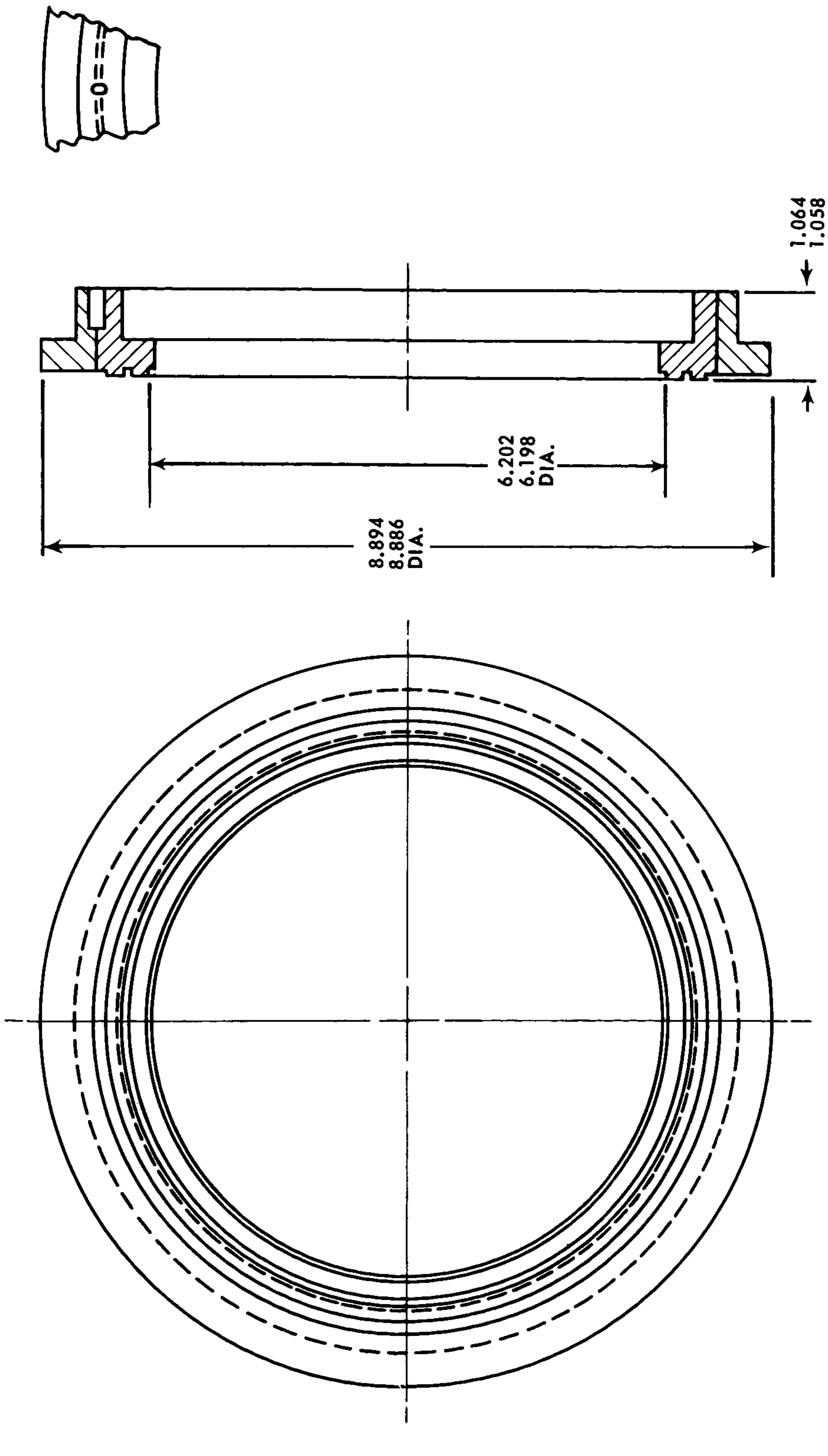

Figure 58 Seal Assembly For Orifice Compensated Seal
PWA Dwg. No. SKZ-70721-C

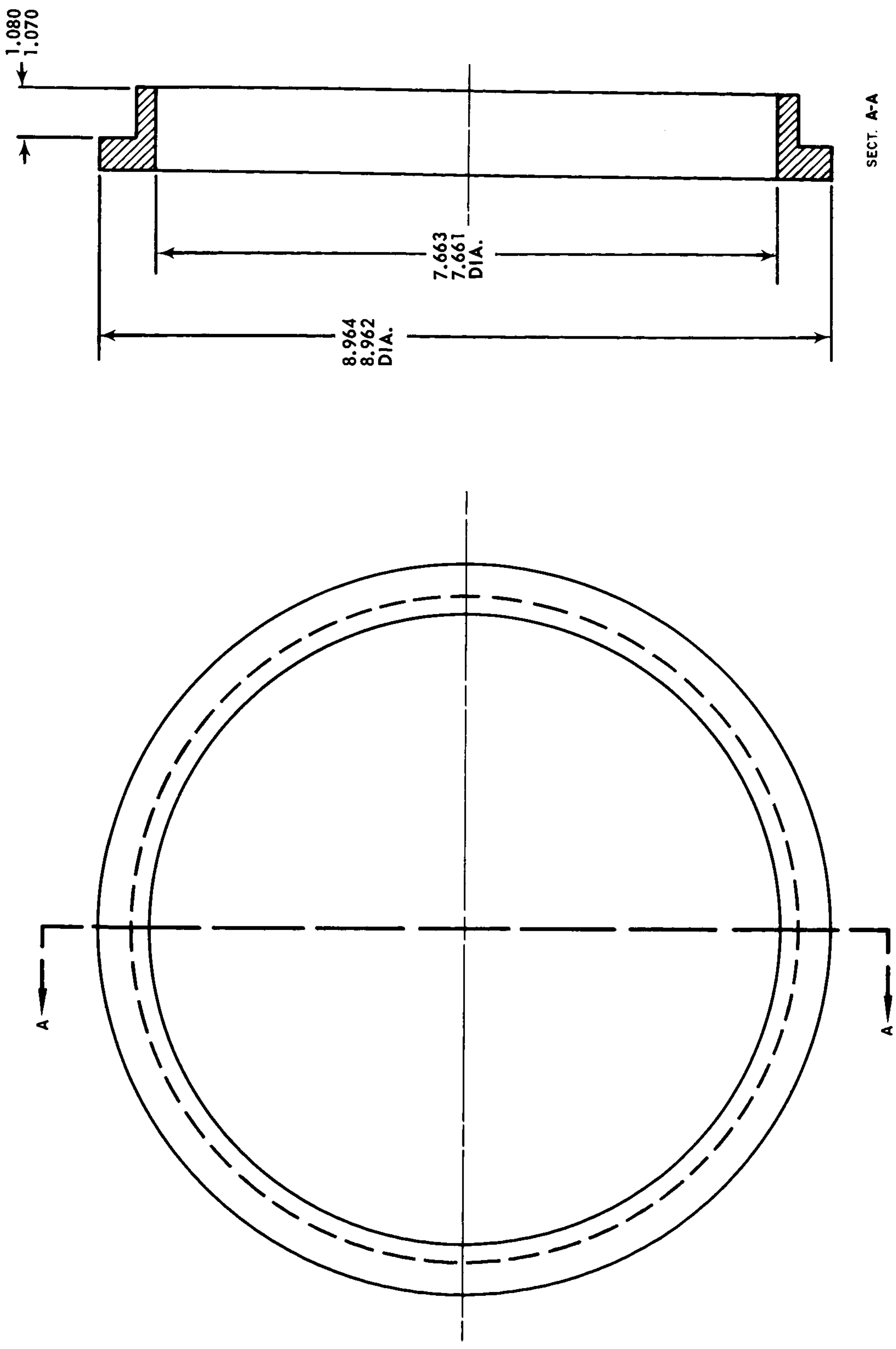

Figure 59 Steel Band For Orifice Compensated Seal
PWA Dwg. No. SKZ-70719-C

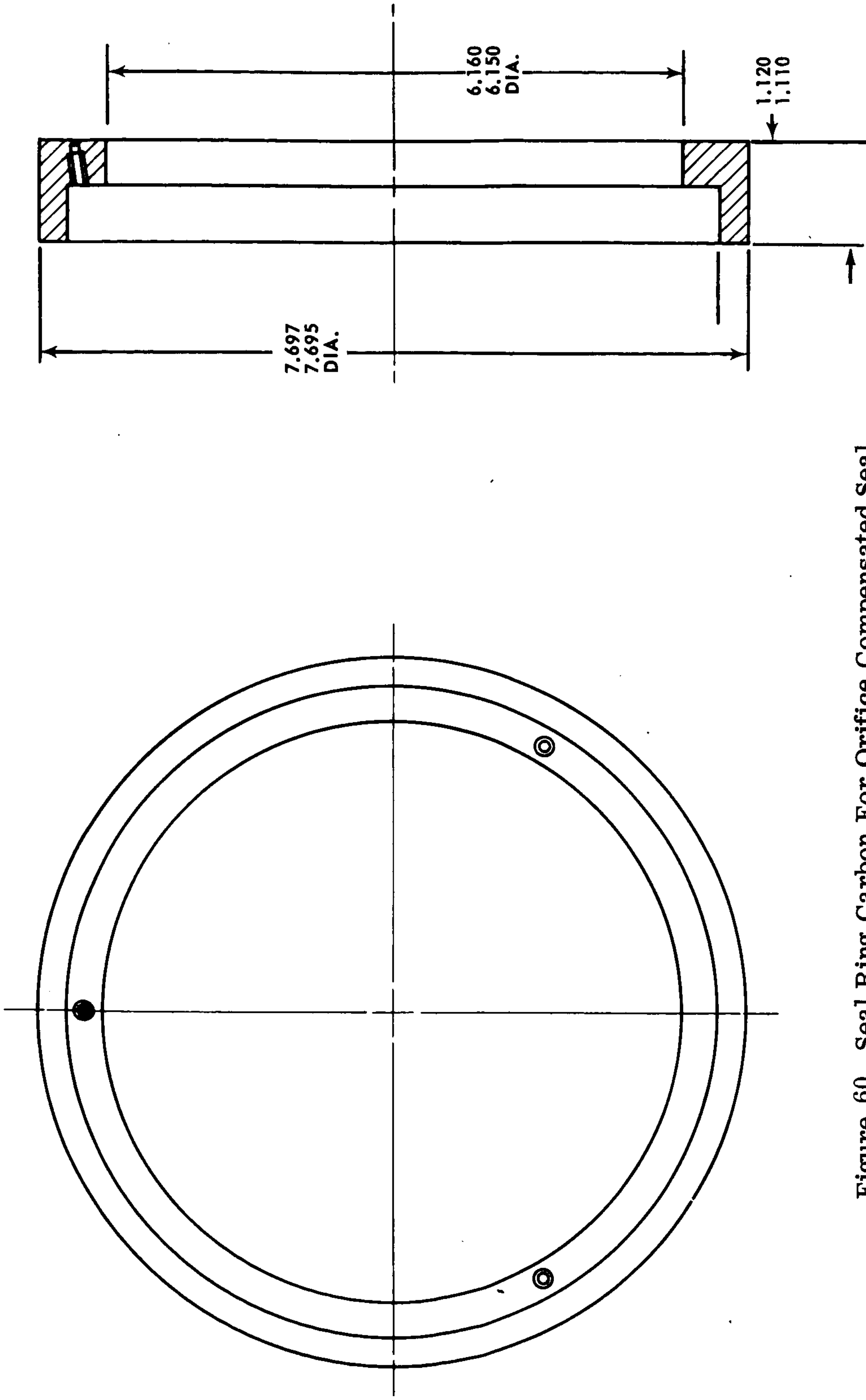

Figure 60 Seal Ring Carbon For Orifice Compensated Seal
PWA Dwg. No. SKZ-70717-C

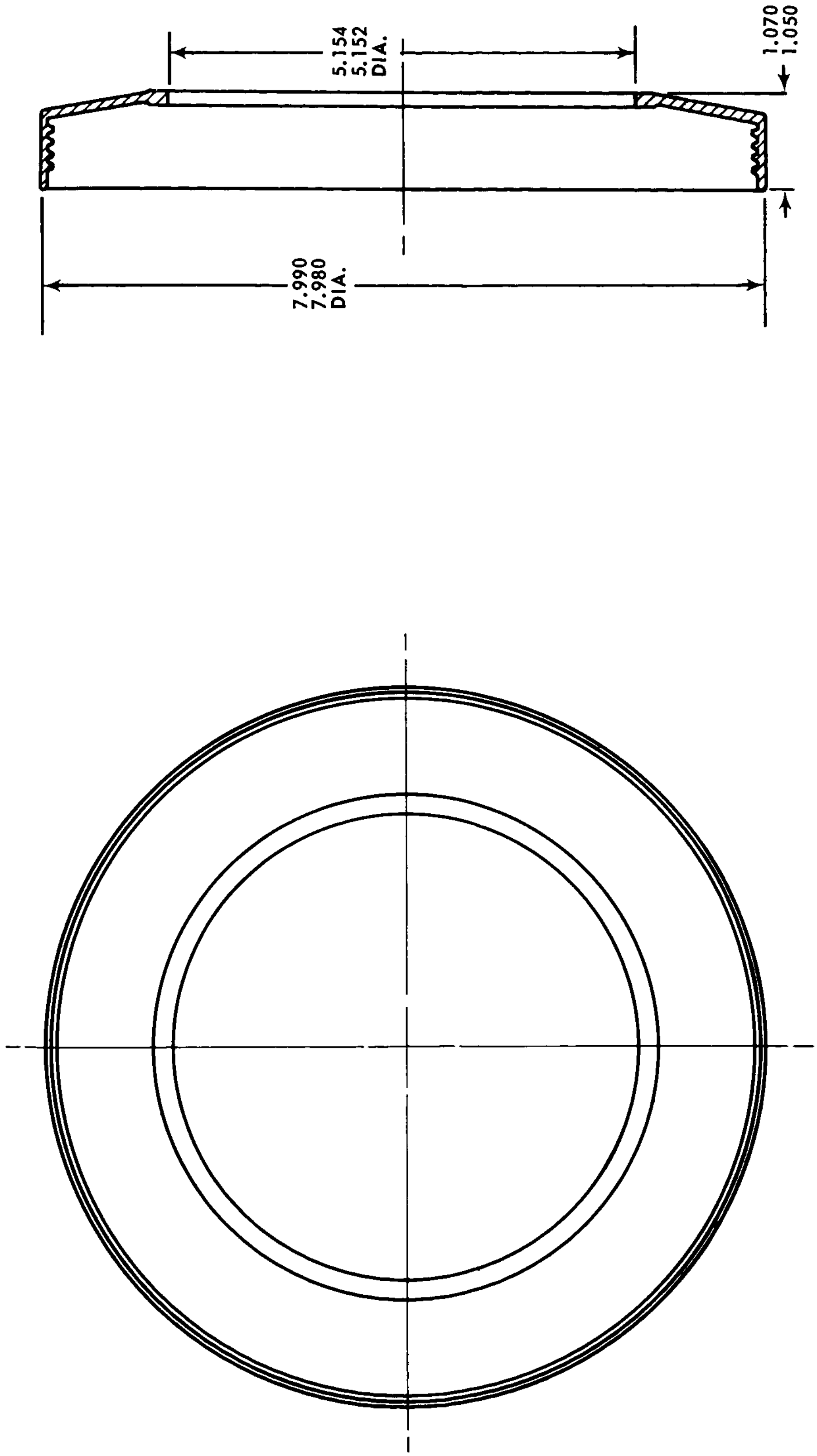

Figure 61 Shroud Windback For Orifice Compensated Seal
PWA Dwg. No. SKZ-70714-C

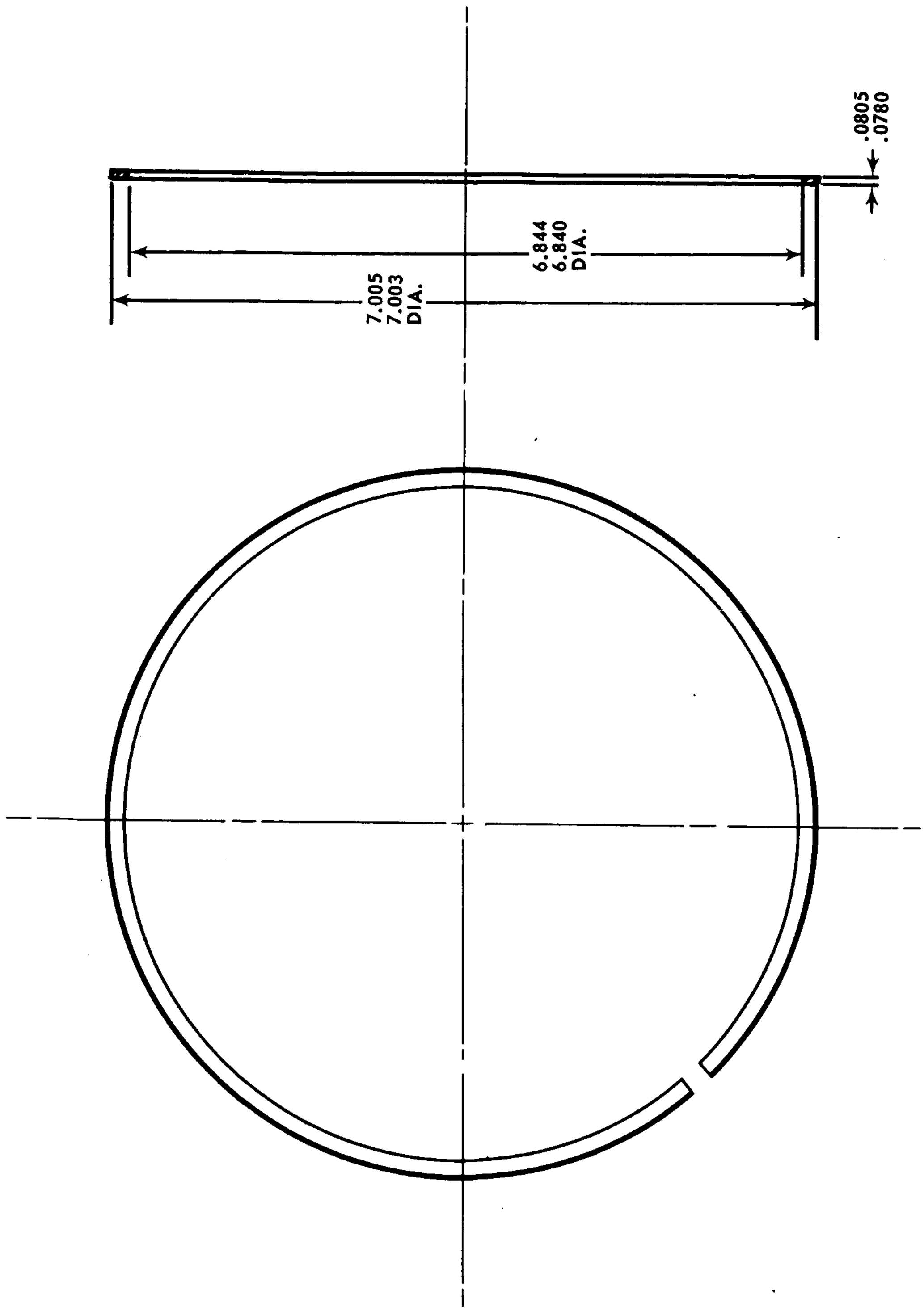

Figure 62 Piston Ring For Orifice Compensated Seal
PWA Dwg. No. SKZ-70715-C

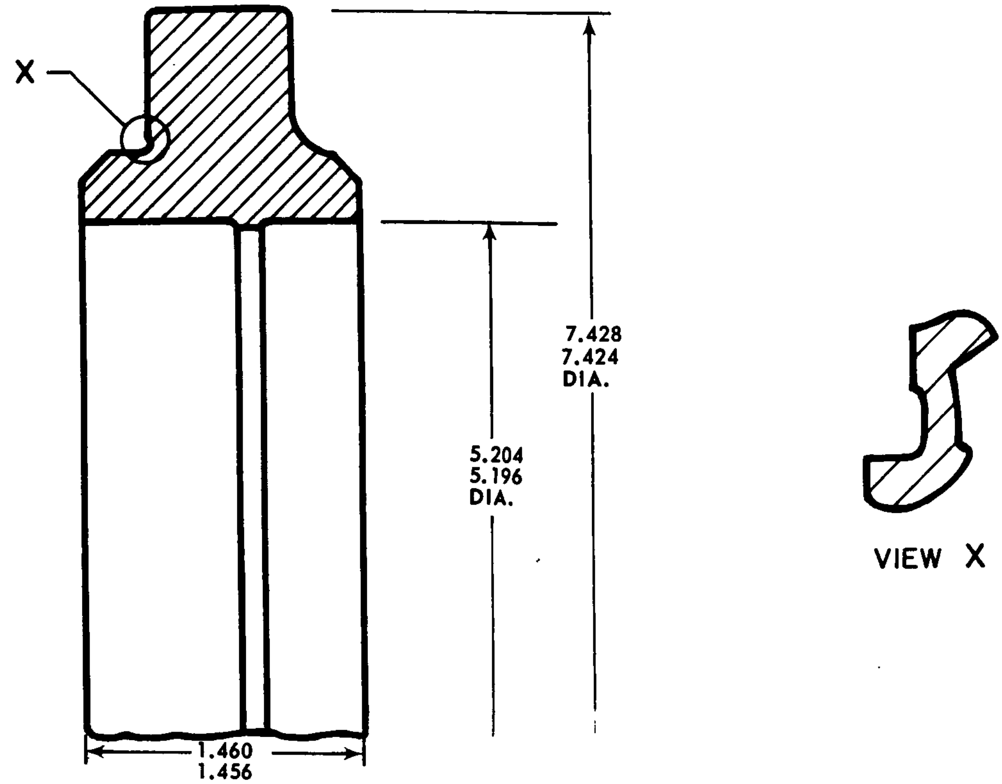

Figure 63 Seal Plate For Orifice Compensated Seal

PWA Dwg. No. SKZ-70711-C

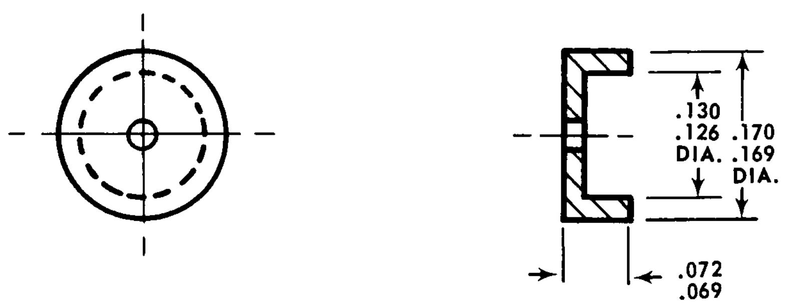

Figure 64 Orifice For Orifice Compensated Seal

PWA Dwg. No. SKZ 70713-C

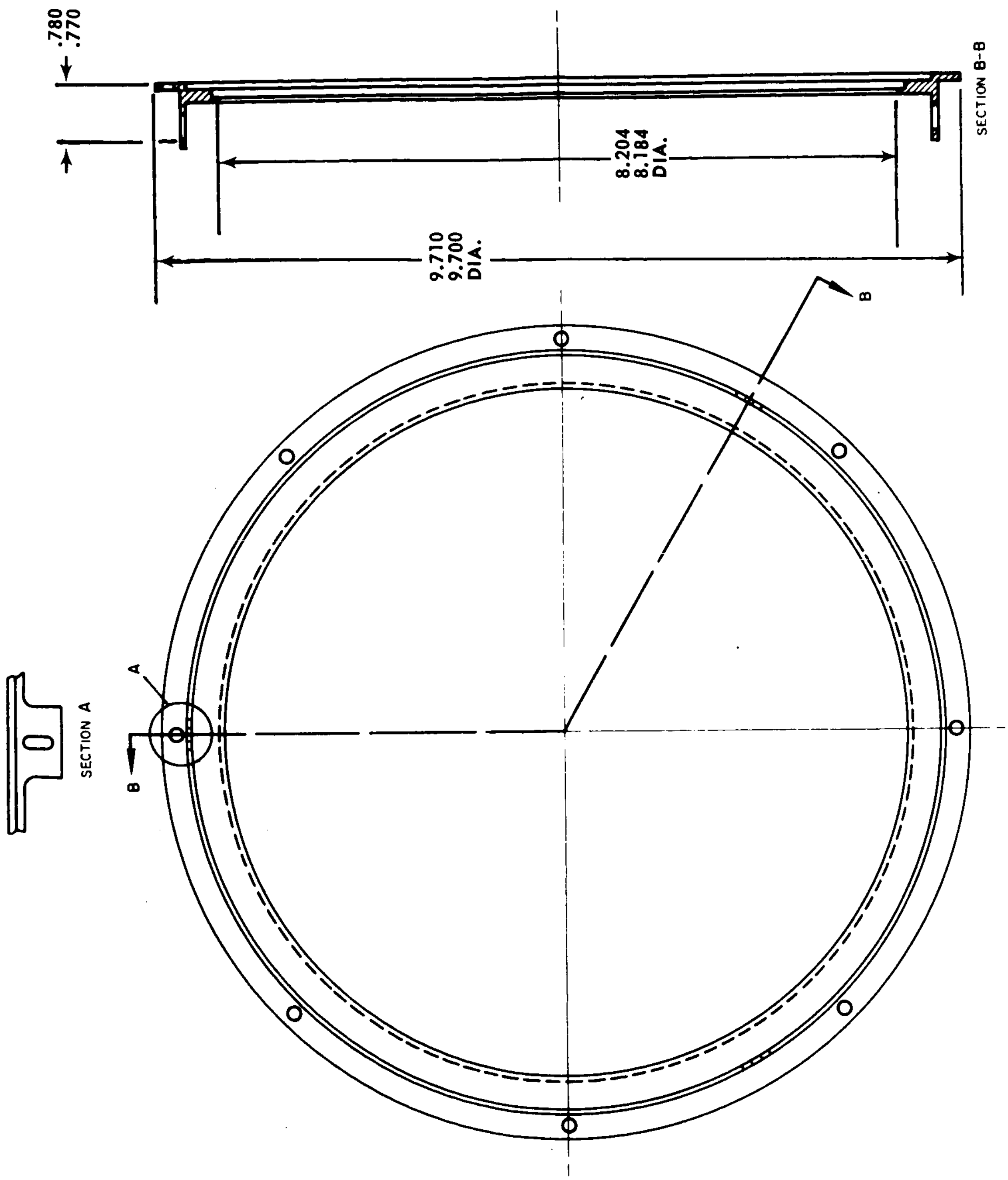

Figure 65 Teflon Holder For Instrumented Version of Orifice Compensated Seal
PWA Dwg. No. SKZ-70718-C

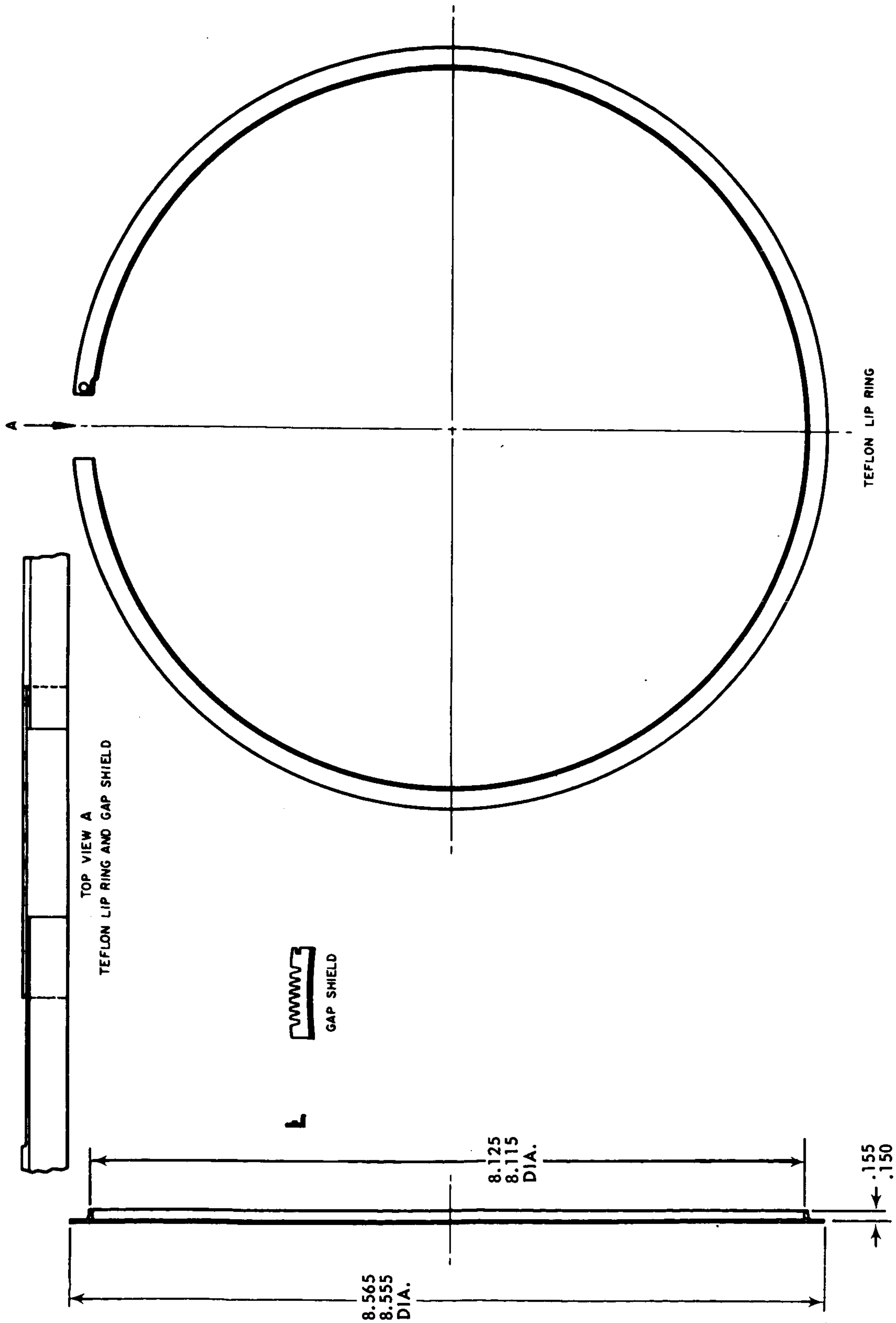

Figure 66 Teflon and Gap Shield for Instrumented Version of Orifice Compensated Seal
PWA Dwg. No. SKZ-70720-C

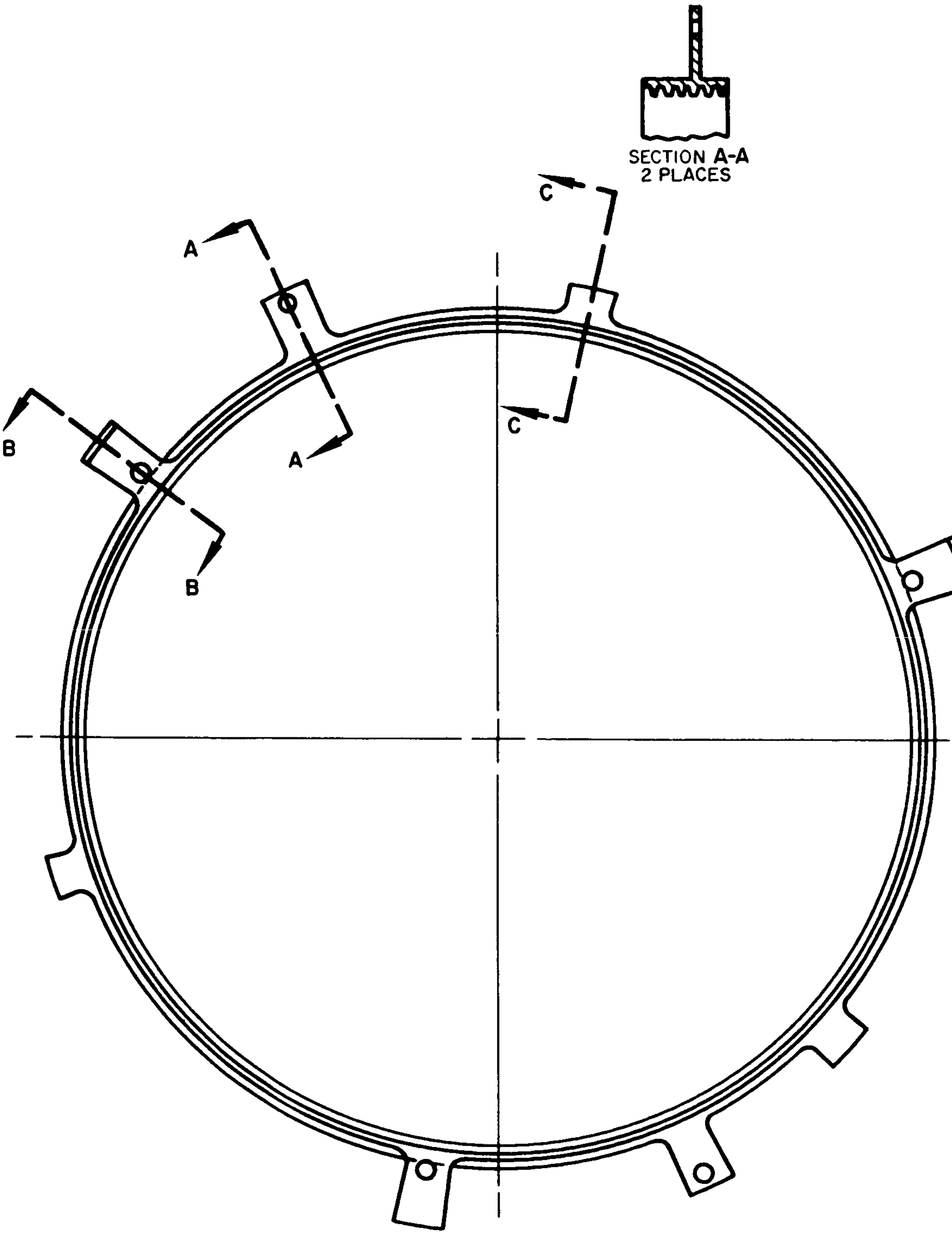
SECTION A-A
2 PLACES
A
A
B
B
C
C

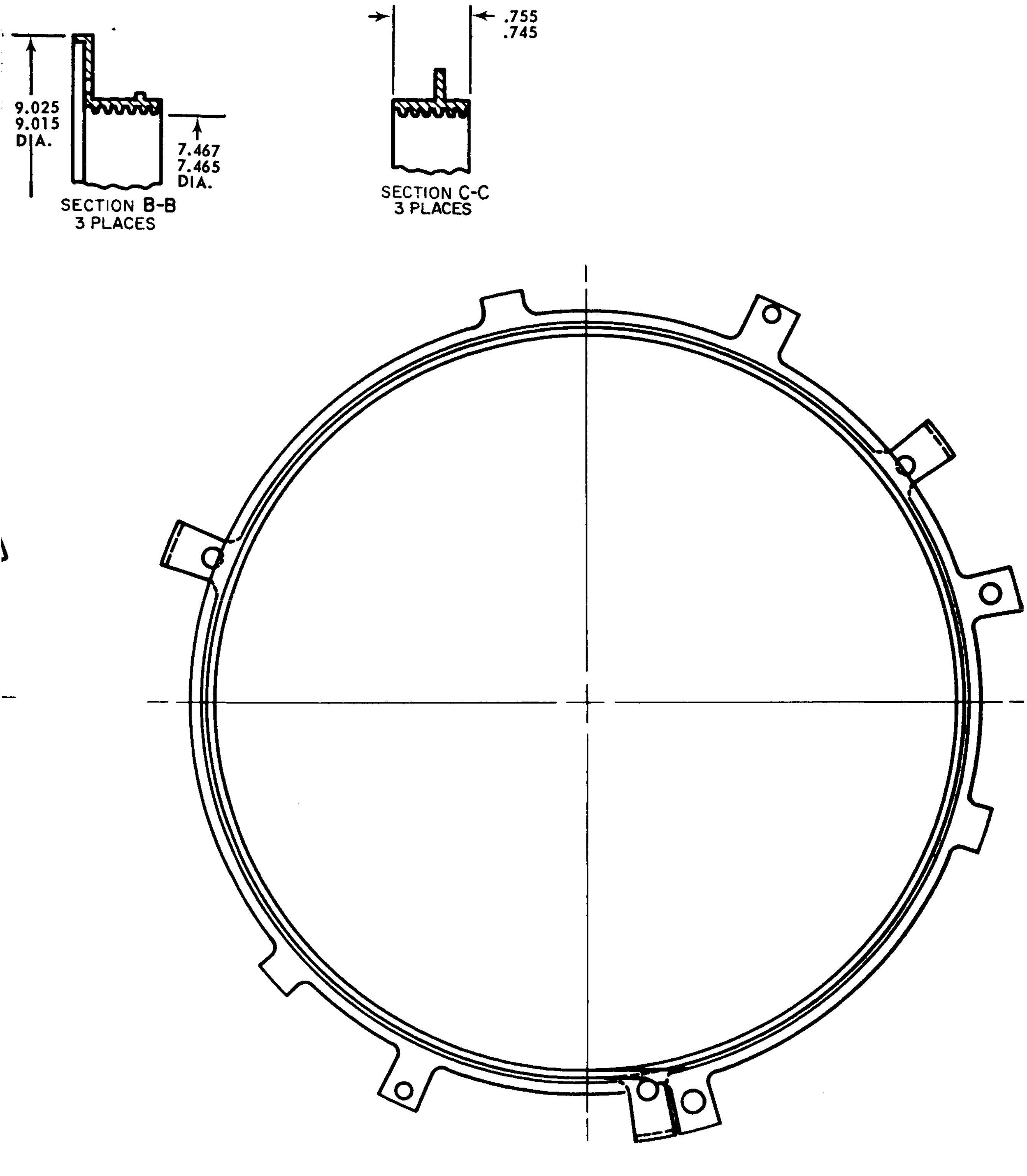

Figure 67 Special Windback for Instrumented Version of Orifice Compensated Seal PWA Dwg. No. SKZ-70712-C

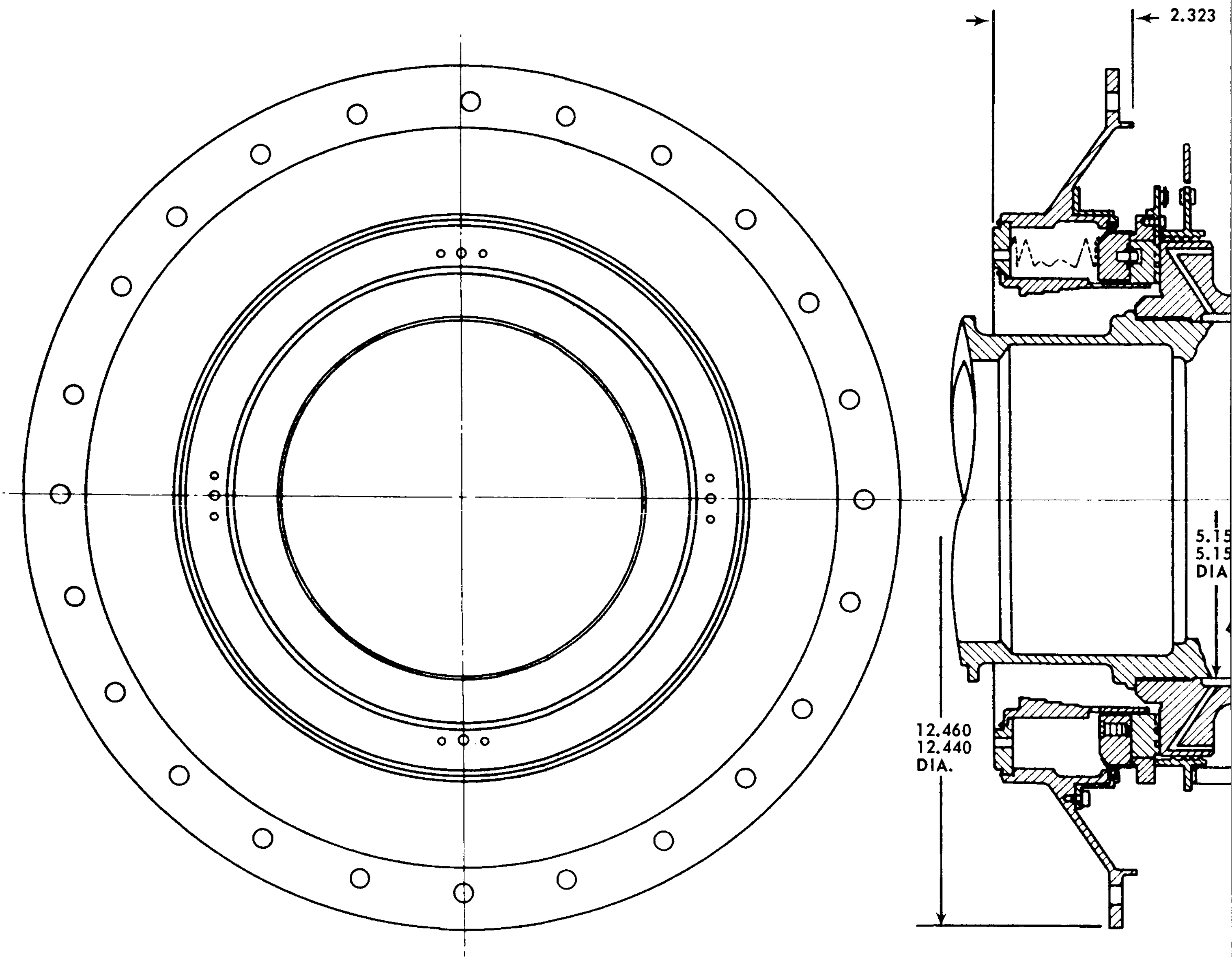
2.323
5.15
5.15
DIA
12.460
12.440
DIA.

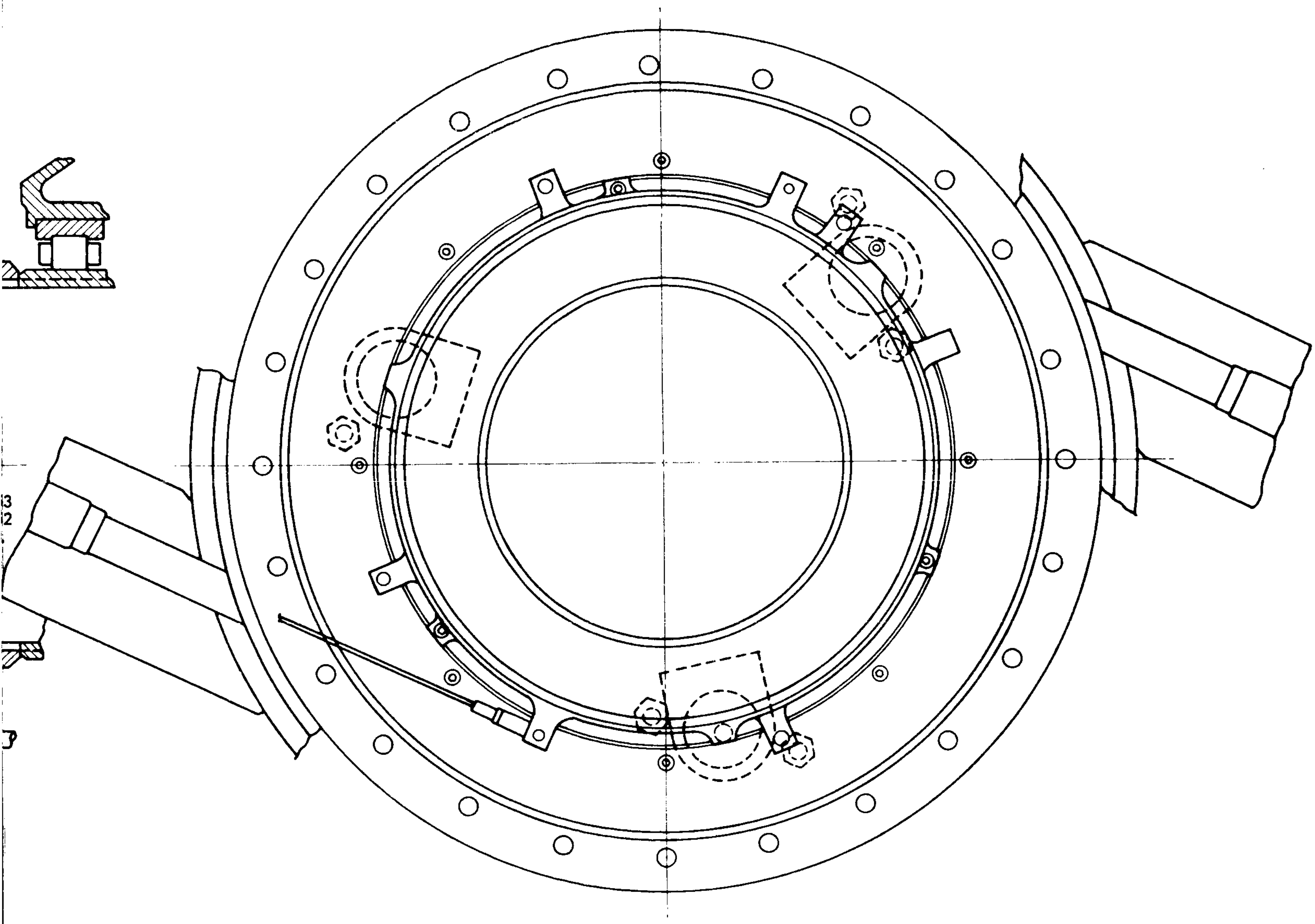

Figure 68 Carbon Face Contact Bellows Secondary Seal Assembly
Stein Seal Co. Dwg. No. 2883-B1

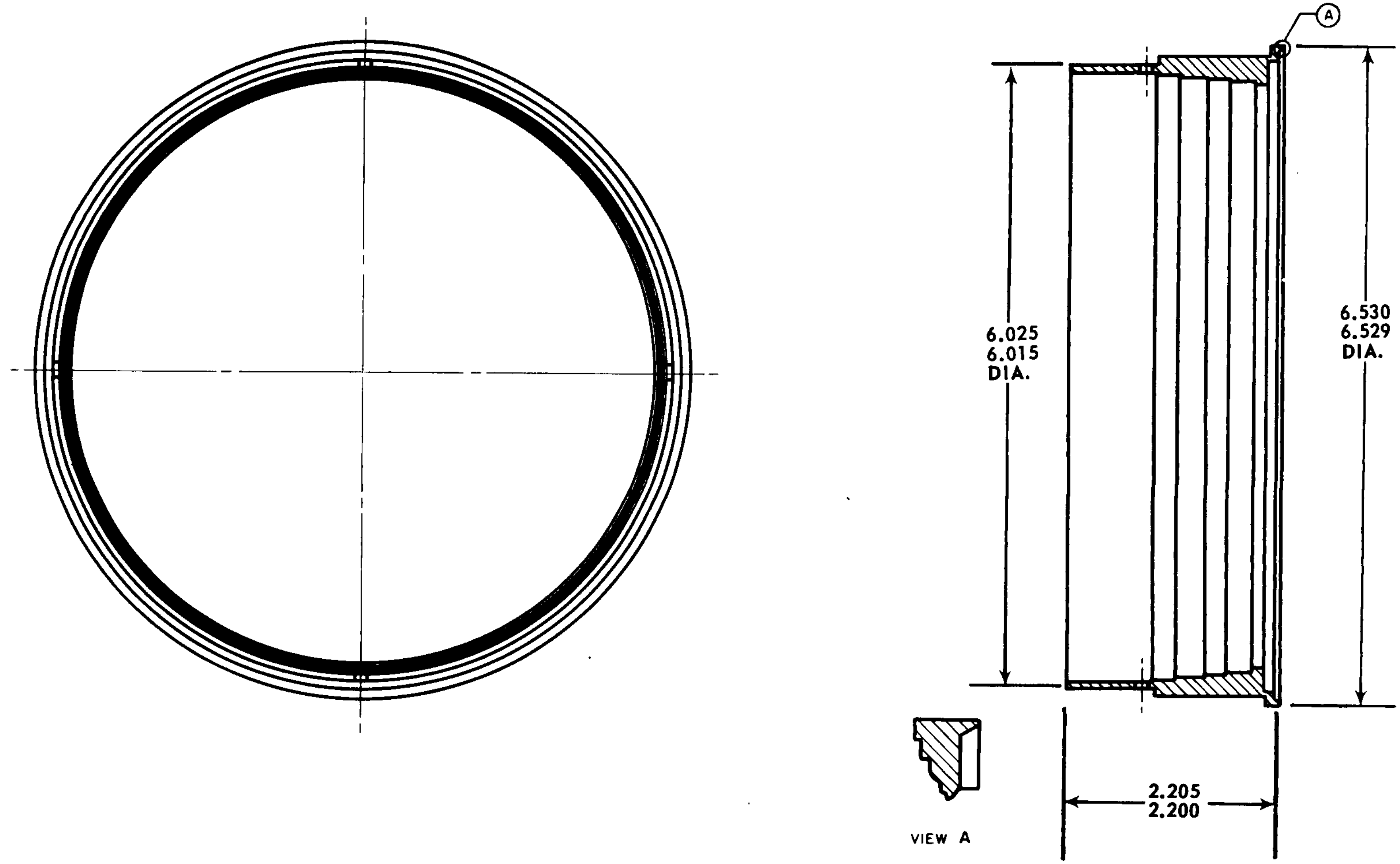

Figure 69 Bore Guide for Face Contact Bellows Secondary Seal
PWA Dwg. No. SKZ 70866-C

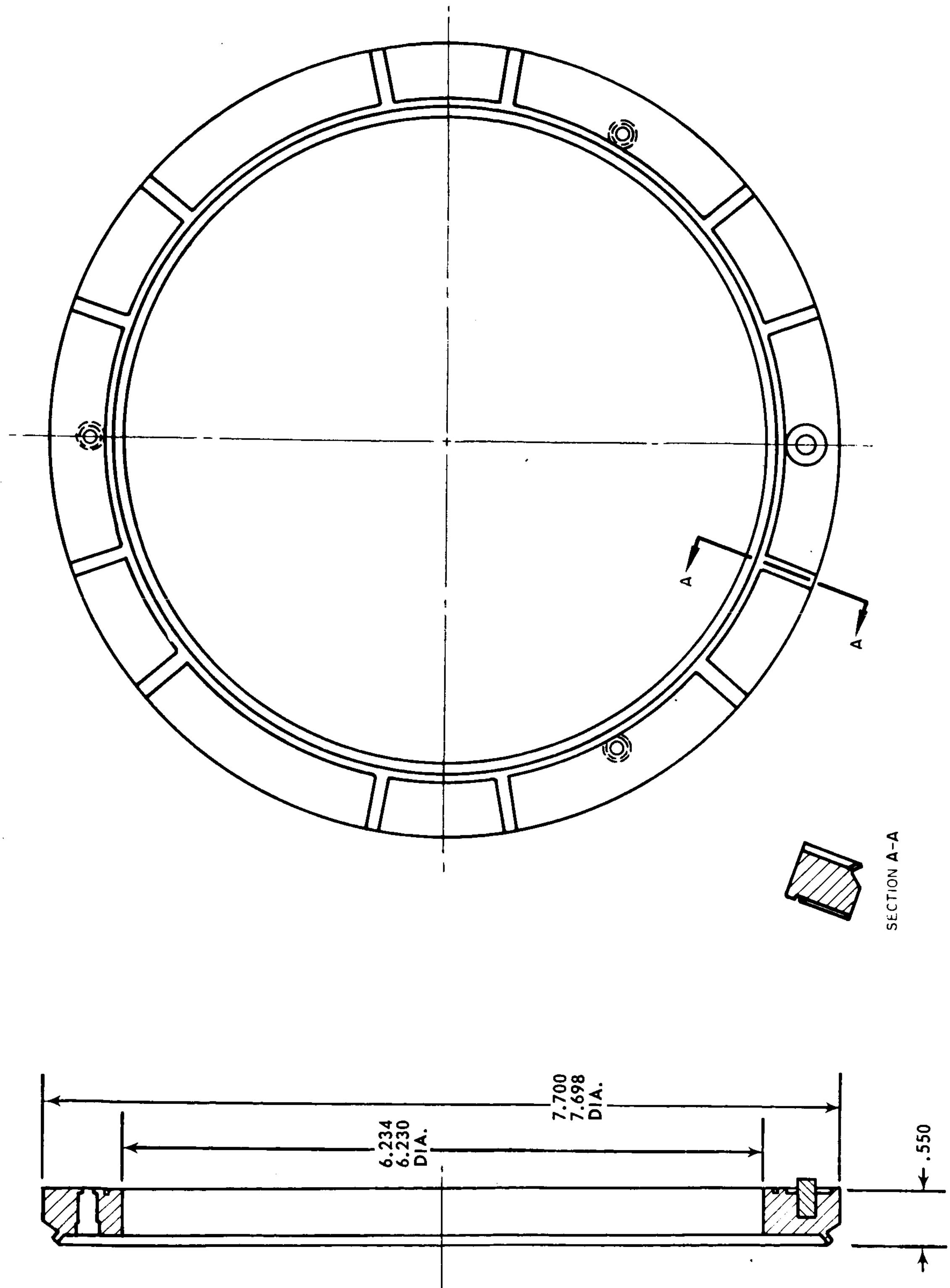

Figure 70 Bellows Front Fitting For Face Contact Bellows Secondary Seal
PWA Dwg. No. SKZ 70862-C

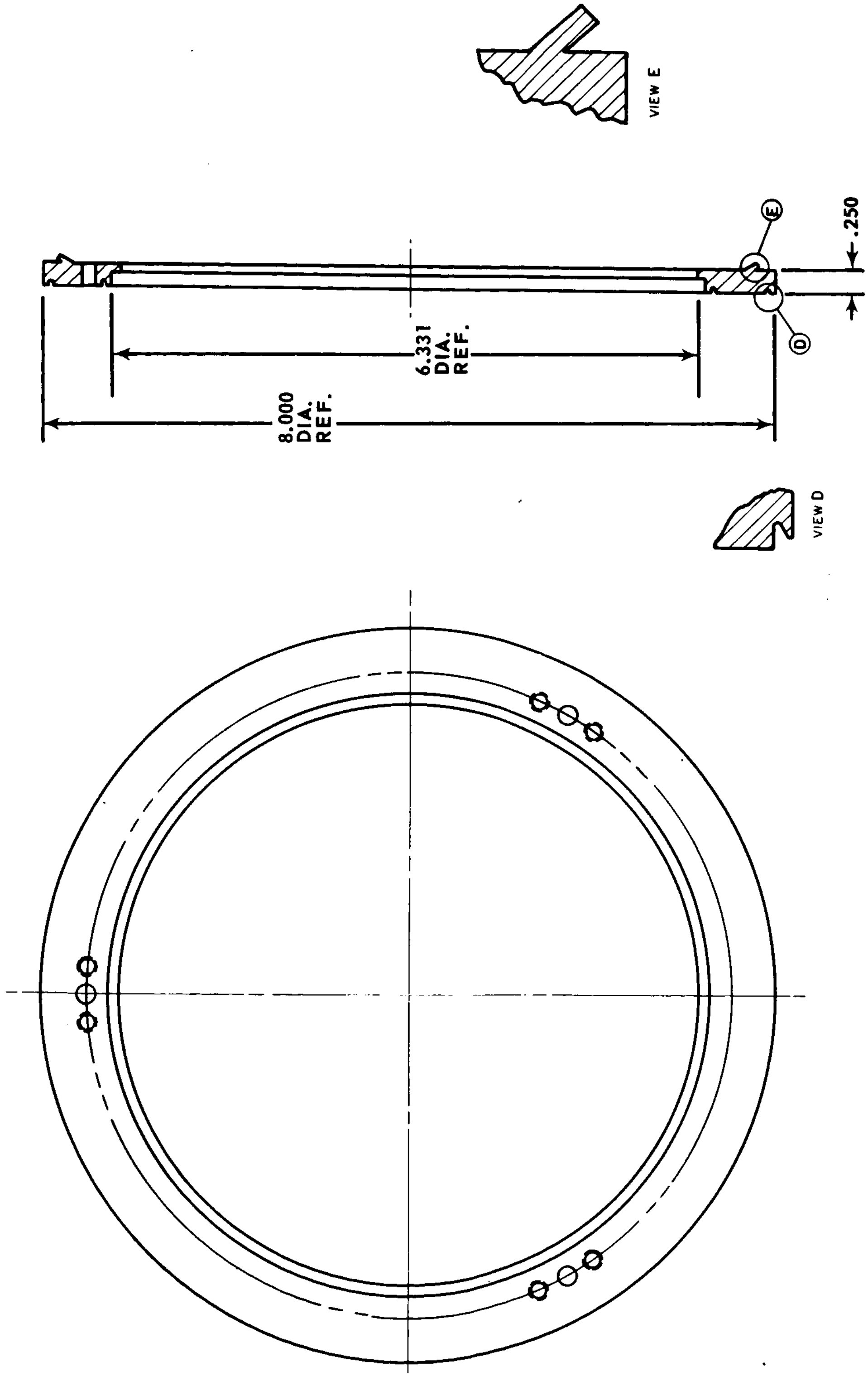

Figure 71 Bellows Rear Fitting For Face Contact Bellows Secondary Seal
PWA Dwg. No. SKZ-70861-C

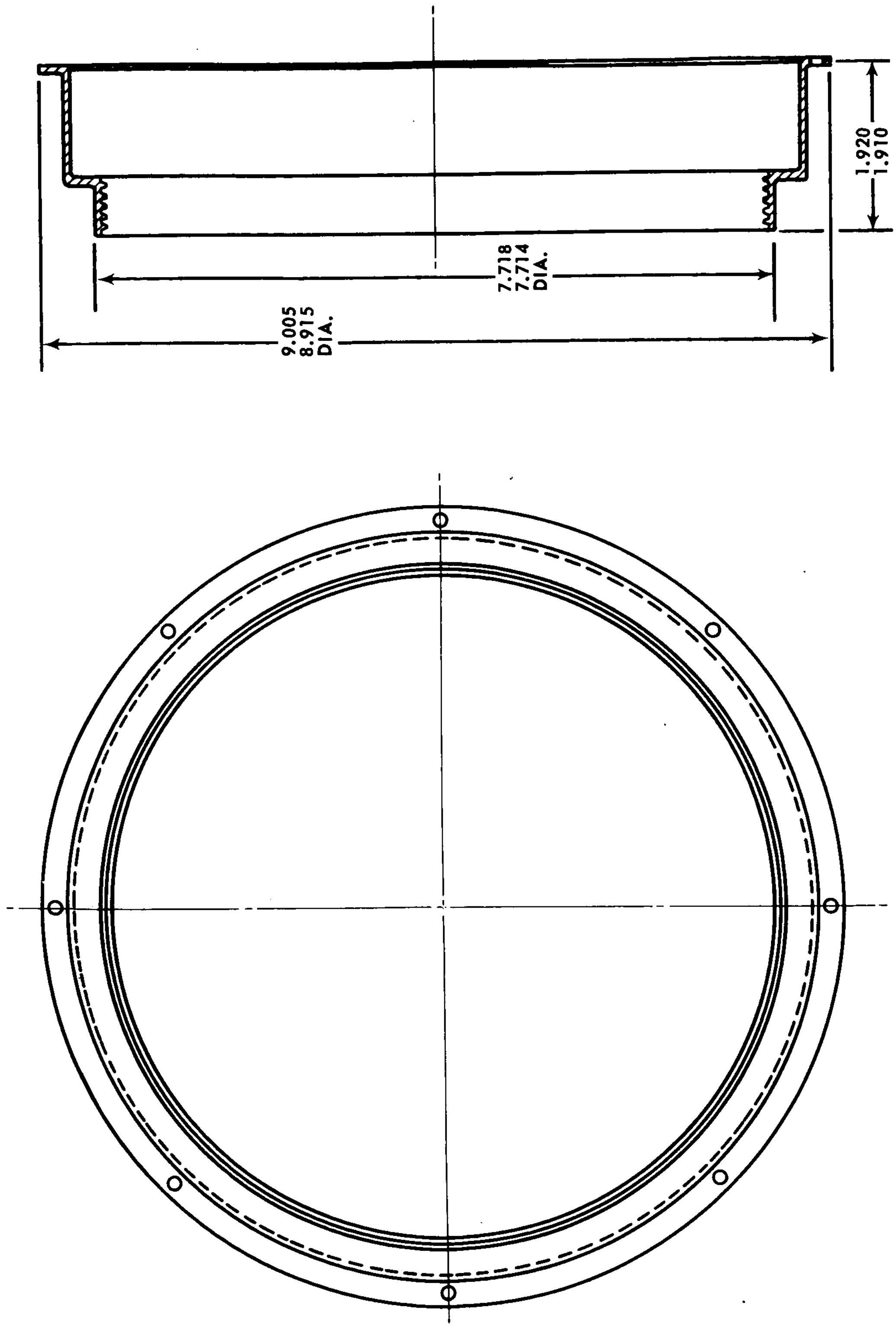

Figure 72 Windback for Face Contact Bellows Secondary Seal
PWA Dwg. No. SKZ-70859-C

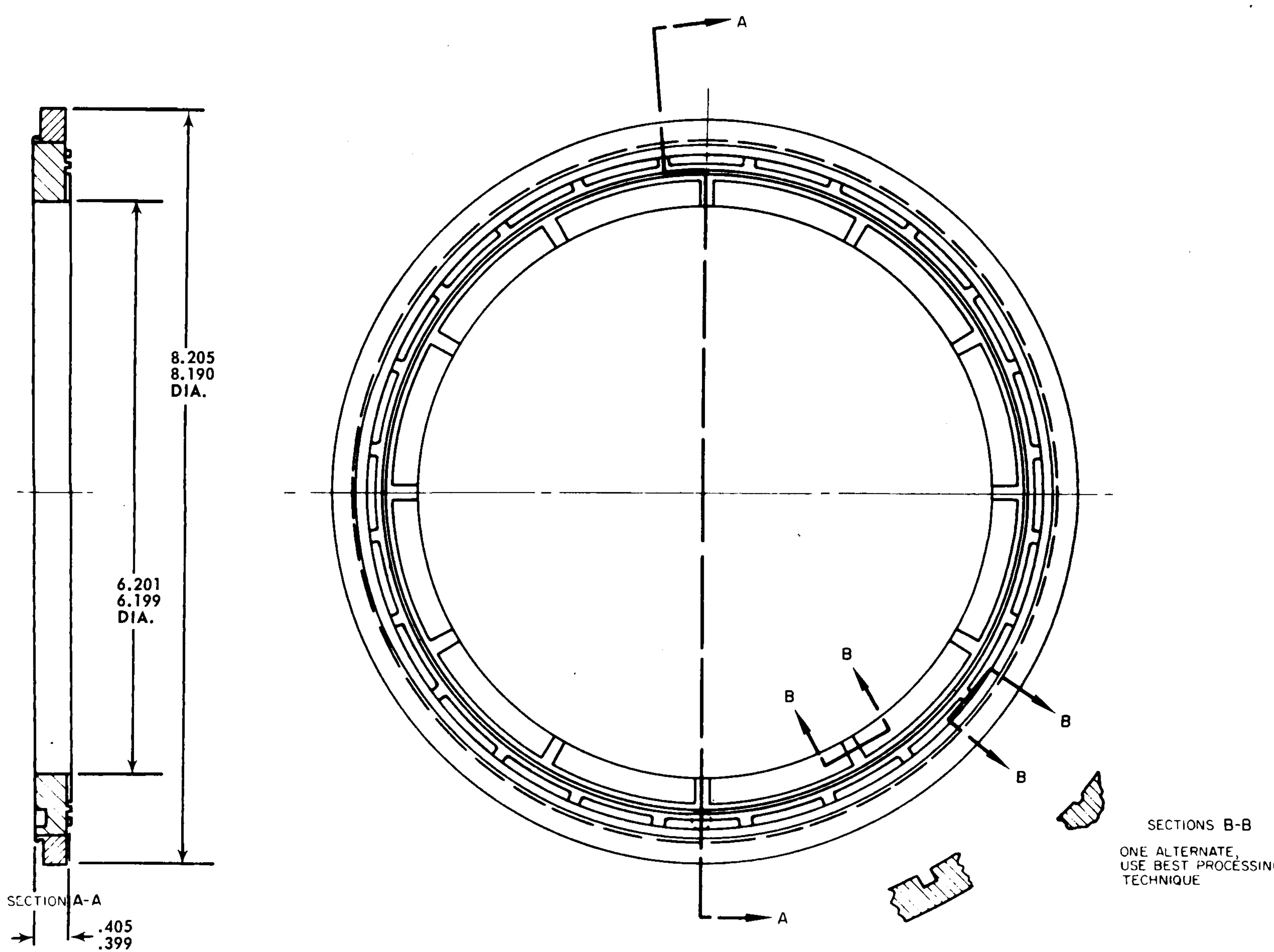

Figure 73 Carbon Seal Assembly For Face Contact Bellows Secondary Seal
PWA Dwg. No. SKZ-70871-C

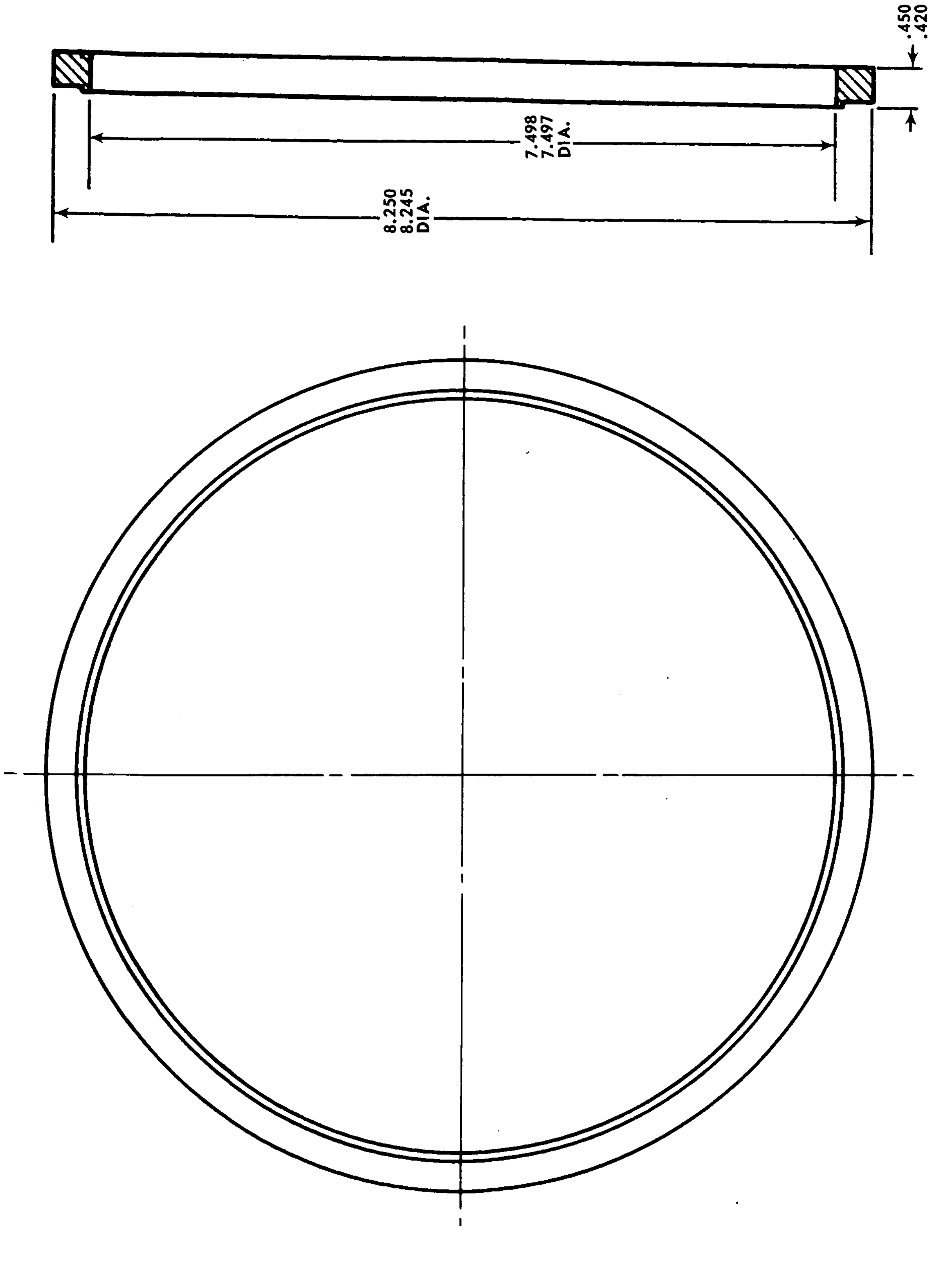

Figure 74 Seal Assembly Band For Face Contact Bellows Secondary Seal
PWA Dwg. No. SKZ-70870-C

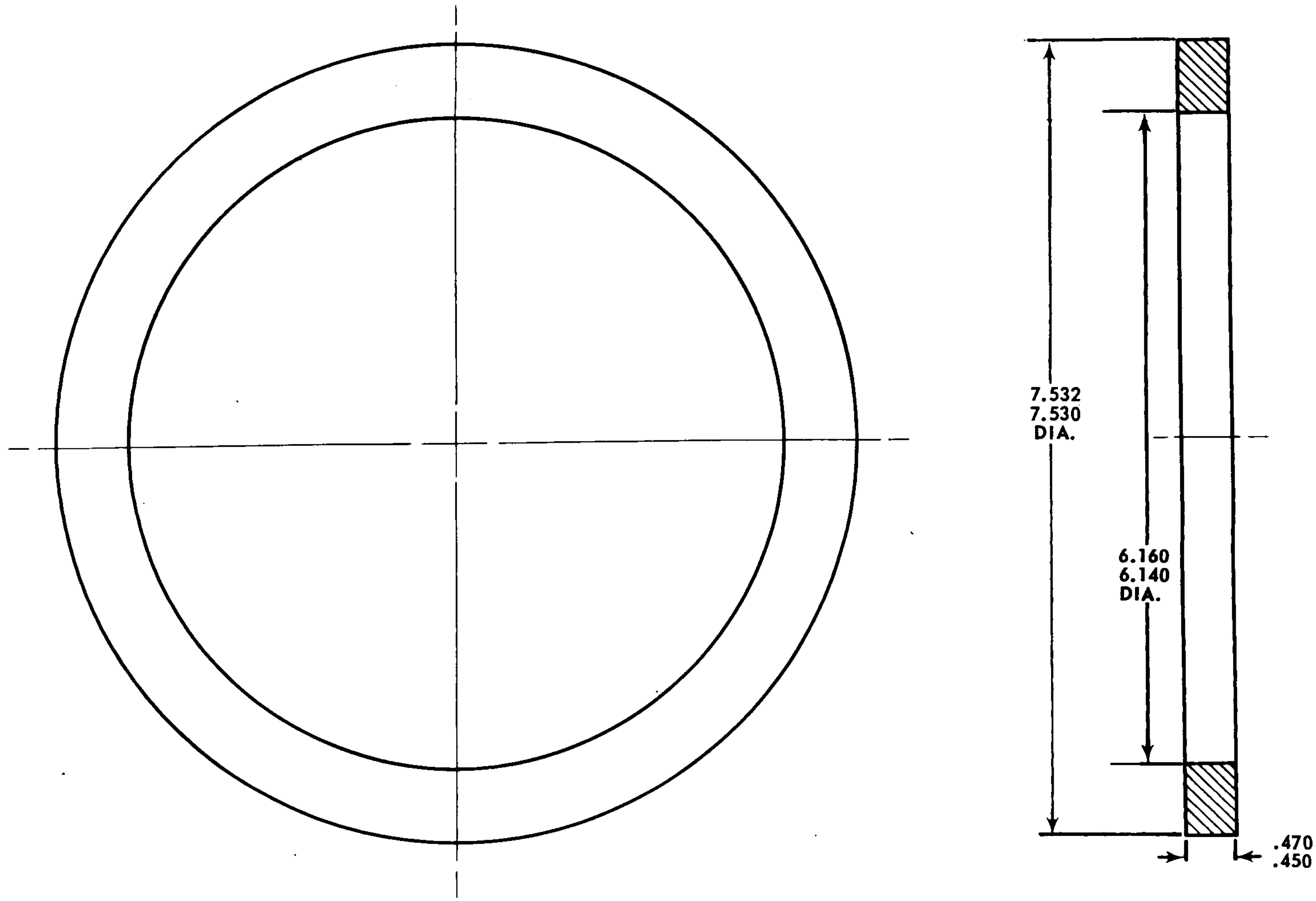

Figure 75 Carbon Wafer for Face Contact Bellows Secondary Seal
PWA Dwg. No. SKZ-70869-C

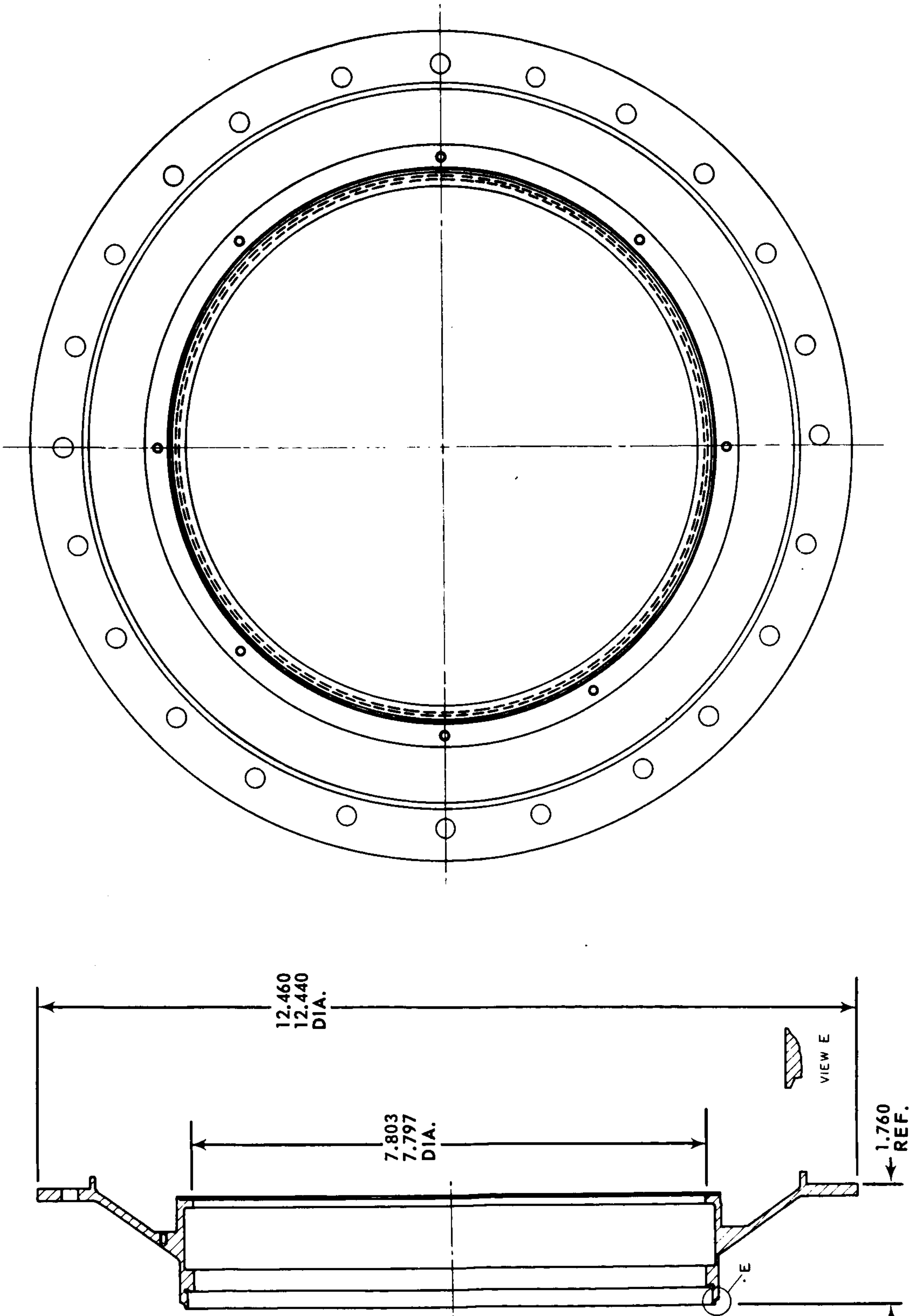

Figure 76 Seal Carrier For Face Contact Bellows Secondary Seal
PWA Dwg. No. SKZ-70867-C

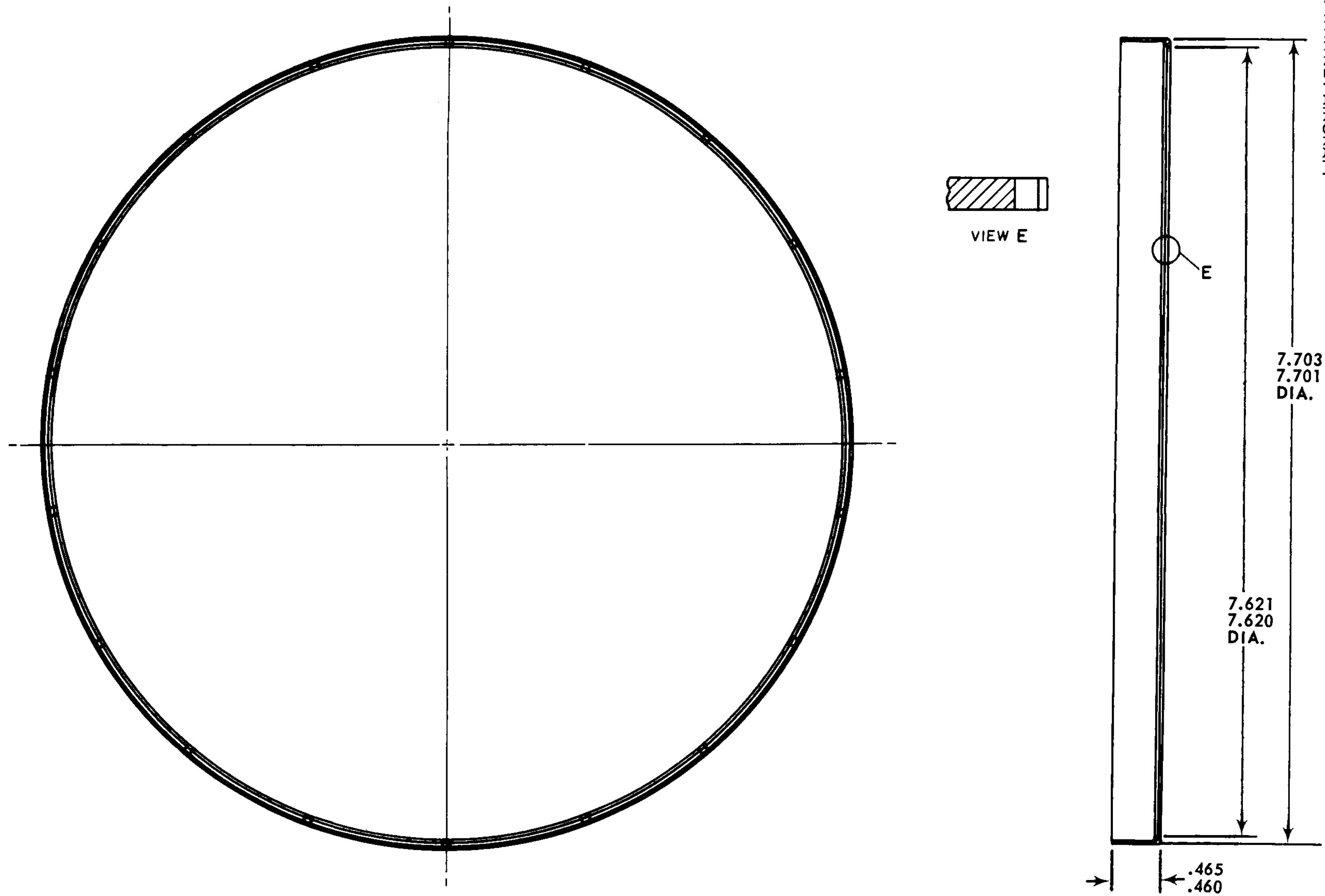

Figure 77 Alignment Ring For Face Contact Bellows Secondary Seal
PWA Dwg. No. SKZ-70868-C

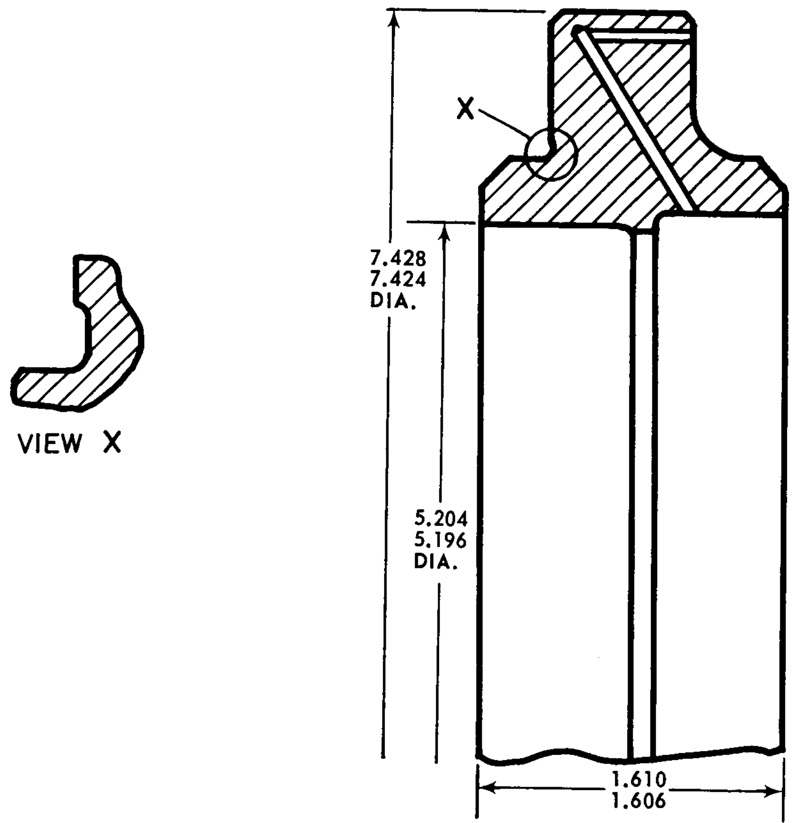

Figure 78 Seal Plate For Face Contact Bellows Secondary Seal
PWA Dwg. No. SKZ-70872-C

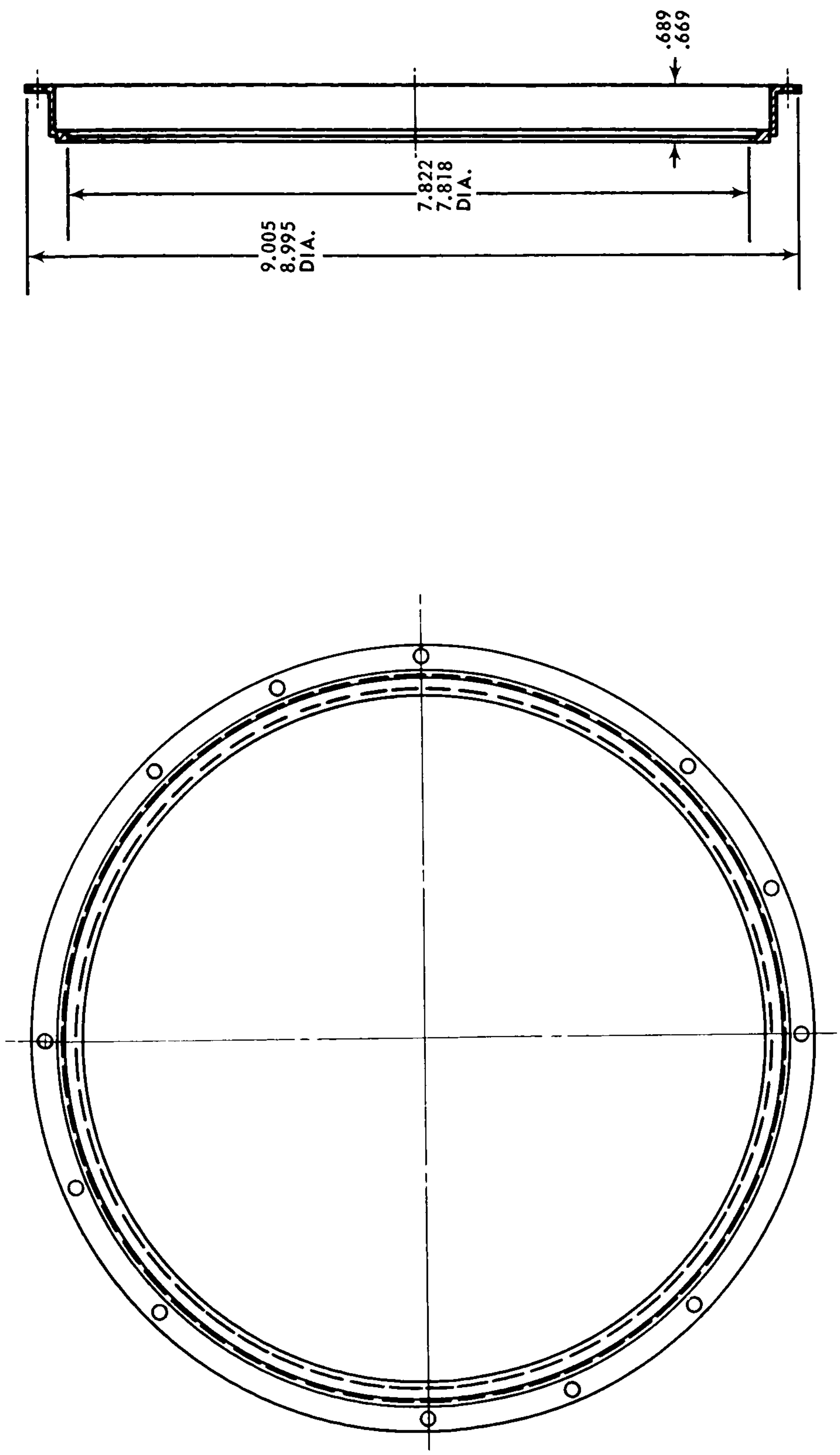

Figure 79 Teflon Holder For Instrumented Version of Face Contact Bellows Secondary Seal
PWA Dwg. No. SKZ-70864-C

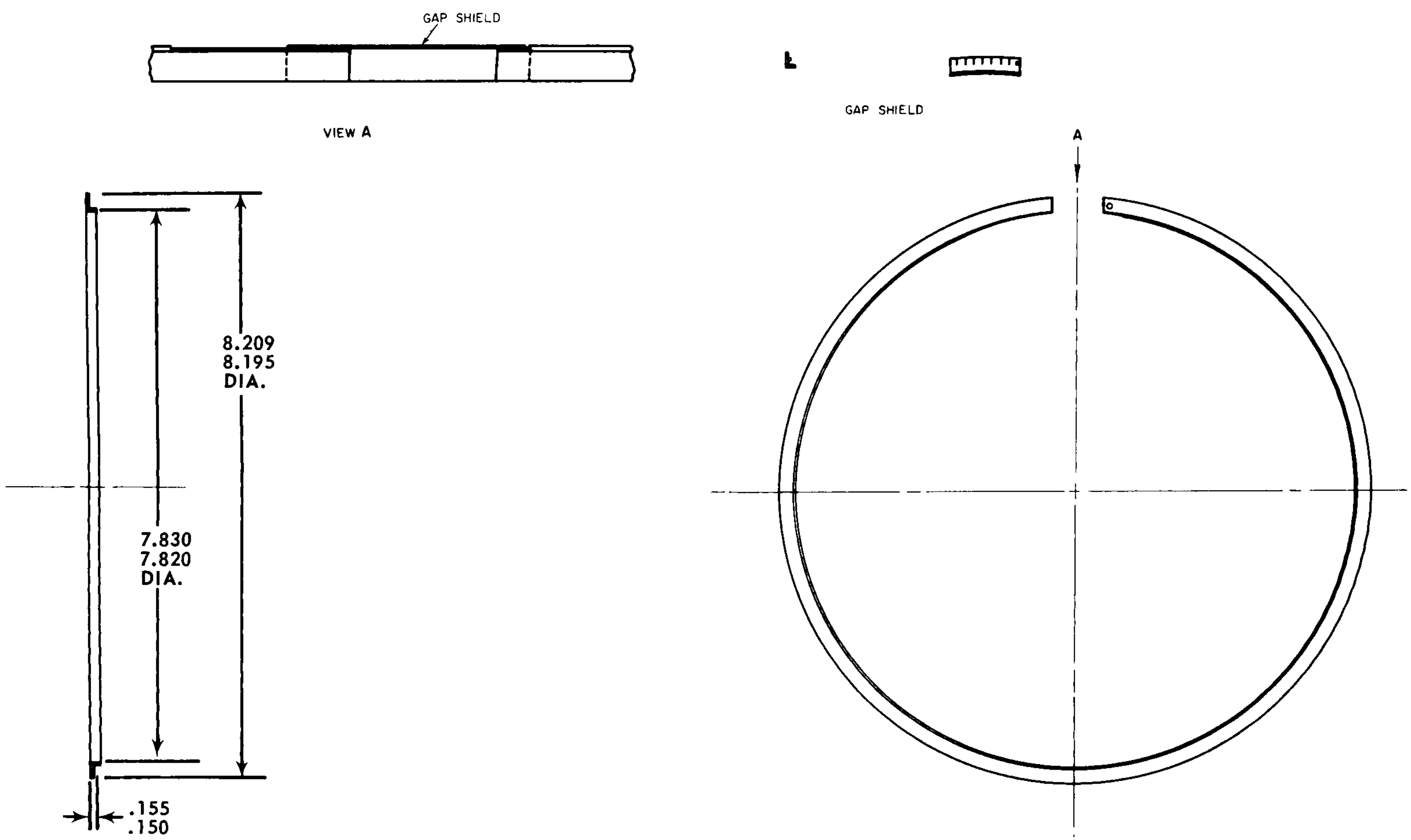

Figure 80 Teflon and Gap Shield For Instrumented Version of Face Contact Bellows Secondary Seal PWA Dwg. No. SKZ-70863-C

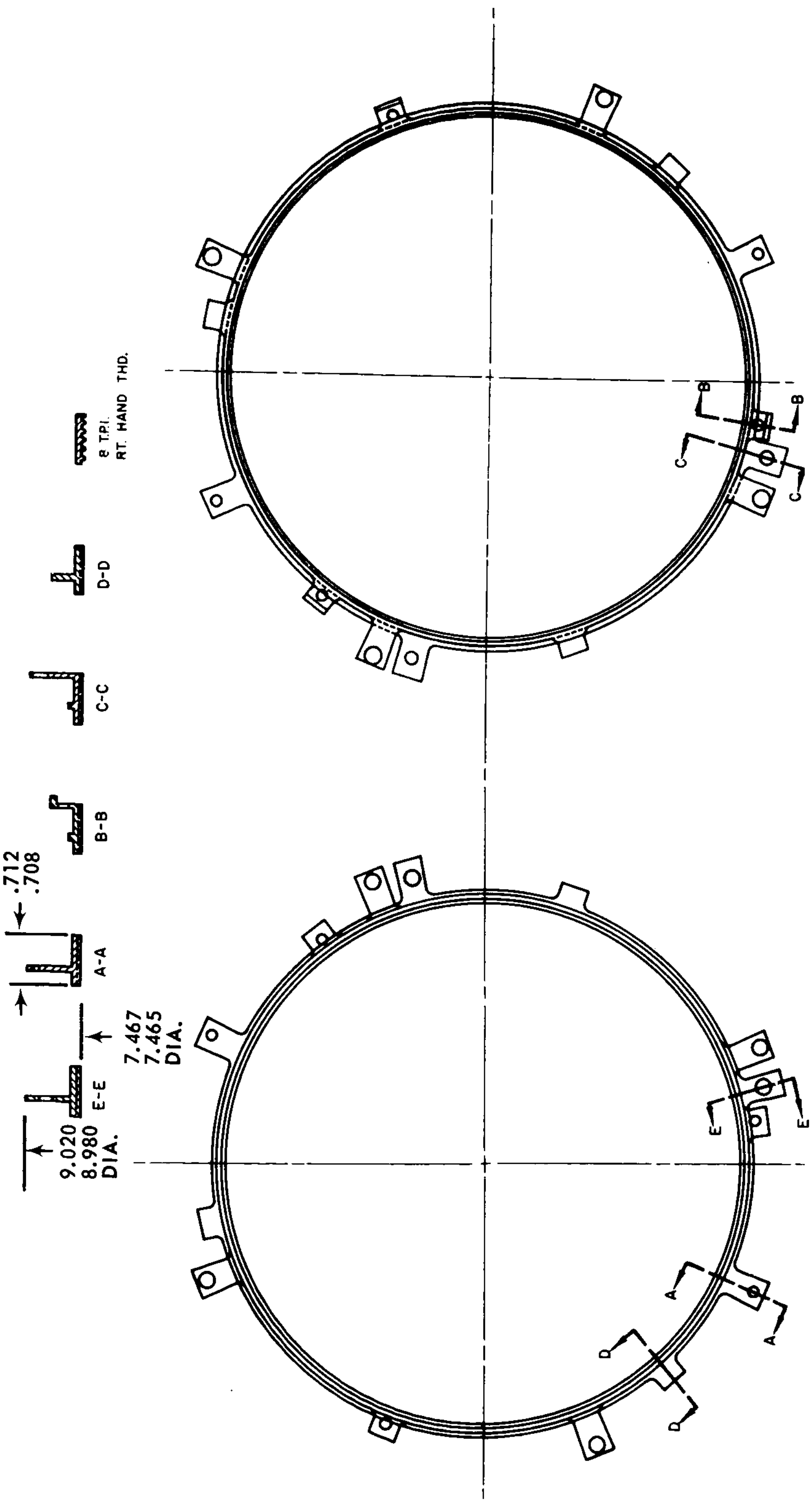

Figure 81 Special Windback For Instrumented Version of Face Contact Bellows Secondary Seal
PWA Dwg. No. SKZ-70865-C

SEMI-ANNUAL REPORTS DISTRIBUTION LIST

NAS3-7609

Addressee		Number of Copies
1. NASA-Lewis Research Center Spacecraft Technology Procurement Section Attention: John H. DeFord		2
2. NASA-Lewis Research Center Air-Breathing Engine Division		
J. Howard Childs	M.S. 60-4	1
W. H. Roudebush	M.S. 60-6	1
D. P. Townsend	M.S. 60-6	4
Lawrence E. Macioce	M.S. 60-6	1
3. NASA-Lewis Research Center Technology Utilization Office Attention: John Weber		1
4. NASA-Lewis Research Center Report Control Office		1
5. NASA-Lewis Research Center Attention: Library		1
6. NASA-Scientific and Technical Information Facility Box 5700 Bethesda, Maryland Attention: NASA Representative		6
7. NASA-Lewis Research Center Fluid System Components Division Attention: I.I. Pinkel		1
E.E. Bisson		1
R.L. Johnson		1
W.R. Loomis		1
L.P. Ludwig		1
M.A. Swikert		1
T.B. Shillito		1

Addressee			Number of Copies
8.	Air Force Materials Laboratory Wright-Patterson Air Force Base, Ohio 45433		
	Attention:	MANL, R. Adamczak	1
		MANE, R. Headrick & J.M. Kelble	1
		MAAE, P. House	1
9.	Air Force Systems Engineering Group Wright-Patterson Air Force Base, Ohio 45433		
	Attention:	SESHS, J.L. Wilkins	1
		SEJPF, S. Prete	1
10.	Air Force Aero Propulsion Laboratory Wright-Patterson Air Force Base, Ohio 45433		
	Attention:	AFAPL (APFL), K.L. Berkey & L. DeBrohum	1
		AFAPL (APTC), C. Simpson	1
		APTP, I.J. Gershon	1
11.	FAA Headquarters 800 Independence Avenue, S.W. Washington, D.C.		
	Attention:	J. Chavkin, SS/120	1
		M. Lott, FS/141	1
12.	NASA Headquarters Washington, D.C. 20546		
	Attention:	N.F. Rekos (RAP)	1
		A.J. Evans (RAD)	1
		J. Maltz	1
13.	NASA-Langley Research Center Langley Station Hampton, Virginia 23365		
	Attention:	Mark R. Nichols	1
14.	Mechanical Technology Incorporated 968 Albany-Shaker Road Latham, New York		
	Attention:	Donald F. Wilcock	1

Addressee		Number of Copies
15.	Clevite Corporation Cleveland Graphite Bronze Division 17000 St. Clair Avenue Cleveland, Ohio 44110 Attention: Thomas H. Koenig	1
16.	Koppers Company, Inc. Metal Products Division Piston Ring and Seal Department Baltimore 3, Maryland Attention: F.C. Kuchler	1
17.	Stein Seal Company 20th Street & Indiana Avenue Philadelphia 32, Pennsylvania Attention: Dr. P.C. Stein	1
18.	Wright Aeronautical Division Curtiss-Wright Corporation 333 West 1st Street Dayton 2, Ohio Attention: S. Lombardo	1
19.	TRW Inc. 23555 Euclid Avenue Cleveland, Ohio 44117 Attention: O. Deckor	1
20.	General Electric Company Advanced Engine and Technology Department Cincinnati, Ohio 45215 Attention: L.B. Venable	1
	G.J. Wile	1
	C. C. Moore H-25	1
21.	Huyck Metals Company P.O. Box 30 45 Woodmont Road Milford, Connecticut Attention: J.I. Fisher	1

Addressee		Number of Copies
22.	Aerojet-General Corporation 20545 Center Ridge Road Cleveland, Ohio 44116 Attention: W.L. Snapp	1
23.	Avco Corporation Lycoming Division Stratford, Connecticut Attention: R. Cuny	1
24.	Battelle Memorial Institute 505 King Avenue Columbus 1, Ohio Attention: C.H. Allen	1
25.	Bendix Corporation Fisher Building Detroit 2, Michigan Attention: R.H. Isaacs	1
26.	Boeing Aircraft Company 224 N. Wilkinson Dayton, Ohio 45402 Attention: H.W. Walker	1
27.	Douglas Aircraft Company Holiday Office Center 16501 Brookpark Road Cleveland, Ohio 44135 Attention: J.J. Pakiz	1
28.	General Dynamics Corporation 16501 Brookpark Road Cleveland, Ohio 44135 Attention: George Vila	1
29.	General Motors Corporation Allison Division Plant #8 Indianapolis, Indiana Attention: E.M. Deckman	1

Addressee		Number of Copies
30.	Lockheed Aircraft Company 16501 Brookpark Road Cleveland, Ohio 44135 Attention: L. Kelly	1
31.	Martin Company 16501 Brookpark Aoad Cleveland, Ohio 44135 Attention: Z.G. Horvath	1
32.	North American Aviation Inc. 16501 Brookpark Road Cleveland, Ohio 44135 Attention: George Bremer	1
33.	Fairchild-Miller Corporation Republic Aviation Division Farmingdale, Long Island New York 11735 Attention: D. Schroeder	1
34.	Westinghouse Electric Corporation 55 Public Square Cleveland, Ohio 44113 Attention: Lynn Powers	1
35.	I.I.T. Research Foundation 10 West 35th Street Chicago, Illinois 60616 Attention: Dr. Strohmeier	1
36.	Pesco Products Division Borg-Warner Corporation 24700 N. Miles Bedford, Ohio	1
37.	Stanford Research Institute Menlo Park, California Attention: R.C. Fey	1

Addressee		Number of Copies
38.	Franklin Institute Laboratories 20th & Parkway Philadelphia 3, Pennsylvania Attention: J. V. Carlson	1
39.	Industrial Tectonics Box 401 Hicksville, New York 11801 Attention: J. Cherubin	1
40.	Pressure Technology Corporation of America 453 Amboy Avenue Woodbridge, New Jersey Attention: A. Dobrowsky	1
41.	Sealol Inc. P.O. Box 2158 Providence 5, Rhode Island Attention: Justus Stevens	1
42.	Continential Aviation & Engineering 12700 Kercheval Detroit 15, Michigan Attention: A.J. Follman	1
43.	Northrop Corporation 1730 K Street N.W. Suite 903-5 Washington 6, D.C. Attention: S.W. Fowler, Jr.	1
44.	Chicago Rawhide Manufacturing Company 1311 Elston Avenue Chicago, Illinois Attention: R. Blair	1
45.	Midwest Research Institute 425 Volker Blvd. Kansas City 10, Missouri Attention: V. Hopkins	1

Addressee		Number of Copies
46.	Socony Mobil Oil Company Research Department Paulsboro Laboratory Paulsboro, New Jersey Attention: E. Oberright	1
47.	Southwest Research Institute 8500 Cuiebra Road San Antonio, Texas Attention: P.N. Ku	1
48.	E. I. duPont de Nemours & Company 1007 Market Street Wilmington 98, Delaware Attention: G. Finn	1
	R. J. Laux	1
	A. J. Cheney	1
49.	Esso Research & Engineering Company P.O. Box 51 Linden, New Jersey Attention: W.O. Taff	1
50.	Monsanto Chemical Company 800 North Lindbergh Blvd. St. Louis, Missouri 63166 Attention: K. McHugh	1
	R. Hatton	1
51.	Sinclair Refining Company 600 5th Avenue New York, New York 10020 Attention: C.W. McAllister	1
52.	Union Carbide Chemicals Company Division of Union Carbide Corporation Tarrytown, New York Attention: W.H. Millott & J.C. Haaga	1

Addressee		Number of Copies
53.	Sun Oil Company Automotive Laboratory Marcus Hook, Pennsylvania Attention: J. L. Griffith	1
54.	Hercules Powder Company, Inc. 900 Market Street Wilmington, Delaware	1
55.	Fairchild Engine and Airplane Corporation Stratos Division Bay Shore, New York	1
56.	Borg-Warner Corporation Roy C. Ingersoll Research Center Wolf and Algonquin Roads Des Plaines, Illinois	1
57.	Kendall Refining Company Bradford, Pennsylvania Attention: F.I.I Lawrence	1
58.	U.S. Naval Air Material Center Aeronautical Engine Laboratory Philadelphia 12, Pennsylvania Attention: A. L. Lockwood	1
59.	U.S. Naval Research Laboratory Washington, D.C. Attention: Charles Murphy	1
60.	Department of the Navy Bureau of Naval Weapons Washington, D.C. Attention: A.D. Nehman, RAAE-3 C.C. Singletorry, RAPP-4	1 1
61.	U.S. Army Ordnance Rock Island Arsenal Laboratory Rock Island, Illinois Attention: R. LeMar	1

Addressee		Number of Copies
62.	Department of the Navy Bureau of Ships Washington 25, D.C. Attention: Harry King, Code 634A	1
63.	Sinclair Research Incorporated 400 E. Sibley Blvd. Harvey, Illinois Attention: M.R. Fairlle	1
64.	SKF Industries, Inc. 1100 First Avenue King of Prussia, Pennsylvania Attention: L.B. Sibley	1
65.	Pennsylvania State University Department of Chemical Engineering University Park, Pennsylvania Attention: Dr. E.E. Klaus	1
66.	Crane Packing Company 6400 W. Oakton Street Morton Grove, Illinois Attention: Harry Tankus	1
67.	B.F. Goodrich Company Aerospace & Defense Products Division Troy, Ohio Attention: L.S. Blalkowski	1
68.	Koppers Company, Inc. Monrosville, Pennsylvania Attention: Billy D. Pfoutz	1
69.	The University of Tennessee Department of Mechanical and Aerospace Eng. Knoxville, Tennessee Attention: Professor W.K. Stair	1 1
70.	Hughes Aircraft Company International Airport Station P.O. Box 90515 Los Angeles 9, California	1

Addressee		Number of Copies
71.	U.S. Navy Marine Engineering Laboratory Friction and Wear Division Annapolis, Maryland Attention: R.B. Snapp	1
72.	Metal Bellows Corporation 20977 Knapp Street Chatsworth, California Attention: Sal Artino	1
73.	Rocketdyne 6633 Canoga Avenue Canoga Prkk, California Attention: M. Butner	1
74.	Carbon Products Division of Union Carbide Corporation 270 Park Avenue New York, New York 10017 Attention: J. Curran	1
75.	Garlock, Inc. Palmyra, New York 14522 Attention: E.W. Fisher	1
76.	Durametallic Corporation Kalamazoo, Michigan Attention: H. Hummer	1
77.	Morganite, Inc. 33-02 48th Avenue Long Island City 1, New York Attention: S.A. Rokaw	1
78.	United States Graphite Company 1621 Holland Saginaw, Michigan Attention: F.F. Ruhl	1
79.	Cartiseal Corporation 3515 West Touhy Lincolnwood, Illinois Attention: R. Voltik	1

Addressee		Number of Copies
80.	Department of the Army U.S. Army Aviation Material Labs. Fort Eustis, Virginia 23604 Attention: John W. White, Chief Propulsion Division	1